# Prediction of Tribological and Rheological Properties of Lubricating Oils by Sound Velocity

**September 2010**

**Department of Engineering Systems and Technology**
**Graduate School of Science and Engineering**
**Saga University, Japan**

**SOBAHAN MIA**

# Prediction of Tribological and Rheological Properties of Lubricating Oils by Sound Velocity

By

**SOBAHAN MIA**

**Supervisor**
**Prof. Nobuyoshi OHNO**


**Department of Engineering Systems and Technology**
**Graduate School of Science and Engineering**
**Saga University, Japan**

**September 2010**

# Prediction of Tribological and Rheological Properties of Lubricating Oils by Sound Velocity

（油中音速による潤滑油レオロジー特性推算法の確立と応用展開の可能性）

By

**Sobahan Mia**

(Master of Engineering, Dept. of Mechanical Engineering
Saga University, Japan, in 2007
B.Sc. Engineering, Dept. of Mechanical Engineering
Rajshahi University of Engineering & Technology, Bangladesh, in 2002)

A dissertation submitted to the Graduate School of Science and Engineering
of Saga University in partial fulfillment of the requirements for
the degree of the Doctor of Philosophy
in the department of Engineering Systems and Technology

Under the supervision of
**Professor Nobuyoshi OHNO**

**September 2010**

I proudly dedicate this thesis to my respectable departed parents,

Askender Mia & Most. Monowara Begum

# Abstract

In recent years, tribological study is very much important to improve the life of machinery. Lubrication is the vital part of tribology; hence lubricant is key term in tribology. Liquid lubricants are mostly used and its properties influences on the life of machine parts to reduce friction and wear, and the application in high pressure. Among the tribological and rheological properties of lubricating oils, pressure-viscosity coefficient and low temperature fluidity is significant for high pressure rheology, elastohydrodynamic lubrication, and for various applications. Pressure-viscosity relationship is an important parameter of lubricating oil to understand its performance. So it is very much important to know the pressure-viscosity coefficient of lubricating oil. With the development of elastohydrodynamic theory, the significance of the high-pressure rheological effect on the lubricant film thickness and traction has been recognized. On the other hand, low temperature behavior of lubricating oil is essential for many applications such as at automobile cold start engine, aircraft or space mechanisms, wind turbine, etc. In the study, the pressure-viscosity coefficient was measured using high pressure viscosity test, and the low temperature fluidity was observed from the occurrence of photoelastic effect by lowering the temperature using liquid nitrogen. But, the measurement required large amount of time, and skill for handling the equipments. There are many correlations to prediction of pressure-viscosity coefficient. Despite the excellent empirical relationships in the researches, a relationship is needed which points out the dependence of pressure-viscosity coefficient on fundamental parameters of lubricating oil. This study found the relationship using the adiabatic bulk modulus. The bulk modulus is the reciprocal of compressibility and indicates the resistance of a fluid to compression. The bulk modulus is an explanation of viscosity-pressure properties in fundamental studies of elastohydrodynamic lubrication. The adiabatic bulk modulus can be calculated from sound velocity in lubricating oil. The sound velocity was measured from passing the supersonic wave in the lubricating oil using Sing around method. The Sing around UVM-2 apparatus was used in this research. Adiabatic bulk modulus was calculated from the measured sound velocity using Wood equation.

First, compared the adiabatic bulk modulus with the experimental pressure viscosity coefficient and a correlation was found between them. Therefore, in this research, prediction equations for pressure viscosity coefficient were proposed which were derived from basic principles based on sound velocity. The results were summarized and compared the calculated values to experimental values. It showed that one correlation does not followed for all lubricating oil. It followed at group basis. So, it existed the effect of sound velocity on the molecular structure of lubricating oils since every group has the different molecular structure. This study proposed three equations to predict pressure-viscosity coefficient, one for the traction oil, one for the mineral oil and polyalphaolefin oil, and another for the unsaturated fatty acid type vegetable oil. Using these equations, pressure-viscosity coefficient can be predicted from the sound velocity in lubricating oil at atmospheric pressure. Next, the adiabatic bulk modulus was compared with the viscoelastic solid transition temperature at atmospheric pressure, which represents the low temperature fluidity of lubricating oil. From the comparison, it has been found that low adiabatic bulk modulus indicates the lower viscoelastic solid transition temperature as well as the good low temperature fluidity in case of same group of oil.

In both cases, relationship depends on the group of oil. On that respect the study investigated the effect of molecular structure of lubricating oil on sound velocity. The study found that sound velocity in lubricating oil is related with their molecular structure and it can be estimated from the properties related to the molecular structure. This study also investigated the effect of sound velocity to the tribological applications. Boundary lubrication is important for tribological applications. Frictional and wear behavior were examined in this research and compared with adiabatic bulk modulus. Low adiabatic bulk modulus indicated the higher wear scar on materials and low adiabatic bulk modulus also indicated lower friction. The adiabatic bulk modulus was also compared with the key property viscosity of lubricating oil. From the comparison, it can be find out the high bulk modulus fluid having low viscosity, which is suitable as hydraulic fluid. In case of wind turbine gear oil, it also can predict the low temperature fluidity from the measured sound velocity in it. Finally, vegetable oils as environment friendly lubricant was also considered on the test and a prediction equation of pressure viscosity coefficient has proposed for unsaturated fatty acid based vegetable oils.

# Certificate of
# Approval

---

Department of Engineering Systems and Technology
Graduate School of Science and Engineering
Saga University
1, Honjo-machi, Saga 840-8502, Japan

---

This is to certify that the Dissertation submitted by

**SOBAHAN MIA**

titled “Prediction of Tribological and Rheological Properties of Lubricating Oils by Sound Velocity” has been approved by the Dissertation Committee for the partial fulfillment of the requirements for degree of the *Doctor of Philosophy* in the department of Engineering Systems and Technology at September, 2010.

Dissertation Committee:

Chairman
Dr. Nobuyoshi OHNO
Professor, Department of Mechanical Engineering
Saga University, Japan.

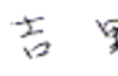

Member
Dr. Hidehiro YOSHINO
Professor, Department of Mechanical Engineering
Saga University, Japan.

Member
Dr. Seiya HAGIHARA
Professor, Department of Mechanical Engineering
Saga University, Japan.

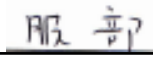

Member
Dr. Nobusuke HATTORI
Professor, Department of Mechanical Engineering
Saga University, Japan.

# Acknowledgements

This work has been carried out under the tribology laboratory (Ohno's Lab) at the department of Mechanical Engineering in Saga University, Saga, Japan.

First, thanks to Almighty Allah for successfully fulfillment of the dissertation. Next, I would like to express my profound gratitude to my supervisor Professor Nobuyoshi OHNO, who has guided and supported me during the research period. I am grateful to him for being a great advisor, an excellent motivator, an intellectual magnet, and most important, never a conservative. I am greatly indebted to him for his valuable guidance, suggestions and encouragement throughout all phases of my research work. I am grateful to his inspiration and support, for shearing many of his insights and for his constant effort to make me a better researcher. I will always be in awe of his creativity, analysis, and comprehension. He tried his best to improve the standard of this thesis. All errors and limitations remaining in this thesis are mine alone.

I would like to express my gratitude to the dissertation committee members, Prof. Hidehiro YOSHINO, Prof. Seiya HAGIHARA and Prof. Nobusuke HATTORI for their fruitful suggestion to improve the thesis. Also expressing my gratitude to Dr. Shigeki Morita for his various advices and help in different stages in laboratory works with providing necessary accessories to the laboratory.

I would like to thank 'Khulna University of Engineering and Technology (KUET)' of Bangladesh for providing support and inspiration and also giving study leave for this study. I would like to acknowledge the Japanese Government (Monbukagakusho) for furnished me with the scholarship which enabled me to study in Japan for these years.

I also addressed my thanks to all the students in my laboratory, also who already graduated within these years, for their help in laboratory works and their support in Japanese environment.

Finally, I would like to acknowledge to my wife Fahima Nasrin Mouri, in grateful thanks for her patience, support, enjoyable home life and continued enthusiasm about my research over last one and half year. Thanks to Dr. Md. Ariful Islam, Dr. Md. Ziaur Rahman and Dr. Md. Tawhidul Islam Khan for their valuable suggestions, and All Bangladeshis in Saga for making my Japan life more comfortable and enjoyable. Also, expressing deepest gratitude to my loving sisters, brothers and their family members, parents-in-law, relatives, friends and colleagues for their continuous support, inspiration and love over these years.

# Contents

# List of Figures

# List of Tables

# Nomenclature

| Symbol | Name |
|---|---|
| A | constant in Doolittle equation |
| *A* | Wear scar area in $mm^2$ |
| B | constant in Doolittle equation |
| C | constant in Johnston equation |
| *C, a, b* | constants in estimated equation of sound velocity |
| $d_e$ | maximum diameter of the drop |
| $d_s$ | level diameter of the drop from $d_e$ |
| dV | decrease in volume |
| $E_v$ | activation energy |
| *f* | fractional free volume |
| g | acceleration of the gravity |
| H | compensation function (for surface tension measurement) |
| *K* | adiabatic bulk modulus |
| $K_T$ | tangent bulk modulus |
| $m_0$ | viscosity temperature property |
| $M_w$ | molecular weight |
| OCP | olefin copolymer |
| *p* | pressure |
| PAO | polyalphaolefin |
| PFPE | perfluoropolyether |
| *R* | Universal gas constant |
| *T* | temperature |
| $T_{VE}$ | Viscoelastic solid transition temperature |
| $T_{VE0}$ | Viscoelastic solid transition temperature at atmospheric pressure |
| *U* | sound velocity |
| $U_{est}$ | estimated sound velocity |
| $U_{exp}$ | experimental sound velocity |
| V | original volume |
| $\alpha$ | pressure-viscosity coefficient |
| $\alpha_{cal}$ | calculated pressure-viscosity coefficient |

| Symbol | Name |
|---|---|
| $\alpha_{exp}$ | experimental pressure-viscosity coefficient |
| $\alpha_T$ | coefficient of thermal expansion |
| $\beta$ | coefficient of compressibility |
| $\gamma$ | surface tension |
| $\eta$ | absolute viscosity |
| $\eta_0$ | absolute viscosity at atmospheric pressure |
| $\kappa$ | the ratio of specific heat at constant pressure and constant volume |
| $\mu$ | coefficient of friction |
| $\nu$ | kinematic viscosity |
| $\nu_0$ | kinematic viscosity at atmospheric pressure |
| $\rho$ | density |
| $\rho^*$ | closest packed solid density |
| $\rho_G$ | density at the gas phase |
| $\rho_L$ | density at the liquid phase |
| $\tau A$ | propagation time into the sample |
| $\tau E$ | propagation time into the circuit |

# Chapter 1

# Introduction

## 1.1 Introduction

Tribology is the “ology” or science of “tribein”. The word comes from the same greek root as “tribulation”. A faithful translation defines tribology as the study of rubbing or sliding. The modern and broadest meaning is the study of friction, lubrication and wear [1]. According to the modern dictionary and handbook, “The branch of science and technology concerned with interacting surfaces in relative motion and with associated matters as friction, wear, lubrication and the design of bearings is Tribology”. Tribology is the art of applying operational analysis to problems of great economic significance, namely, reliability, maintenance and wear of technical equipment, ranging from spacecraft to household appliances. The understanding of the underlying mechanism requires a combination of knowledge from the fields as varied as physics, chemistry, materials science, mechanical engineering and mathematics and makes tribology all the more interesting [2]. Tribology is crucial to modern machinery, which uses in sliding and rolling surfaces. Examples of productive friction are brakes, clutches, driving wheels on trains and automobiles, bolts and nuts. Examples of productive wear are writing with pencil, machining, polishing and shaving. Examples of unproductive friction and wear are internal combustion and aircraft engines, gears, cams, bearings and seals. Ignorance of tribology of machines and moving parts, results the huge losses in industrial sectors. The importance of friction and wear control cannot be overemphasized for economic reasons and long-term reliability. Any country can save money by better tribological practices. The savings are both substantial and significant, and these savings can be obtained without the development of large capital investment. The purpose of research in tribology is understandable the minimization and elimination of loses resulting from friction and wear at all levels of technology where the rubbing of surface is involved. Research in tribology leads to greater plant efficiency, better performance, fewer breakdowns, and significant savings. It is important that all designers of mechanical systems use appropriate means to reduce friction and wear, through proper selection of bearings and the selection of appropriate lubricants and materials for all interacting surfaces [3]. Another important key word of this study is

rheology. Rheology is the study of the flow of matter: mainly liquids but also soft solids or solids under conditions in which they flow rather than deform elastically [4].

It would be difficult to imagine any type of machinery without lubrication. The role of lubrication is an important part in the field of tribology. Lubrication is simply the use of material to improve the smoothness of movement of one surface over another, and the material, which is used in this way called a lubricant [5]. Lubricants are commonly used for lubrication to reduce the friction and wear of interacting surfaces and provides smooth running and a satisfactory life for machine elements. Most lubricants are liquids (such as mineral oils, synthetic oil, silicon fluids, water, etc.), but they may be solids (such as polytetrafluoroethylene, or PTFE) for use in dry bearings, greases for use in rolling element bearings or gases (such as air) for use in gas bearings. The physical and chemical interactions between the lubricant and the lubricating surfaces must be understood in order to provide the machine elements with satisfactory life. Selection of lubricant is very important. To select an appropriate lubricant, it is necessary to know the properties of lubricant, lubrication system of applied machinery, conditions of machinery, cost of lubricant etc. Common properties of lubricating oil are: viscosity, viscosity index, density, compressibility, surface tension, cloud point, pour point or low temperature property, flash point, friction coefficient, etc. The most important property is its viscosity. Viscosity is a function of temperature and pressure. Relationship between the viscosity with temperature and relationship between viscosity with pressure is also important in lubricant rheology as well as for the life of machine elements. Just as temperature rise reduces the viscosity of lubricating oil, again, an increase in pressure produces a rise in its viscosity. Barus expressed a relation between viscosity and pressure introducing a constant $\alpha$ named pressure-viscosity coefficient [6]. In recent years, pressure viscosity relationship is an important parameter of lubricating oil to understand its performance, especially in high-pressure applications. So it is very much significant to know the pressure-viscosity coefficient of lubricating oil.

Low temperature fluidity is another important property in lubricant rheology. The pour point is an indicating parameter of low temperature fluidity, which is defined in ASTM–D-97-39 as the lowest temperature at which the oil will pour or flow when it is chilled without disturbance under definite prescribed conditions. Bondi [7] reports that a large number of oils show glassy solidification due to higher

viscosity at the pour point. Viscoelastic solid transition temperature $T_{VE}$ also represents the low temperature fluidity of lubricating oil. The physical and practical significance of viscoelastic solid transition temperature is much better than the pour point.

Sound velocity in the lubricating oil can be measured as like the other lubricant properties. Sound is a molecular disturbance and the disturbance is caused by vibration. It depends on the nature of the medium through which it travels and also the gap between the molecules. Sound velocity depends on the molecular structure of any substance. Sound velocity in the liquid is lower than that of solid. So, it directly related to the bulk modulus or modulus of elasticity of the substances. Adiabatic bulk modulus, which is an important parameter of lubricating oil, can calculate from the measured sound velocity. The bulk modulus of a substance measures the substance's resistance to uniform compression. It is defined as the pressure increase needed to cause a given relative decrease in volume.

Pressure-viscosity coefficient, Viscoelastic solid transition temperature and other properties of lubricating oils are measured experimentally. There are many correlations to predict the lubricant properties also. Pressure-viscosity coefficient $\alpha$ can be directly determined by measuring the viscosity at various pressures. Many correlations exist to predict $\alpha$, but most of them suffer from disadvantages of containing complex equation forms, requiring data difficult to access and providing low accuracy. In this research, author proposed a simple correlation to predict pressure-viscosity coefficient $\alpha$. The relation emphasized on adiabatic bulk modulus $K$, which was calculated from the sound velocity in the lubricating oil. $K$ is related to the intermolecular force and high-pressure physical properties, which depends on free volume. If sound velocity can measure in high accuracy then accurate bulk modulus can be easily calculated. Then anyone can easily predict the pressure-viscosity coefficient of lubricating oil. Again, viscoelastic solid transition temperature at atmospheric pressure $T_{VE0}$ can be measured experimentally from the occurrence of photo elastic effect by lowering the temperature using liquid nitrogen. The measurement is quite difficult and requires low temperature apparatus for handling the liquid nitrogen. Since $T_{VE0}$ is related with the free volume of the substances, it has

a relation with the sound velocity of the substances. Upon this basis, a relation has found between the sound velocity and the low temperature fluidity.

Testing lubricating oils were considered on group basis, such as traction oil, polyalphaolefin (PAO) oil, paraffinic mineral oil, perfluoropolyether (PFPE) oil, Ester oil, Vegetable oil and Glycerol. PAO and paraffinic mineral oil can also named as Hydrocarbon oil. Molecular structure of these groups is different compare to each other. Measured sound velocity also shown different value as the group basis. At this instant, author found the effect of sound velocity on the molecular structure of lubricating oils. To clarify this effect, density and surface tension of testing oils were measured by conventional method. Some times measurement of sound velocity in lubricating oil became difficult. Considering this difficulty, author found a relation to estimate sound velocity. Since, sound velocity is related with the molecular structure and the lubricant property: surface tension and density are also related with molecular behavior of the lubricant, it can estimate the sound velocity of lubricating oil from the surface tension and its density. Here author proposed an estimation formula for sound velocity from the surface tension and its density.

Frictional property and wear behavior of lubricating oil is important in the applied tribology. Adiabatic bulk modulus of the lubricating oil is also compared with the friction coefficient of the lubricating oil and with the wear scar in steel ball using the oil. Adiabatic bulk modulus is also compared with the viscosity of lubricating oils. From the relations, lubricating oils can be distinguished for the appropriate application.

## 1.2 Literature Review

Sound is a travelling wave which is an oscillation of pressure transmitted through a solid, liquid, or gas, composed of frequencies within the range of hearing and of a level sufficiently strong to be heard, or the sensation stimulated in organs of hearing by such vibrations [8]. Sound velocity is the rate of travel of a sound wave through an elastic medeum. Sound travels faster in solid than in liquid, and faster in liquid than it does in gases. Sound velocity depends of the medium's compressibility and density. Calculating adiabatic compressibility or adiabatic bulk modulus from sound velocity measurement is a well-established practice [9-11]. Molecular compressibility was determined from Wood equation [12]. The compressibility and

density are combined using the Urick equation [11], which is based on an idea suggested by Wood [12].

The measurement of sound velocity in fluid systems is the subject of numerous research studies. There are many studies concerned with single-phase fluids and the fluid systems composed of two or more different fluid phases, such as liquid and gas. Nichita et al. [13] proposed a method to calculate the isentropic compressibility and the sound velocity in both single-phase and two-phase states for various mixtures. The thermodynamic limits for compressibility and sound velocity were the subject of their study, correspond to a regime of slowly varying pressures and/or small gas domains in the liquid: the liquid and gas phases were considered to be in thermodynamic equilibrium at any instant. Okazaki [14] presented a universal method for describing the speed of sound from the perspective of physicochemical reaction kinetics. He shown that the speed of sound changes with temperature according to a thermodynamically derived formula and that the motion and propagation phenomena of sound energy can also be regarded as chemical reaction. Povey et al. [15] studied on the relationship between the sound velocity and chain length. They used Cygnus UVM1 ultrasound velocity meter to measured sound velocity. They derived a model from the detailed analysis of the mechanisms involved. That model can give very precise estimations of the composition of pure liquid. They envisage that the ultrasound velocity method, with the mentioned units ease of use and in-line capability, can provide a powerful new method of characterizing polymetric fluids, as well as contributing to understanding of fluid compressibility and of the propagation of sound in terms of specific intermolecular and intramolecular physicochemical behavior. The weaker molecular forces involved are difficult to probe by other methods but they hope that their method will offer new perspectives on the molecular basis of the liquid state, leading to practical applications where identification and/or purity are issues.

There are many literatures on the lubricant properties. The pressure-viscosity characteristics of liquids are important in understanding the behavior of lubrication and hydraulic system. Bell and Kannel [16] and Cheng [17] studied on the elastohydrodynamic theory and suggested that the lubricant film thickness under a bearing is governed largely by the pressure-viscosity effect in the low-pressure region. As long ago as 1893, Barus [6] established an empirical equation to describe the

isothermal pressure-viscosity relationship for a given liquid. Based on the concept that the mobility of the molecules in a liquid is governed by their free volume, different models were later derived to describe molecular transport phenomena, such as viscous flow and diffusion. The basic concept underlying free volume theories implies that each molecule in a liquid is confined to a cage bounded by its immediate neighbors. Therefore, knowledge of pressure-viscosity relationship of lubricants is important for the design and construction of the lubrication elements, such as rolling bearings, valve cams and gear. Pressure-viscosity coefficient $\alpha$ is the parameter of pressure-viscosity relationship.

Many correlations [18-20] were proposed to predict pressure-viscosity coefficient $\alpha$, but most of them suffer from the disadvantages of containing complex equation forms, requiring data difficult to access and providing low accuracy. Most of all, as pointed out by Johnston [21], these correlations are entirely empirical and not related to the fundamental liquid theories. At the same time, Johnson has derived an equation to relate $\alpha$ to the bulk properties of liquids based on Eyring's thermal activation energy model for viscous flow. However, his result gives a low level of precision when it was compared to the experimental data of some oil samples. So and Klaus proposed a viscosity-pressure correlation of liquids [22]. The parameters used for this correlation were the atmospheric viscosity and density at the temperature of interest and the constant which indicates the atmospheric viscosity-temperature property $m_0$. This equation has a rather complex form, but it only requires physical properties which are very easy to measure. In 1989, Wu et al. [23] developed a method for the prediction of pressure-viscosity coefficients of lubricating oils based on free volume theory. The accuracy of this method was only compared to So's method. The failure of this method to predict the pressure behavior of some synthetic hydrocarbons and non-hydrocarbons appears to be related to the unusual high, or low bulk moduli of these fluids. Bair and Kottke [24] concluded their research as numerical simulations of elastohydrodynamic lubrication have generally failed to accurately describe pressure-viscosity response and a complete pressure viscosity curve can be accurately represented piecewise by well-known empirical equations. They also mentioned that free volume theory could be used to arrive at accurate expressions although these may be complicated. Leeuwen [25] describes a method to

deduct pressure-viscosity coefficient through an accurate film thickness measurements. In this research, he compared eleven film thickness approximation formulas related in the film thickness of a test fluid. Among those, the Roelands [26] pressure-viscosity equation is most popular in EHL work. Bair discussed about the missing of Roelands equation in one of his research [27]. He also described clearly the effect of pressure, viscosity and temperature of lubricant in his several researches [28-30]. In the EHL, film thickness also can be measured using the pressure-viscosity coefficient of lubricating oil. From the above studies, there is no doubt that pressure-viscosity coefficient is an important parameter of lubricating oil.

Low temperature behavior of lubricant is another important parameter. Yukhno et al. [31] investigated the frictional and wear behavior at low temperature. They found that the coefficient of friction is somewhat higher at low than at room temperature. The effect of temperature decrease on the wear life of solid lubricant coatings is ambiguous. Matveevsky [32] showed the influence of low temperature on the lubricating capacity of mineral oils using 4-ball wear test. Recently, Sharma and Stipanovic [33] reported a process for predicting low temperature rheology using nuclear magnetic resonance spectroscopy and mass spectrometry. They found the effect of hydrocarbon base oil composition on the low temperature rheology of lubricants. Ohno [34] reported that the $T_{VE0}$ is related with free volume and free volume also related with tangential bulk modulus ($K_T$). There is a well-known relation between tangent bulk modulus $K_T$ and adiabatic bulk modulus $K$, which can be expressed as $K = \gamma K_T$, where $\gamma$ is the ratio of specific heat at constant pressure and constant volume [7].

Also there are many publications related to the lubricant properties. In 2001, Kagathara and Parsania [35] found that density, absolute viscosity and sound velocity decreased with rise in temperature and increased with concentration, except chloroform. The decrease in sound velocity with temperature indicated weakening on intermolecular forces due to thermal agitation. The decrease of viscosity and density with increase in temperature are due to increase the kinetic energy and volume expansion of the solution, respectively. The increase in volume causes increase in intermolecular free length. So, sound velocity is related to the molecular structure. Hsu [36] explained the molecular basis of boundary lubrication in terms of tribophysic of the tribochemical films formed under rubbing conditions. Molecular

structures influence the individual additive functions as well as the overall balance of the mixture.

## 1.3 Objectives of the Research

It is important to know the behavior of lubricant rheology in the field of tribology. Pressure-viscosity coefficient and low temperature fluidity of lubricating oil is important parameters in lubricant rheology. These properties are also important in applied tribology. Sound velocity is also an important property of a substance to know the elastic behavior as well as molecular structure of the substance. The main objectives of this research is given as follows:

i. To measure the sound velocity in lubricating oils and makes the relation with other important properties of lubricating oils.
ii. To introduce the sound velocity as a predicting parameter for tribological properties and lubricant rheology.
iii. To find out a relation for the prediction of pressure-viscosity coefficient of lubricating oil based on sound velocity measurement.
iv. To find out a relation between the low temperature fluidity and Sound velocity of lubricating oils.
v. To find out the effect of sound velocity on the molecular structure of the lubricating oils and estimate sound velocity from the properties related to molecular structure of lubricating oil.
vi. To find out the effect of sound velocity in the lubrication oil to the tribological applications and the boundary lubrication.
vii. To apply the sound velocity in environment-friendly vegetable oils and find out the relationship with the tribological properties for these environment-friendly lubricant.

## 1.4 Outline of the Research

This thesis paper has written in several sections mentioning as chapter. Current chapter (chapter 1) is the first section provides an overall introduction to the thesis. Objectives of the thesis and literature cited are mention in this chapter. Though the

main objective of the thesis is to measure the sound velocity and to introduce the sound velocity as a predicting parameter for tribological properties and lubricant rheology. Prediction of pressure-viscosity coefficient, relation between low temperature fluidity and the application of sound velocity is the key term of this thesis. In addition, molecular effect of lubricating oil is also discussed in separate chapter. Each chapter required to fulfilling the objectives of the thesis.

Chapter 2 describes about the sound velocity measurement. Details description of the Sing around apparatus, which is the major experimental apparatus of this thesis work, is mentioned in this chapter. The list of tested lubricating oils and their physical properties are given in chapter 3. Other experimental apparatus and experimental procedure for the properties measurement of lubricating oil is described in this chapter.

The main thesis work and outcomes started from the chapter 4. Sound velocity is an important parameter to know the performance of the lubricating oil. Importance of pressure-viscosity coefficient in the field of tribology for lubricating oil is given in the chapter 4. Then I have tried to find out the relation between pressure-viscosity coefficient and sound velocity of lubricating oil. The prediction methodology also mentioned in this chapter and finally prediction correlations of pressure viscosity coefficient have found for the lubricating oils according to the group basis. Again, low temperature fluidity is an important parameter in lubricant rheology. Chapter 5 describes the importance of low temperature fluidity and mentioned that viscoelastic solid transition temperature represents the low temperature fluidity of lubricating oil. Correlation of the viscoelastic solid transition temperature at atmospheric pressure and the adiabatic bulk modulus for the lubricating oil is given in this chapter. This chapter also mentioned that, the prediction of low temperature fluidity of blend oil can possible from the base oil viscoelastic solid transition temperature and the adiabatic bulk modulus. Since the prediction correlations of pressure-viscosity coefficient, and the relation between viscoelastic solid transition temperature and adiabatic bulk modulus depend on the group of lubricating oil, Chapter 6 describes the effect of sound velocity on the molecular structure of lubricating oils. In this chapter I have explained the properties with are related to the molecular structure and graphically present the relationship with sound velocity. From these relationship we can roughly identified the group of lubricating oils. Studied groups of lubricating oils are traction

oil, polyalphaolefin oil, paraffinic mineral oil, perfluoropolyether oil and glycerol. To overcome the difficulty of sound velocity measurement, an estimation equation is proposed in this chapter considering the molecular structure of lubricating oils.

Effect of sound velocity to the tribological application is given in chapter 7. Boundary lubrication is most important in the tribological applications. This chapter describes the relation between the sound velocity and the frictional and wear properties of lubricating oil. Also mentioned the relation with viscosity of lubricating oil. From the relation, it has been found that the high adiabatic bulk modulus fluid having low viscosity is suitable for hydraulic systems. The prediction of low temperature fluidity of wind turbine gear oil can be possible from the sound velocity in the gear oil, also illustrated in this chapter. There has been growing concern for the use of mineral oils as lubricants because of the worldwide interest in environmental issues. Vegetable oils are environment friendly lubricant with some excellent properties as high viscosity index, high lubricity, high bio-degradability etc. The sound velocity in the vegetable oils is measured in this thesis, which is given in chapter 8. A prediction correlation also proposed for the vegetable oils as like traction, polyalphaolefin and paraffinic mineral oils.

Finally, the summery of the thesis work and recommendation for future research are given in chapter 9.

# Chapter 2

# Measurement of Sound Velocity in Lubricating Oils

## 2.1 Introduction

Sound is nothing more than a local disturbance whose propagation is facilitated by the collisions between particles; this disturbance propagates in a longitudinal wave; imagine one molecule hitting the next molecule, and then that molecule hitting the next, and so forth. The rate of travel of sound wave is known as sound velocity. The square of the sound velocity is proportional to the ratio of an elastic modulus to the mass density of the material. The sound velocity is usually larger in solids than in liquids and usually larger in liquids than in gases is because of the elastics constants of the material. In case of liquids, the elastic constant is known as adiabatic bulk modulus.

Sound velocity through a substance can be measured using various techniques. Passing the ultrasonic wave in the sample is mostly used technique to measure sound velocity. Many apparatus are available to measure sound velocity. In this study, author used Sing around UVM-2 apparatus to measure the sound velocity in lubricating oil.

## 2.2 Details of the Apparatus

Sound velocity in the lubricating oils was measured by Sing around UVM-2 apparatus. The apparatus is made by Cho-Onpa Kogyo Company, Japan. Specification of the device and the function of the parts of the device are given in appendix A. UVM-2 apparatus is shown in Fig. 2.1. The apparatus also consists of an oil container with 2 ultrasonic transducers, temperature control bath, a 9821 series PC with Sing around cycle control software. The Sing around device combines with the ultrasonic transducer and measures the supersonic wave spread time of a solid or liquid sample. The basic principle of this device is the ultrasonic wave pulse launched from the transmission oscillator propagates in the sample and is received to the reception oscillator. It is converted into mono pulse after auto gain control amplified, the delay circuit passes and the trigger does the transmission circuit to the received supersonic wave pulse again. Sing around device displayed total propagation time of the cycle including delay time. It also displayed only delay time of the circuit. The propagation time of the sample inside can be measure from the difference of the

above mentioned times of the cycle when propagation will be steady. Sound velocity was calculated from the propagation time and sample length.


Fig 2.1 Sing around UVM-2 apparatus

Fig. 2.2 Sing around sound velocity measuring oil container with transducers

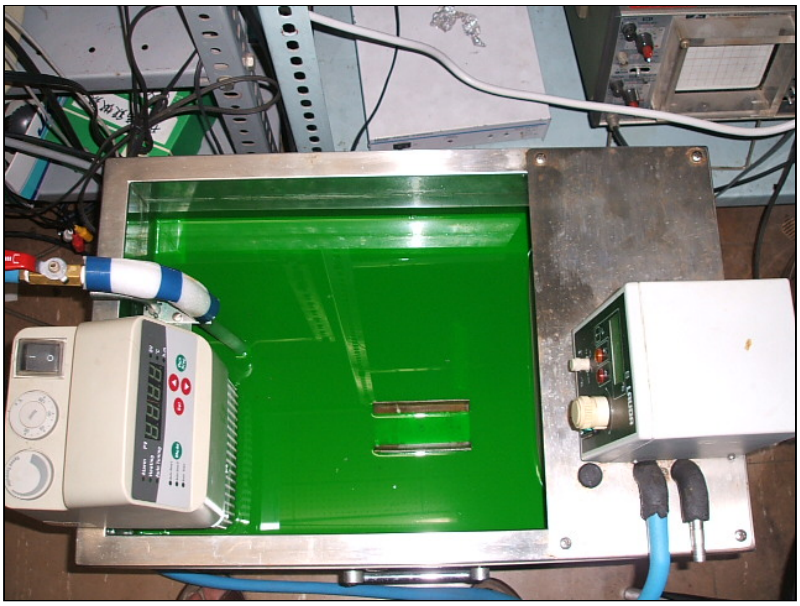

Fig.2.3 Sample oil temperature control bath

The propagation time of the sample inside can be requested by measuring the cycle of the faction that keeps oscillating repeating the loop (Sing around cycle).

Sing around cycle,

$$T = \tau A + \tau E$$

where, $\tau A$ : The propagation time of the sample inside

and $\tau E$ : The propagation time of the circuit

Then,

$$U = \frac{L_1 - L_2}{\tau A} = \frac{L_1 - L_2}{T_1 - T_2 - (\tau E_1 - \tau E_2)} = \frac{L_1 - L_2}{T_1 - T_2}$$

where, $U$ : Sound velocity of the sample and $\tau E_1 = \tau E_2$

and $L_1$, $L_2$ : Length of the sample

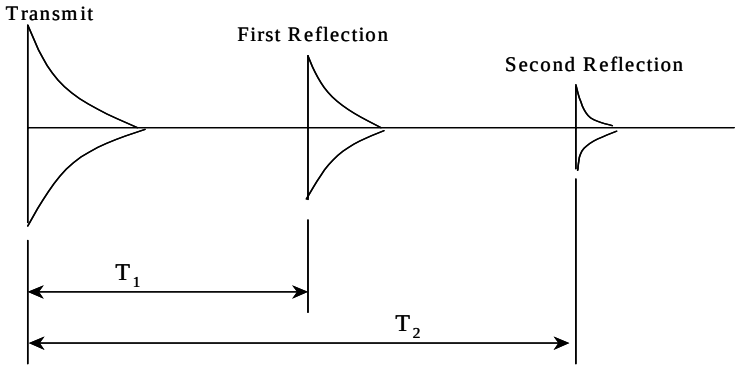


Fig.2.4 Sound wave propagation

The photographic of Sing around apparatus is shown in Fig. 2.1, and the line diagram of the apparatus is given in Fig. 2.5. Here also given the sound propagation through the sample oil in Fig. 2.4, indicating the propagation time. Sample lubricating oil was taken in the container of 60.8 mm length shown in Fig. 2.2. There was another oil container of 50 mm in length. Length of the container also indicates the distance between the transducers (i.e. $L_1$-$L_2$) and $T_1 - T_2$ is the propagation time of the sample inside during Sing around cycle. Temperature of sample oil was controlled using a temperature control bath, inserting the oil container into the liquid of the bath. Temperature control bath is shown in Fig 2.3. Heater for increasing the temperature and cooler for decreasing the temperature has attached with the temperature control bath. Sound wave propagation in the tested sample is shown in the display of the UVM-2 apparatus. Data was taken when wave propagated smoothly. That was observed by Sing around cycle software in 9821 series PC. Then sound velocity of the sample lubricating oil was calculated.

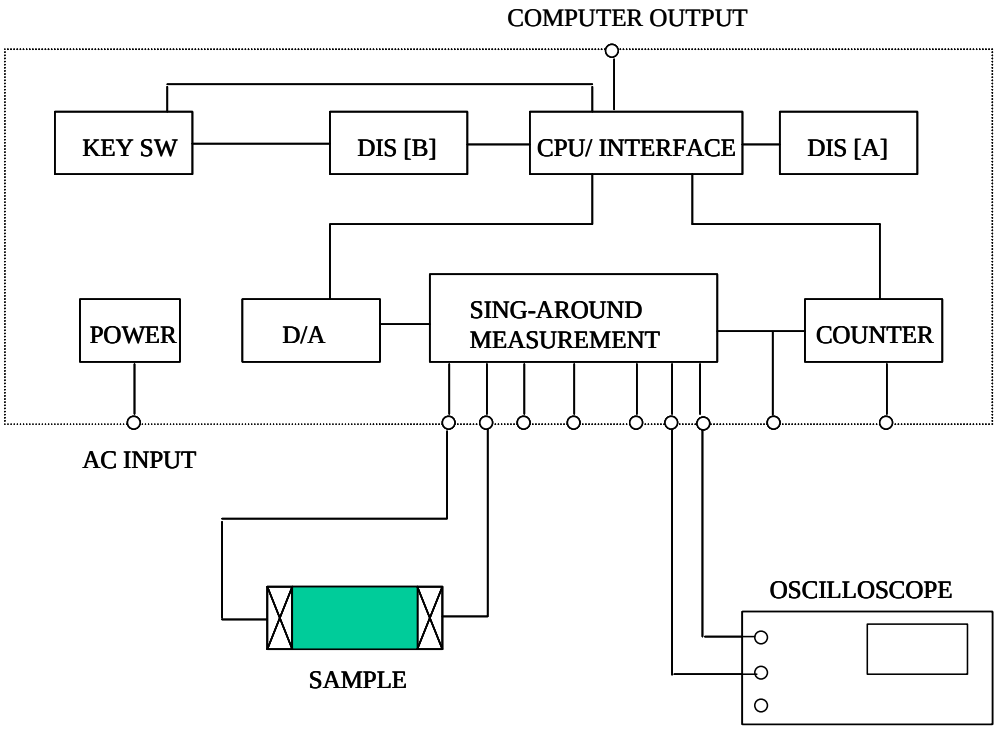


Fig.2.5 Configuration of the Sing around apparatus

## 2.3 Configuration of the Apparatus

1) Sing around measurement part

The Sing around measurement part is the mail part of the container, and it consists of the transmission, the reception amplifier, the delay circuit, and the windows circuit.

2) Counter

The counter measures the cycle of the Sing around by using TCXO of 10 MHz.

3) Display part [A]

The time measurement such as the Sing around cycles and windows is displayed.

4) D/A

A digital signal is converted into the analog signals of the transmission voltage, the transmission pulse, the trigger level, and the AGC voltage, etc.

5) Display part [B]

The display is related to D/A, and it uses as a monitor.

6) Key switch

Various settings are done by this key operation.

7) CPU/ Interface

Various interrupt such as keys and RS232C, the time controls, and data are managed by the microprocessor.

8) Power

The input is AC100V power supply. The DC voltage to which ±5V, ±12V, ±300V, and ±12V (floating) stabilize is supplied to each part.

## 2.4 Measuring Procedure

Sound velocity in the lubricating oil was calculated using Sing around technique. Measuring procedure is described as follows:

1. First clean the oil container using acetone or hexane, then again clean using petroleum ether or ethanol. During the cleaning the container should shack several time to clean the container properly. And then dry the container using the hot air.
2. Tested sample oil inserts in the oil container. About 15 ml of oil is necessary to

full the container, and then lock the container by cap.

3. There are two ultrasonic transducer sensors in the two sides of the container. So at this stage, it should connect to the main UVM-2 device using the connecting cable. After that, the container puts in the temperature control bath.
4. Switch on the UVM-2 Sing around apparatus and temperature control bath. Sets the test temperature.
5. Power on the systems PC 98 series computer. Open the Sing around software and set the criteria for the software as mentioned in appendix A, and run the software.
6. Wait 10 to 15 minute after the temperature reach the tested temperature. Set the signal pulse from Sing around apparatus if necessary, Details are given in appendix A. Check the Sing around cycle from the display of the apparatus and also from the software in the computer. Software averages the data of each 5 cycle and expressed by green circle. Observes the steadiness of the propagation by the green circle in the computer. If the green circles stay in parallel to a given line in the computer software, then the propagation become steady.
7. Data can taken, when the propagation become steady. There are two data in the display of the apparatus. Propagation time with delay, and another is system delay only. Both times is shown in micro second. From the difference between these two times, the wave propagation time inside the sample oil can be found.
8. Sound velocity in the lubricating oil can calculate from the distance of two sensors, i.e. length of sample and the wave propagation time inside the sample. If we use distance in meter and time in second then the sound velocity will be express in meter per second (m/s).

# Chapter 3

# Properties of Lubricating Oil and Their Measurement

## 3.1 Introduction

Experimental details for the measurement of lubricant properties of the study are explained in this chapter. List of the tested lubricating oils is also mentioned here. The explanation of lubricating oils is given here. The physical properties are listed as the group basis of lubricating oil. Experimental apparatus rolls an important part for accuracy and good result of any research. So, it is necessary to know details of the experimental apparatuses. The experimental setup and working principle is described in this chapter. Sound velocity is also an important property of lubricating oil since it is related to the bulk property of lubricating oil. Sound velocity can measured accurately using Sing around apparatus, which is described in previous chapter. Early mentioned that pressure viscosity relation is the important parameter to know the performance of lubricating oil. Viscosity at different pressure was measured using falling ball viscometer. From that data pressure-viscosity coefficient can be measured at any temperature.

Another important property considered in this research is surface tension of lubricating oil. Liquids are often characterized by the tendency of their boundaries to contract to the smallest possible area, as is explained by the spherical form of liquid droplets. Since this contraction occurs spontaneously, a free energy change must be associated with it, or conversely work must be done by the liquid to extend the surface. This distribution of lubricant in a bearing can be affected by wet ability [37], surface tension [38] and at high speed by oil-air surface tension force [39]. Moreover, surface wet ability, surface tension and contact angle of different materials or lubricating oils effects on friction and wear [40-41].

## 3.2 Lubricating Oils

The term lubricating oils is generally used to include all those classes of lubricating materials that are applied as fluids [42]. Lubricants are functional materials in the mechanical system [43]. A lubricating oil or lubricant is any substance used to separate two surfaces in relative motion which can be readily sheared while adhering the surfaces. Mainly lubricating oils are characterized by their

viscosity, but other properties are also important. There are many kinds of lubricating oil. The most used lubricants are mineral or synthetic lubricants. Perfluoropolyether (PFPE) fluids are another type of lubricating oil used on magnetic recording media, aerospace industry and satellite instrument satisfactorily [44-45]. Recently these oils have been used as hydraulic fluids, high temperature liquid lubricants in turbine engine [46] and the base oils of high-temperature greases.

In this study, lubricating oils were considered as group basis. The groups were traction oil, polyalphaolefin oil, paraffinic mineral oil, perfluoropolyether oil, glycerol ester oils and vegetable oil. The tested lubricating oils and their physical properties are listed in the following tables:

Table 3.1 Physical properties of traction oils

| Oil name | Density ρ, g/cm$^3$ | Kinematic Viscosity ν, mm$^2$/s | |
|---|---|---|---|
| | at 15 °C | at 40 °C | at 100 °C |
| SN32 | 0.9140 | 30.95 | 4.44 |
| SN100 | 0.9289 | 99.50 | 7.94 |
| CVTF | 0.9579 | 32.06 | 5.56 |
| BBPH | 0.9280 | 40.57 | 4.78 |
| SNHV | 0.9895 | 311.00 | 12.10 |

Table 3.2 Physical properties of polyalphaolefin (PAO) oils

| Oil name | Density ρ, g/cm$^3$ | Kinematic Viscosity ν, mm$^2$/s | |
|---|---|---|---|
| | at 15 °C | at 40 °C | at 100 °C |
| PAO32 | 0.8270 | 30.50 | 5.90 |
| PAO68 | 0.8305 | 71.84 | 11.41 |

Table 3.3 Physical properties of mineral oils

| Oil name | Density ρ, g/cm$^3$ | Kinematic Viscosity ν, mm$^2$/s | |
|---|---|---|---|
| | at 15 °C | at 40 °C | at 100 °C |
| P60N | 0.8552 | 8.02 | 2.38 |
| P150N | 0.8620 | 29.93 | 5.28 |
| P500N | 0.8716 | 89.79 | 10.99 |
| PBSN | 0.8772 | 379.3 | 29.10 |
| N1200 | 0.9046 | 228.20 | 29.10 |

Table 3.4 Physical properties of perfluoropolyether (PFPE) oils

| Oil name | Density ρ, g/cm$^3$ | Kinematic Viscosity ν, mm$^2$/s | |
|---|---|---|---|
| | at 15 °C | at 40 °C | at 100 °C |
| Fombline | 1.8470 | 141.70 | 41.89 |
| Demnum | 1.8860 | 194.56 | 34.72 |
| Krytox | 1.9100 | 168.16 | 18.24 |

Table 3.5 Physical properties of glycerol

| Oil name | Density ρ, g/cm$^3$ | Kinematic Viscosity ν, mm$^2$/s | |
|---|---|---|---|
| | at 15 °C | at 40 °C | at 100 °C |
| Glycerol | 1.2631 | 209.30 | 12.00 |

Table 3.6 Physical properties of Ester oils

| Oil name | Density ρ, g/cm$^3$ | Kinematic Viscosity ν, mm$^2$/s | |
|---|---|---|---|
| | at 15 °C | at 40 °C | at 100 °C |
| Ester A | 1.0653 | 31.44 | 4.69 |
| Ester B | 1.2268 | 25.56 | 3.61 |
| Ester C | 1.1657 | 17.85 | 3.16 |
| Ester D | 1.1523 | 18.23 | 3.67 |
| Ester + PMA | 1.0610 | 44.47 | 6.88 |
| Phosphate Ester | 1.1766 | 21.86 | 3.73 |
| DOS | 0.9170 | 11.56 | 3.24 |

Table 3.7 Physical properties of vegetable oils

| Oil name | Density ρ, g/cm$^3$ | Kinematic Viscosity ν, mm$^2$/s | |
|---|---|---|---|
| | at 15 °C | at 40 °C | at 100 °C |
| Castor oil | 0.9666 | 241.0 | 17.5 |
| Olive oil | 0.9137 | 39.62 | 8.24 |
| Rapeseed oil | 0.9456 | 39.10 | 8.30 |
| Coconut oil | 0.9260 | 27.55 | 5.89 |
| Mustard oil | 0.9180 | 44.11 | 9.41 |
| Camellia oil | 0.9168 | 39.32 | 8.28 |

## 3.3 Experimental Apparatus For the Properties Measurement of Lubricating Oils

### *3.3.1 High Pressure Falling Ball Viscometer*

Viscosity of the test oils at high pressure was measured by the falling body (ball) viscometer. It is simple and inexpensive measuring systems that can be used to determine the steady shear viscosity of viscoelastic fluids at low shear rates if appropriate analytical and experimental procedures are adopted. The principle is that a solid body, having a higher density than the liquid to be tested, slowly falls through a liquid-filled tube. The density difference and the gap between the falling body and the tube wall determine the viscosity of the falling body. The oil container is compensated by formulae for different temperature expansion.

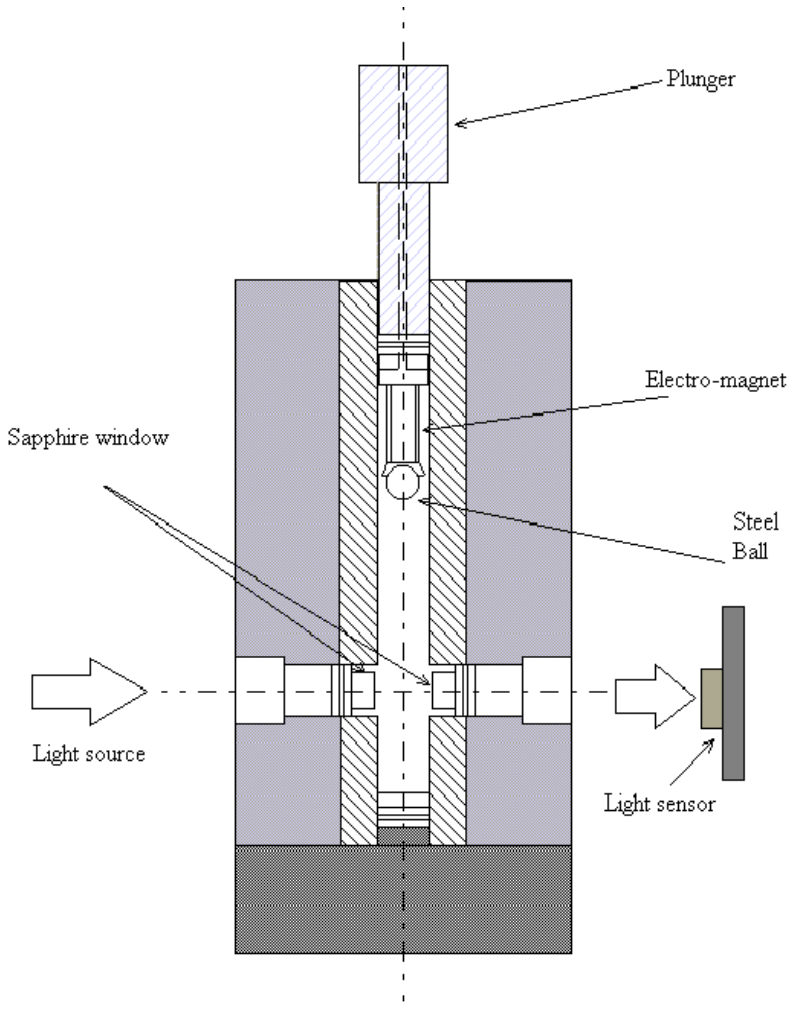


Fig.3.1 High pressure falling ball viscometer

The viscometer is made of nickel-chromium-molybdenum steel with 12 mm inner diameter. A steel ball of 7.94 mm diameter was dropped into the viscometer with oil which passed through the 3.0 mm diameter sapphire observation window. The falling ball passing time through the sapphire window was measured by a sensor, and the viscosity measurement was done from simple calculations. Pressure was applied using a 30 ton hydraulic power unit. The experiment was done at the oil temperature of 20 °C to 100 °C in the range of viscosity $\eta<10^3$ Pas and the pressure up to 0.4 GPa. In addition, the relaxation time, a measure of the elasticity of the tested lubricating oils, was determined. These rheological properties are necessary for the analysis of the fluid's (oils) mechanical and heat transfer behavior of viscoelastic fluids. A schematic diagram of the high pressure falling ball viscometer is shown in Fig. 3.1. Appendix B shows the complete mathematical derivation of high-pressure viscosity measurement formulae.

### *3.3.2 High Pressure Densitometer*

At low pressures, the lubricating oils behave like a normal liquid and the same type of properties as for liquid lubricants can be used to analyze the pressure build up, oil film thickness and elastic deformations of the bearing surfaces. At high pressure, where the lubricant is solidified, the pressure build-up is governed by the shear strength and the compressibility of the solidified oil and the elastic properties of the bearing surfaces. Depending on the pressure gradients in the lubricant film, two different types of behavior of the solidified oil are conceivable. Either the oil sticks to the rolling surfaces and moves with the same velocity and in the same direction as the surfaces, or the solid oil slides along the bearing surfaces in the direction of the local pressure gradient. Which of these two possible scenarios actually takes place depends on the shear stress at the oil-bearing interface. If the shear stress is less than the local shear strength of the interface or the solidified oil, the oil will stick to the surfaces and move like a solid layer without slip between the bearing surfaces. When the stress reaches the shear strength, slip will take place in the direction of the maximum stress. To be able to calculate the total pressure build-up in the different region of the lubricated contact, continuity of the mass flow must be guaranteed at all boundaries between the regions with different lubricant behavior. The lubricant properties in the

solidified state have to be determined experimentally by high pressure densitometer to solve this lubrication problem numerically.

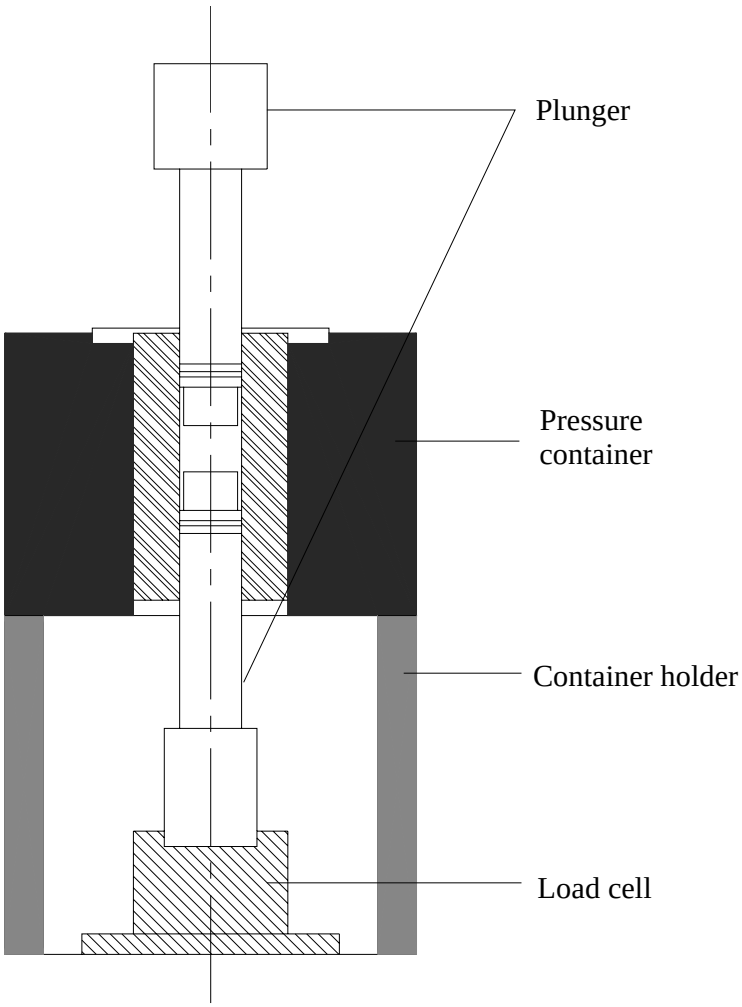


Fig. 3.2 High pressure densitometer

The lubricant behavior in the solidified state was investigated using a high pressure densitometer made by Saga university, Japan as shown in Fig. 3.2. This high-pressure chamber was designed to measure both the pressure when the oil converted to a solid, and the shear strength of the oil at higher pressure. Isothermal tangent bulk modulus and isothermal secant bulk modulus can measure from the high pressure density measurement using this apparatus.

***Working Principle***

Density measurement was done by using plunger type high pressure densitometer. The apparatus is shown in Fig.3.2. The outer cylinder, with an outer diameter of 80.0 mm, and inner diameter of 29.93 mm, made of nickel-chromium-

molybdenum steel. The inner cylinder, with an outer diameter of 30 mm and inner diameter of 12 mm, made of die steel and it was shrinkage fitted to the outer cylinder. The plunger and plug each have a high-pressure seal. The high-pressure seal is comprised of the O ring, back up ring and the anti-extrusion ring made of beryllium copper. The volume of tested oils at ambient pressure was V=2.0 mL. The oil is contained in a high pressure chamber closed at the bottom by plug and at the top by a plunger. The plug rests on a load cell which records the total force on the plug. A plunger was pushed into the cylinder by a 30 ton hydraulic power unit. The chamber pressure p is given by $(W_1+W_2)/2A$, where $W_1$ is the force on hydraulic power unit, $W_2$ is the force on load cell, and A is the area of the bore in the high pressure chamber. The volume of lubricant in the chamber corresponding to a pressure was determined from the displacement of the plunger by using a linear gauge. A correction for the volume of the lubricant was done to take account of the elastic deformation of the plunger, plug and before area at high pressure. Fluid volume measurements at test temperatures and pressures were converted to density. The time for compressing the lubricant from 0 to 1.2 GPa was taken about 60 min to ensure isothermal compressibility of the lubricants.

Appendix C shows a complete mathematical derivation of high pressure density measurement formulae.

### *3.3.3 Low Temperature Photoelasticity Observation Apparatus*

Photoelastic investigation on solidification of lubricants at low temperature was done by the low temperature photoelasticity apparatus. It is widely known that transparent polymer, e.g. urethane rubber, exhibits a high photoelastic effect together with its high deformability. Even in the glassy state with low deformability this effect is also recognized though its sensitivity becomes much lower. The experimental set up is given Fig. 3.3.

When a minute hemispherical air bubble is closed into a space between test oil and a cover glass plate and cooled, its volume apparently expands as a result of contraction of the oil. Thus expanded bubble generates tensile stresses along its interface under solidification condition. At the same time the photo elastic effect appears under a dark polarized field. Thus, the photoelastic patters exhibited by lubricants were visualized through quartz window in a polarized light beam. This

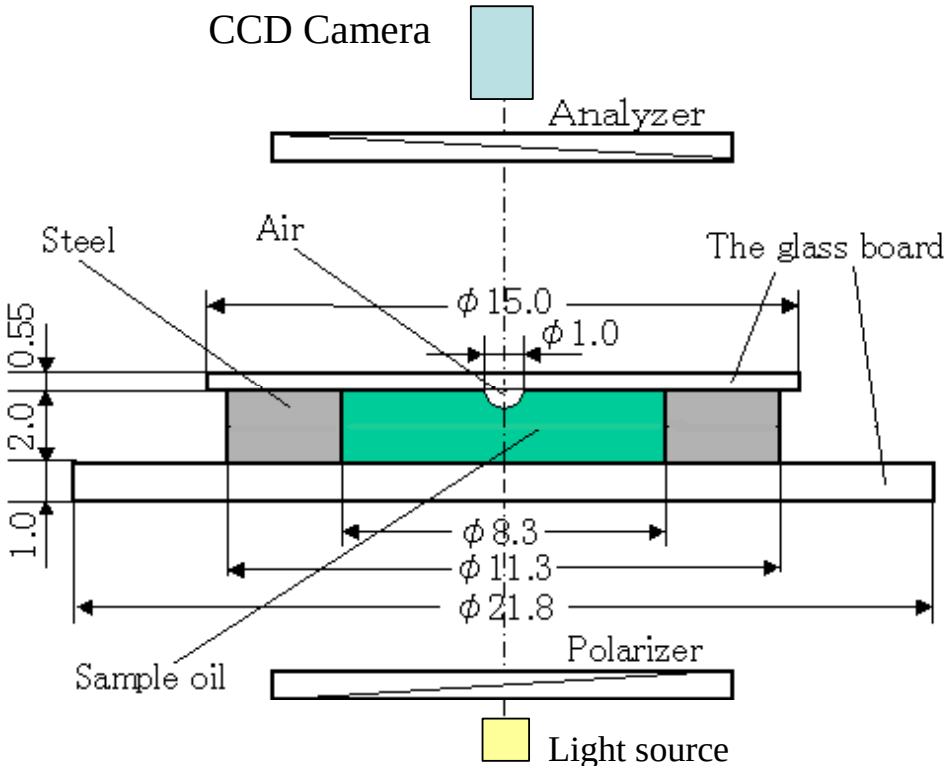


Fig. 3.3 Experimental set up of low temperature photoelasticity observation

enables the stress analysis and estimation of mechanical properties of the solidified oil.

Fig. 3.3 Shows the main part of the apparatus. A hemispherical air bubble, 0.5 – 1.0 mm in diameter enclosed in a space between a cover glass plate and oil in a container expands apparently as a result of contraction of surrounding oil at lowering temperature. For observing the solidification of oils the double refraction effect in polarized light was utilized. This enables not only to determine the glass transition temperature by occurrence of the photoelastic effect but also to detect the elastic-plastic transition by observing the change in diameter of hemispherical air bubble statically under the isobaric condition. The observation also can detect the wax content in the oil or the crystal formation temperature of the sample.

### *3.3.4 Surface Tension Measuring Apparatus*

Surface tension is a measurement of the cohesive energy present at an interface. The molecules of a liquid attract each other. The interactions of a molecule in the bulk of a liquid are balanced by an equal attractive force in all directions. Molecules on the surface of a liquid experience an imbalance of forces. The net effect of this situation is

the presence of free energy at the surface. The excess energy is called surface free energy and can be quantified as a measurement of energy/area. It is also possible to describe this situation as having a line tension or surface tension which is quantified as a force/length measurement. The common units for surface tension are dynes/cm or mN/m.

Surface tension of lubricating oils was measured using Pendant drop shape analysis as like Fig. 3.4. Contact angel apparatus and a digital video camera were used to measure the surface tension of lubricating oils. Photograph of the contact angle apparatus is shown in Fig. 3.5. It consists of a low power microscope for horizontal observation of oil drop. A micro syringe was used to produce a single drop and video camera was placed behind the low power microscope of the contact angle apparatus. Photograph of a micro syringe is given in Fig 3.6. A light source was allowed for back illumination of the drop. Video was taken of 3 drop of oil off the light source and anther 3 drops of oil on the light source. From this video, Pendant drop shape analysis was given the value of surface tension. Surface tension was measured at 20 °C and 40 °C.

The surface tension at the liquid interface can be related to the drop shape through the following equation:

$$\gamma = \frac{g\rho d_e^{\,2}}{H} \qquad (2.1)$$

where $\gamma$ : Surface tension

H: Compensation Function

$d_e$ = the maximum diameter of the drop

$d_s$ = the level diameter of the drop in the distance of the tip of liquid to $d_e$

$\rho$ : density

and g: acceleration of the gravity.

The compensation function is taken from the table 6.69 [47] where $S = d_s/d_e$.

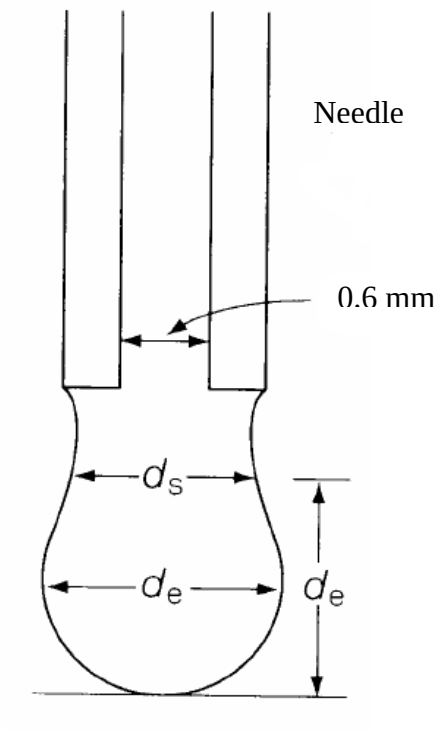


Fig. 3.4 Pendant drop analysis


Fig. 3.5 Contact angle apparatus for surface tension measurement


Fig. 3.6 Used micro syringe to produce the drop of oil

### *3.3.5 Density and Viscosity Measuring Apparatus*

Density of the sample oils was measured using a digital density meter (Model: DA-130, Kyoto Electronics Manufacturing Co. Ltd., Japan) as shown in Fig. 3.7. Density was measured at room temperature and at 40°C temperature. From these two temperatures I have calculate the density at 15°C temperature.

Fig. 3.7 Digital density meter

Kinematic viscosity of the sample oil was measured in the laboratory. Conventional capillary viscometer was used for the measurement. Viscosity was measured at 40°C and at 80°C. Then, using the ASTM-Walther viscosity temperature relation I have calculated the viscosity at 100°C. Kinematic viscosity at 40°C and 100°C is tabulated in the physical properties of sample oils.

## 3.4 Conclusion

All the experimental setups were handled carefully according to safety rules. Cleaning is important in the tribological performance for lubricating oils. After every experiment cleaning of the set up involved in the experiment and lubricating oils were clean properly. Acetone, Petroleum ether, n-hexane etc were used as cleaning agent. Ultrasonic cleaner also used for the cleaning and compressed air and hot air was used after the cleaning for dried the apparatus parts. As a result, apparatus gave accurate results. During the experiment, I have tried to find out the accurate results. All the experiments were repeated twice for the accurate result. When repeatability was good, then data was taken for the experiment.

# Chapter 4

# Sound Velocity as a Prediction Parameter for Pressure Viscosity Coefficient of Lubricating Oils

## 4.1 Introduction

Pressure-viscosity behavior of lubricating oil is very much essential in the field of tribology and high-pressure rheology. Tribology, the study of the interaction between surfaces in contact, spans many disciplines from physics and chemistry to mechanical engineering and material science, and is of extreme technological importance. The important purposes of tribology are prevention of damage and frictional control. The significant parameter for the prevention of damage under the EHL condition is $\alpha\eta$ and for traction control is $\alpha p$ ($\alpha$: pressure-viscosity coefficient, $\eta$: viscosity, p: average Hertzian pressure) [48]. In both cases $\alpha$ is a common parameter. So it is very much important to know the pressure-viscosity coefficient of lubricating oil. Bair also noted that $\alpha$ depends on the lubricant at hand, and on the pressure, temperature, and shear rate in the contact [49]. It is recognized that the pressure-viscosity coefficient is an indispensable property in the elastohydrodynamic (EHD) lubrication.

Pressure-viscosity coefficient can be calculated from high-pressure viscosity measurement. The measurement of the effect of pressure on viscosity has a history reaching back for more than a century. Bridgman [50] developed the geometry of the falling body that is used in the majority of instrument today. A falling body or sinker of roughly cylindrical form is disposed within a cylindrical tube so that the sinker can move axially (fall) within the tube. Irving and Barlow [51] worked out the relationships between viscosity and the geometry, the falling velocity and the densities of the sinker and the liquid. Bair and Winer [52] improved the device in their laboratory; they utilized a linear variable differential transformer to detect the position of a magnetic sinker within a non-magnetic pressure vessel. Ohno et al. [53,54] established a falling ball viscometer in Saga University based on the previous concept. Same Viscometer is used to measure the high pressure viscosity in this study. Detail of the apparatus is given in experimental apparatus chapter. Pressure viscosity coefficient $\alpha$ can calculate from the pressure viscosity relation. But the measurement

requires long haul, being in addition to require the skill for handling the high-pressure equipment. So it is better to calculate α on the easy way. It can be calculated from physical properties under the atmospheric pressure whose measurement is easy.

There are many correlations to predict α. Bair and Qureshi showed many correlation (including Barus equation and Roeland equation) of pressure viscosity coefficient in their research [55] and compared with their measurement. They claim that the high pressure falling body viscometers produce sufficiently accurate and repeatable data to test rheological model of EHL film thickness and traction. They also measured the reciprocal assymtotic isoviscous pressure α*. The reciprocal asymptotic isoviscous pressure, α*, is a coefficient that characterizes the piezoviscous response for general EHL film thickness calculations. Blok [56] showed that film thickness calculations with the assumption of exponential behavior (α(p) = constant) could be applied to general pressure-viscosity behavior by substituting α* for the constant, α.

So and Klaus [22] combined both linear and nonlinear regression analyses with atmospheric viscosity, density and $m_0$ as independent variables used to obtain the flowing third order empirical correlation:

$$\begin{aligned}\alpha &= 1.216 + 4.143\,(\log \nu_0)^{3.0627} \\ &+ 2.848 \times 10^{-4}\, m_0{}^{5.1903}\,(\log \nu_0)^{1.5976} \\ &- 3.999\,(\log \nu_0)^{3.0975}\, \rho^{0.1162}\end{aligned} \tag{4.1}$$

Where α = Pressure-viscosity coefficient,

$\nu_0$ = Atmospheric kinematic viscosity,

$m_0$ = Viscosity-temperature property, and

ρ = Atmospheric density.

Johnston [21] derived a relation based on fundamental properties of a liquid lubricant rather than to propose an empirical correlation. His relation is as follows:

$$\alpha = \frac{\beta E_v}{\alpha_T 2CRT^2} \tag{4.2}$$

Where, β is the coefficient of compressibility, $E_v$ is the activation energy, $\alpha_T$ is the coefficient of thermal expansivity, C is a constant, R is the universal gas constant and T is the temperature. Both of the relations present better results, but the resulting

accuracy depends on parameters accuracy. Again, most of the correlations suffer disadvantages due to their containing complex equation forms, requiring data, which are difficult to access. These disadvantages provide low accuracy.

In this research, the authors emphasize on the bulk modulus, rather than the other parameters. Bulk modulus is related to the intermolecular force and the high-pressure physical properties, and also depends on the free volume. Cohen and Turnbull [57] gave physical meaning to the free volume. They hypothesized that molecular transport occurs when a fluctuation in the free volume opens up a void greater than some critical size required to allow movement of a molecule into that void. Cutler et al. [58] found the effect of high molecular weight hydrocarbons on the compressibility of oil. Compressibility is the reverse of bulk modulus. There are four types of bulk modulus, isothermal secant, isothermal tangent, adiabatic secant and adiabatic bulk modulus. Determining the density change directly provides the isothermal secant bulk modulus. Tangent bulk modulus is obtained by differentiation of the data and sound velocity measurement provides the adiabatic bulk modulus [59]. Ohno and Hirano [53] calculated tangent bulk modulus $K_T$ from the high-pressure density test of sample oil utilizing the high-pressure densitometer. The adiabatic bulk modulus $K$ can be calculated from the sound velocity. Sound velocity is also related to the molecular structure of lubricating oil, it could also be estimated from the molecular properties. In this study, sound velocity is measured from the supersonic wave spread time in the lubricating oil using the Sing around method. Then, compared the experimental pressure-viscosity coefficient $\alpha$ with the adiabatic bulk modulus $K$ at the same temperature. It has been found that an exponential relationship between pressure viscosity coefficient and adiabatic bulk modulus exists. The relationship demonstrates that, the pressure-viscosity coefficient $\alpha$ can be predicted only from the adiabatic bulk modulus $K$ [60].

## 4.2 Sample oils

Sample oils were taken on the group basis. These are traction oil (SN32, SN100 and CVTF), polyalphaolefin oil (PAO32, PAO68), paraffinic mineral oil (P60N, P150N, P500N, PBSN), perfluoropolyether oil (Fomblin, Demnum and Krytox), and glycerol. Physical properties of tested oils are given in Table 3.1 to Table 3.5.

## 4.3 Methodology of Prediction

The knowledge of the pressure-viscosity relationship of lubricants is important for the design and construction of lubrication elements, such as rolling bearings, valve cams and gears. Many correlations were proposed to predict pressure-viscosity coefficient. As like on the basis of free volume theory [23], bulk properties of liquid [21]. Also, there are many researches [18,19] for the prediction of pressure-viscosity coefficient α. Prediction process and methodology of this research is given as follows.

Pressure-viscosity coefficient α can calculate by high-pressure viscosity measurement, using the Barus's equation (Eq. 4.3) [6], where, $\eta_0$ is an absolute viscosity under the atmospheric pressure and η is the absolute viscosity at corresponding pressure p.

$$\eta = \eta_0 \exp(\alpha p) \tag{4.3}$$

In addition, Doolittle has indicated high-pressure viscosity by the Eq. 4.4, which is known as Doolittle free volume equation, where *f* is fractional free volume, and *A* and *B* are constant.

$$\eta = A \exp(B / f) \tag{4.4}$$

Since at atmospheric pressure, $\eta_0$ is the absolute viscosity and $f_0$ is the fractional free volume; therefore, the Doolittle equation can be written as

$$\eta = \eta_0 \exp\left\{ B\left( \frac{1}{f} - \frac{1}{f_0} \right) \right\}$$

$$= \eta_0 \exp\left\{ B\left( \frac{1}{\ln \rho^* - \ln \rho} - \frac{1}{\ln \rho_0^* - \ln \rho_0} \right) \right\} \tag{4.5}$$

Ohno and Hirano [53] also measured the fractional free volume by the closest packed solid density ρ*. They used it in their research on the prediction of viscosity and showed that fractional free volume *f* could be indicated with $f = \ln(\rho^*/\rho)$. From the Eqs. (4.3) and (4.5), the following equation can be found.

$$\alpha p = B\left( \frac{1}{\ln \rho^* - \ln \rho} - \frac{1}{\ln \rho_0^* - \ln \rho_0} \right) \tag{4.6}$$

Again, one of the basic equations for the compression of oils is the equation of volumetric change, which is used in the strength of materials. The volumetric strain ε is defined as the ration of the decrease in volume to the original volume.

$$\varepsilon = \frac{dV}{V} = \left( -\frac{\partial \ln \rho}{\partial p} \right)_T dp + \left( -\frac{\partial \ln \rho}{\partial T} \right)_p dT$$

$$= \left( -\frac{1}{K_T} \right) dp + 3\partial dT \qquad (4.7)$$

where $V$ is the volume, ρ is density, $p$ is pressure, $T$ is temperature, $K_T = (\partial n\rho/\partial p)^{-1}$ is the bulk modulus and δ is coefficient of thermal expansion. Ohno and Hirano [53] expressed clearly the measuring process of tangent bulk modulus using high pressure density measurement. The change in density ρ against pressure for traction oil CVTF at 40°C is shown in Fig. 4.1. The density increases linearly at high pressures region. The effect of solidification is seen clearly in the abrupt change in ∂lnρ/∂p. Extending the straight line from solid region into lower pressure ranges as shown Fig. 4.1, the idealized closest packed solid density was expressed by ρ*.

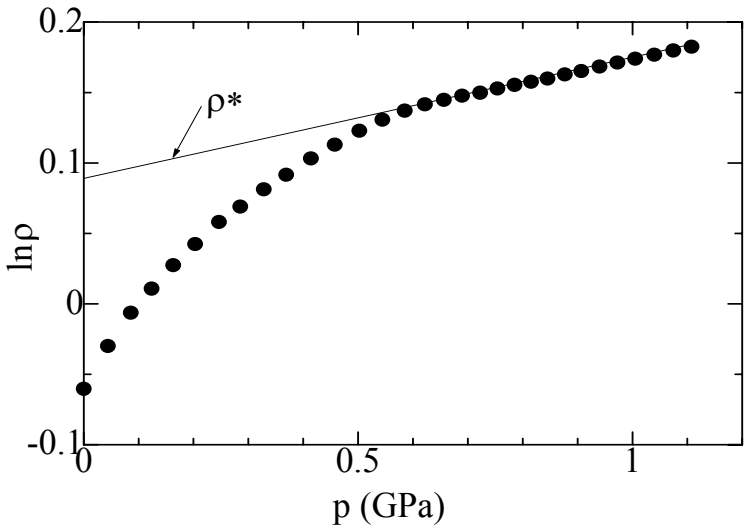


Fig. 4.1 Density pressure curve for traction oil CVTF at 40 °C

When Eq. 4.6 is differentiated with pressure $p$ considering the constant $\rho_0$* and $\rho_0$, the pressure-viscosity coefficient α can be pointed out by the Eq. 4.8, where $K_T$ is the tangent bulk modulus.

$$\alpha = \frac{B}{(\ln \rho^* - \ln \rho)^2} \cdot \frac{d}{dp}(\ln \rho) = \frac{B}{K_T f^2} \qquad (4.8)$$

Figure 4.2 shows the relationship between the tangent bulk modulus $K_T$, pressure $p$ and the fractional free volume $f$ of traction oil CVTF at 40°C. The $f$ is inversely proportional to $K_T$ at lower pressure region and then from Eq. 4.8, it is clear that the pressure-viscosity coefficient α is related to tangent bulk modulus $K_T$. Tangent bulk modulus is also related with the adiabatic bulk modulus $K$, as $K = \kappa K_T$, where κ is the ratio of specific heat at constant pressure and constant volume. The numerical value of κ is almost constant for same group of oil (for mineral oil κ=1.135) but differ slightly from group to group of lubricating oils [7]. The above methodology shows that the pressure-viscosity coefficient can be predicted from the adiabatic bulk modulus.

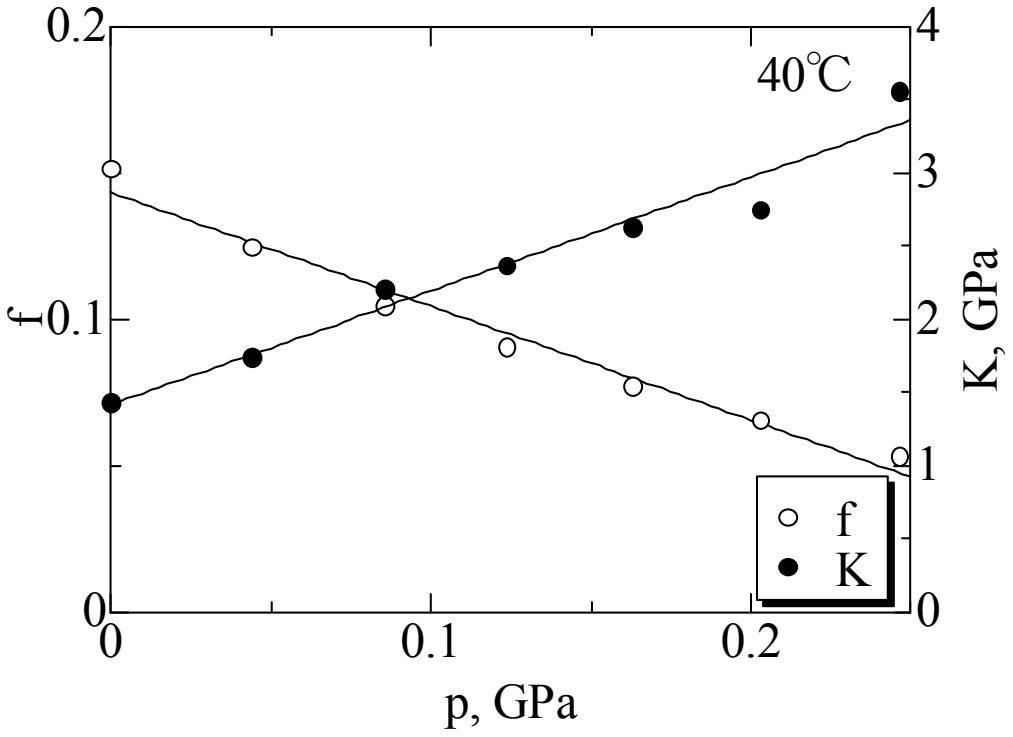


Fig. 4.2 Relation between the bulk modulus, pressure and free volume of CVTF

## 4.4 Experimental Procedure

### *4.4.1 High Pressure Viscosity Measurement*

Viscosity of test oils at high pressure is measured by the falling ball viscometer, the same apparatus used by Ohno et al. [54]. It is a simple and inexpensive measuring system that is used to determine the steady shear viscosity of viscoelastic fluids at low shear rates. The principle is that, a solid body having a higher density than the liquid to be tested, falls slowly through a liquid filled tube. The density difference and the gap between the falling body and the tube wall determine the viscosity of the sample. The expansion of the oil container is compensated by the formulas for different temperature. Experiments are done at the oil temperature of 20°C to 100°C in the range of viscosity $\eta < 10^3$ Pa·s and the pressure up to 0.4 GPa. The actual measured values of the pressure and absolute viscosity of CVTF at different temperatures are shown in Fig. 4.3. The pressure-viscosity coefficient $\alpha$ is calculated from the graph using Barus's equation (Eq.4.3). The pressure-viscosity coefficient for other samples are measured experimentally by this method, and the values is shown in Table 4.1 to Table 4.5.

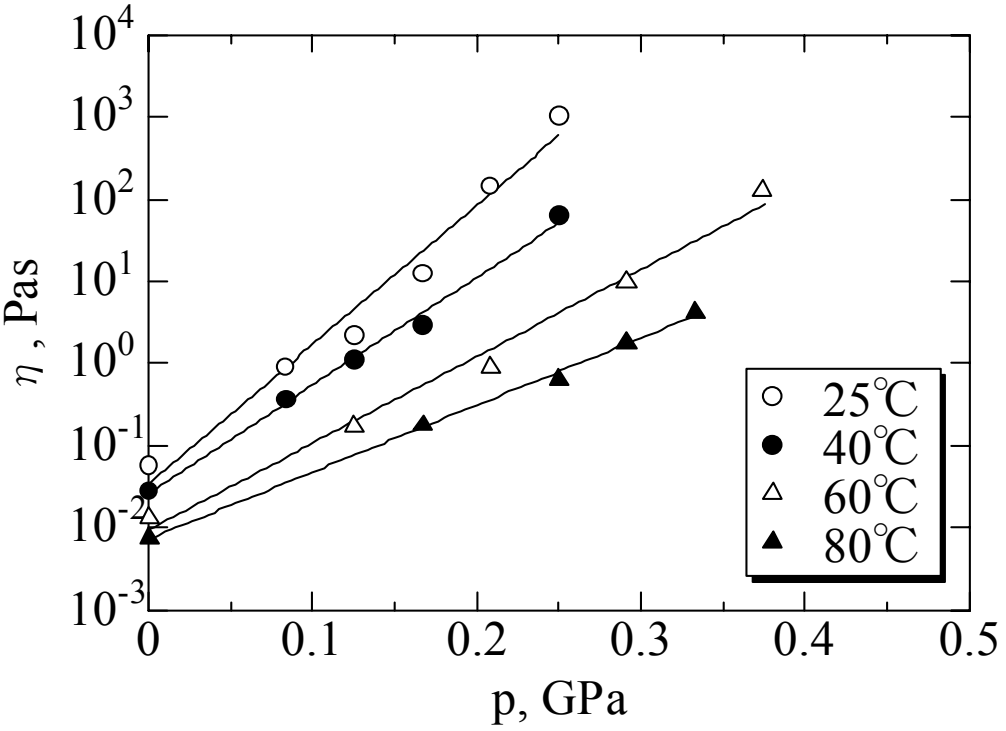


Fig. 4.3 Pressure, viscosity and temperature relationship of traction oil CVTF

### *4.4.2 Measurement of Sound Velocity and Adiabatic Bulk Modulus*

Sound is a molecular disturbance and the disturbance is caused by vibration. Sound velocity is measured in distance per time, which is the multiplication of wavelength and frequency. It depends on the nature of the medium through which it is traveling and also how molecules are close together. So sound velocity is directly related to its bulk modulus and density. Laplace (after then Wood) expressed the sound velocity $U = 1/(\beta\rho)^{0.5}$ in terms of adiabatic compressibility β and density ρ which is known as Wood equation. If $U$ can measure in high accuracy, then adiabatic bulk modulus $K$ $(K=1/\beta)$ can be calculated accurately. Sound velocity of sample oils was measured by the Sing around technique in the actual experiment. Sing around device displayed total propagation time of the cycle including delay time. It also displayed only delay time of the circuit. The propagation time of the sample inside was measured from the difference of the above mentioned times of the cycle when propagation became steady. Details explanation of the Sing around apparatus and sound velocity measurement has given in chapter 2. Here, adiabatic bulk modulus $K$ is calculated from the measured sound velocity $U$ of each sample oils at different oil temperatures. Figures 4.4 to 4.8 have shown the changes of sound velocity of lubricating oils with temperature.

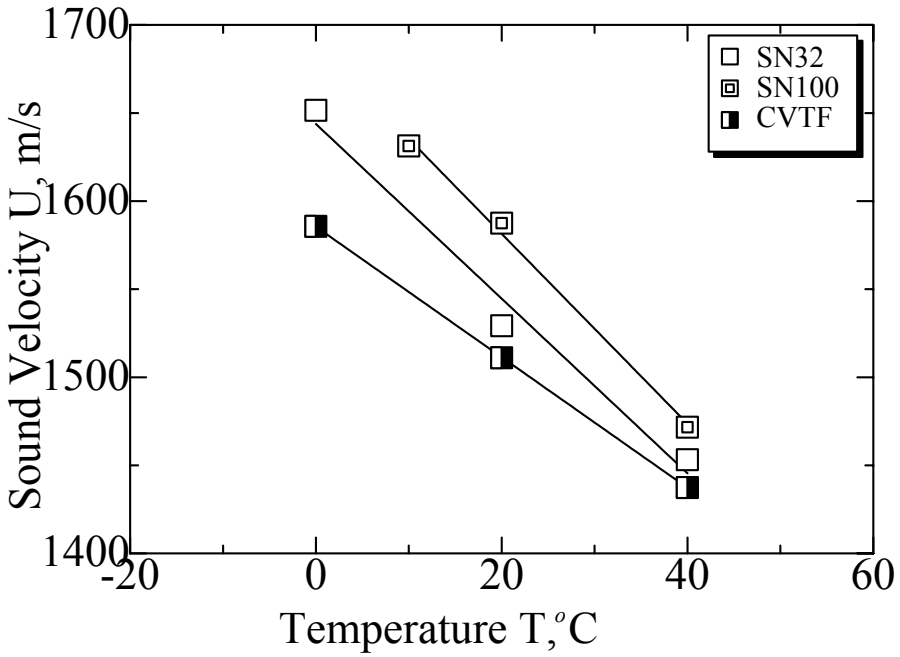


Fig. 4.4 Changes of sound velocity of traction oils with temperature

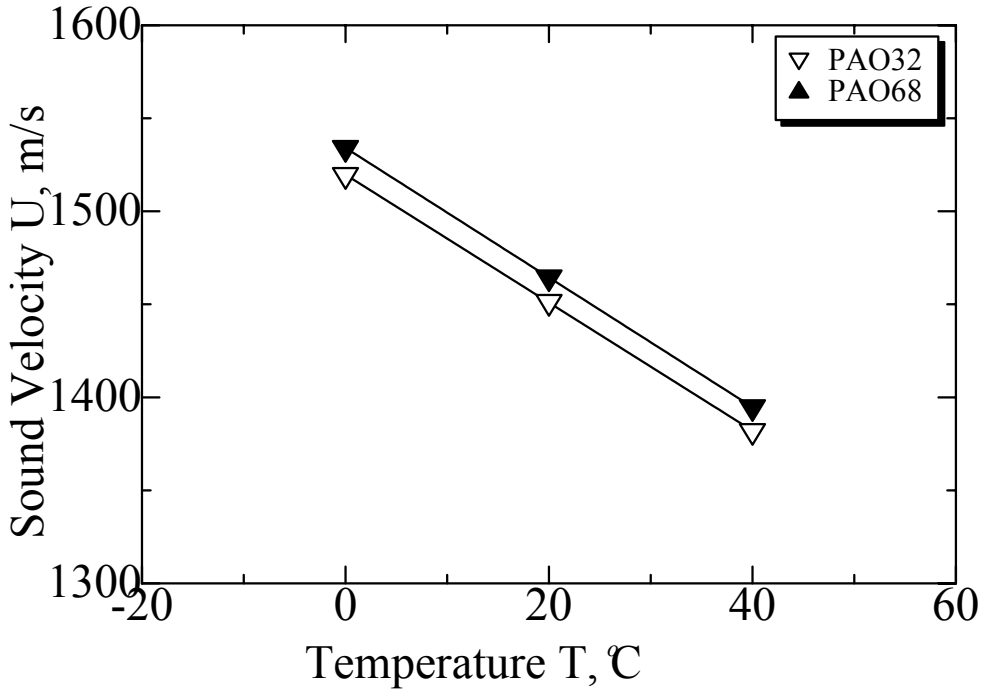


Fig. 4.5 Changes of sound velocity of polyalphaolefin oils with temperature

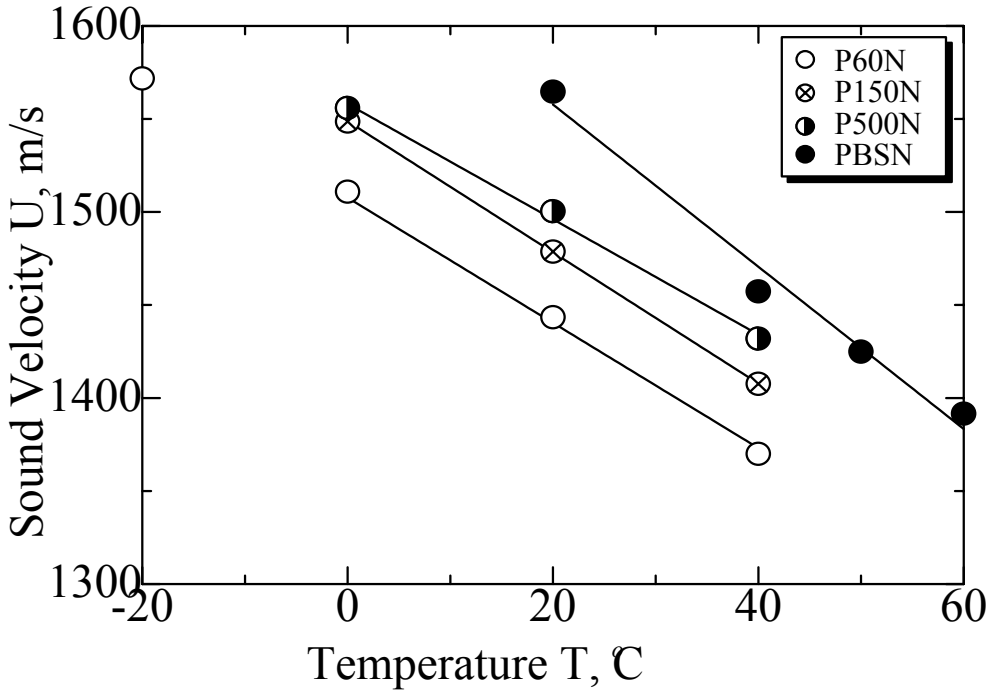


Fig. 4.6 Changes of sound velocity of paraffinic mineral oils with temperature

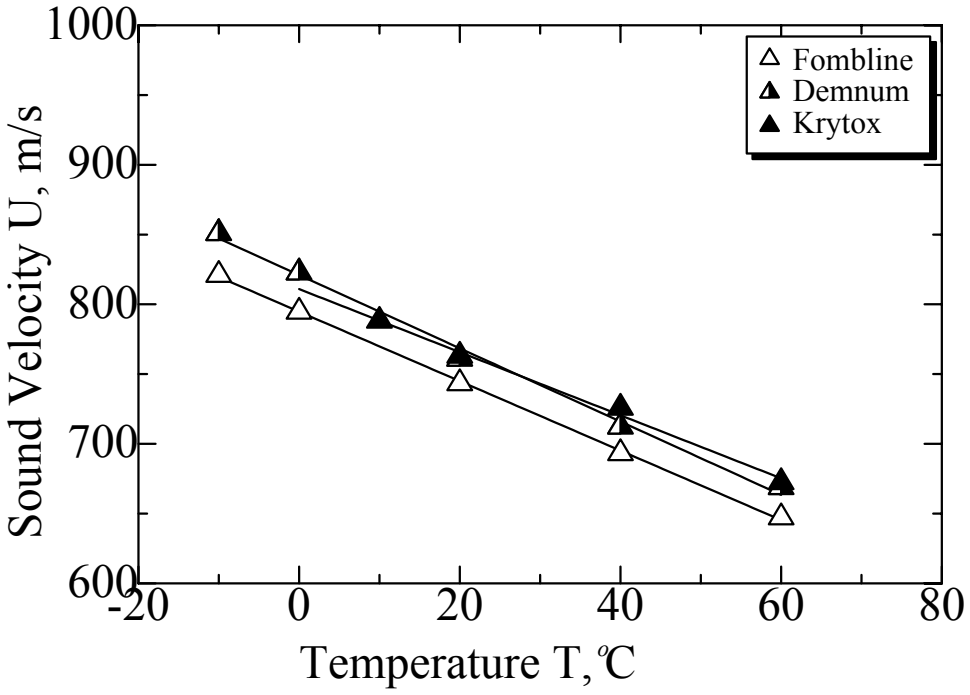


Fig. 4.7 Changes of sound velocity of perfluoropolyether oils with temperature

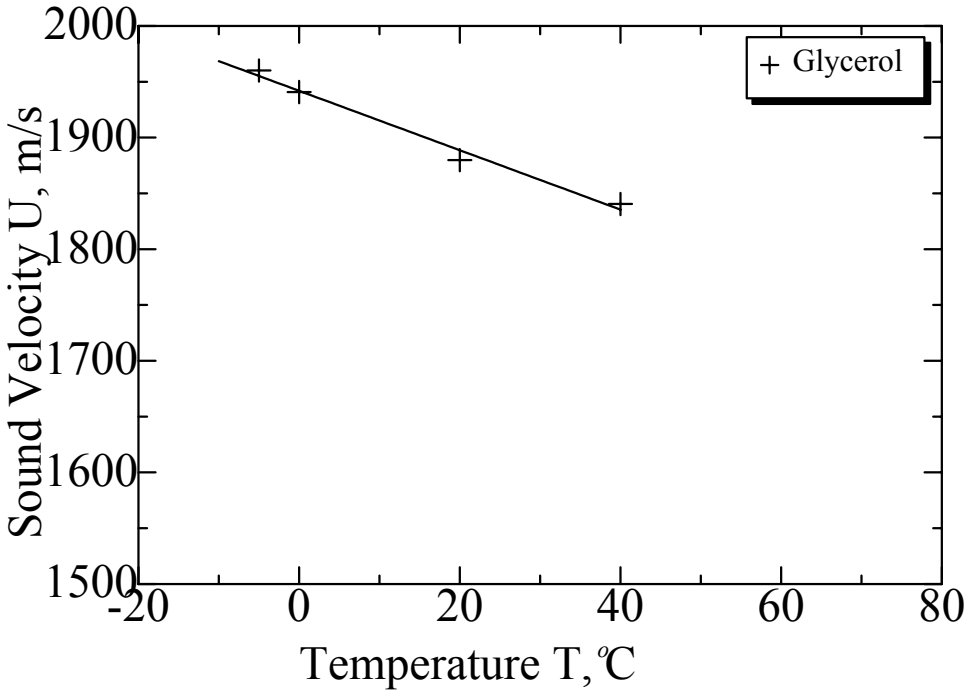


Fig. 4.8 Changes of sound velocity of glycerol with temperature

## 4.5 Results and Discussion

The experimental pressure viscosity coefficient $\alpha_{exp}$ was calculated from the high pressure viscosity measurement. The adiabatic bulk modulus $K$ was calculated from the measured sound velocity. The experimental results are listed in Table 4.1 to Table 4.5.

Table 4.1 Experimental results for traction oils

| Sample oil | Temperature $T$ | Sound velocity $U$ | Ad. Bulk modulus $K$ | Experimental pressure viscosity coefficient $\alpha_{exp}$ |
|---|---|---|---|---|
| | °C | m/s | GPa | GPa$^{-1}$ |
| SN32 | 40 | 1453 | 1.87 | 30.2 |
| | 100 | 1156 | 1.12 | 14.2 |
| SN100 | 20 | 1588 | 2.31 | 51.5 |
| | 40 | 1472 | 1.95 | 40.0 |
| | 60 | 1365 | 1.65 | 29.8 |
| | 80 | 1259 | 1.37 | 22.7 |
| | 100 | 1152 | 1.13 | 16.9 |
| CVTF | 25 | 1493 | 2.11 | 40.2 |
| | 40 | 1437 | 1.93 | 30.4 |
| | 60 | 1363 | 1.70 | 24.8 |
| | 80 | 1289 | 1.49 | 18.8 |

Table 4.2 Experimental results for polyalphaolefin oils

| Sample oil | Temperature $T$ | Sound velocity $U$ | Ad. Bulk modulus $K$ | Experimental pressure viscosity coefficient $\alpha_{exp}$ |
|---|---|---|---|---|
| | °C | m/s | GPa | GPa$^{-1}$ |
| PAO32 | 20 | 1451 | 1.74 | 13.6 |
| | 40 | 1382 | 1.55 | 11.2 |
| | 60 | 1313 | 1.37 | 9.1 |
| | 80 | 1244 | 1.20 | 9.0 |
| | 100 | 1176 | 1.05 | 8.9 |
| PAO68 | 25 | 1447 | 1.73 | 15.2 |
| | 40 | 1395 | 1.59 | 14.0 |

Table 4.3 Experimental results for paraffinic mineral oils

| Sample oil | Temperature $T$ | Sound velocity $U$ | Ad. Bulk modulus $K$ | Experimental pressure viscosity coefficient $\alpha_{exp}$ |
|---|---|---|---|---|
| | °C | m/s | GPa | GPa$^{-1}$ |
| P60N | 22 | 1431 | 1.74 | 18.1 |
| | 40 | 1370 | 1.57 | 11.7 |
| | 100 | 1168 | 1.07 | 6.7 |
| P150N | 40 | 1408 | 1.68 | 12.7 |
| | 70 | 1302 | 1.40 | 12.1 |
| | 100 | 1196 | 1.16 | 6.8 |
| P500N | 40 | 1432 | 1.75 | 14.1 |
| | 70 | 1339 | 1.49 | 11.8 |
| | 100 | 1246 | 1.26 | 6.9 |
| PBSN | 20 | 1565 | 2.15 | 27.1 |
| | 40 | 1457 | 1.83 | 16.4 |
| | 50 | 1425 | 1.74 | 16.2 |
| | 80 | 1308 | 1.43 | 11.7 |
| | 100 | 1224 | 1.23 | 8.3 |

Table 4.4 Experimental results for perfluoropolyether oils

| Sample oil | Temperature $T$ | Sound velocity $U$ | Ad. Bulk modulus $K$ | Experimental pressure viscosity coefficient $\alpha_{exp}$ |
|---|---|---|---|---|
| | °C | m/s | GPa | GPa$^{-1}$ |
| Fombline | 20 | 743 | 1.02 | 14.4 |
| | 40 | 693 | 0.86 | 13.8 |
| Demnum | 20 | 761 | 1.09 | 21.5 |
| | 40 | 712 | 0.93 | 18.6 |
| Krytox | 20 | 763 | 1.11 | 44.4 |
| | 40 | 726 | 0.98 | 33.2 |

Table 4.5 Experimental results for Glycerol

| Sample oil | Temperature $T$ | Sound velocity $U$ | Ad. Bulk modulus $K$ | Experimental pressure viscosity coefficient $\alpha_{exp}$ |
|---|---|---|---|---|
| | °C | m/s | GPa | GPa$^{-1}$ |
| Glycerol | 28 | 1872 | 4.40 | 4.7 |
| | 40 | 1840 | 4.21 | 3.7 |

From the experimental results as mentioned in the above tables and Fig. 4.9 to Fig. 4.13, it is clear that sound velocity is proportional to its bulk modulus. Figure 4.13 shows that glycerol has higher bulk modulus and it's sound velocity also superior at measured temperature because hydrogen bond of glycerol shown greater intermolecular force and grown high bulk modulus. On the other hand perfluoropolyether oils have low bulk modulus and the value of sound velocity in them have found the lower value, because PFPE has higher free volume at testing temperature, low intermolecular force due to its fluorine bond and shown low bulk modulus. Figure 4.12 shows the relation between the adiabatic bulk modulus and the sound velocity of PFPE oils.

Figures 4.9 to Fig 4.11 show the relation between adiabatic bulk modulus and sound velocity of traction oils, polyalphaolefin oils and paraffinic mineral oils consequently. When adiabatic bulk modulus and sound velocity of all tested oils are plotted in a single graph, it will be easy to compare each other. Figure 4.14 shows this comparison.

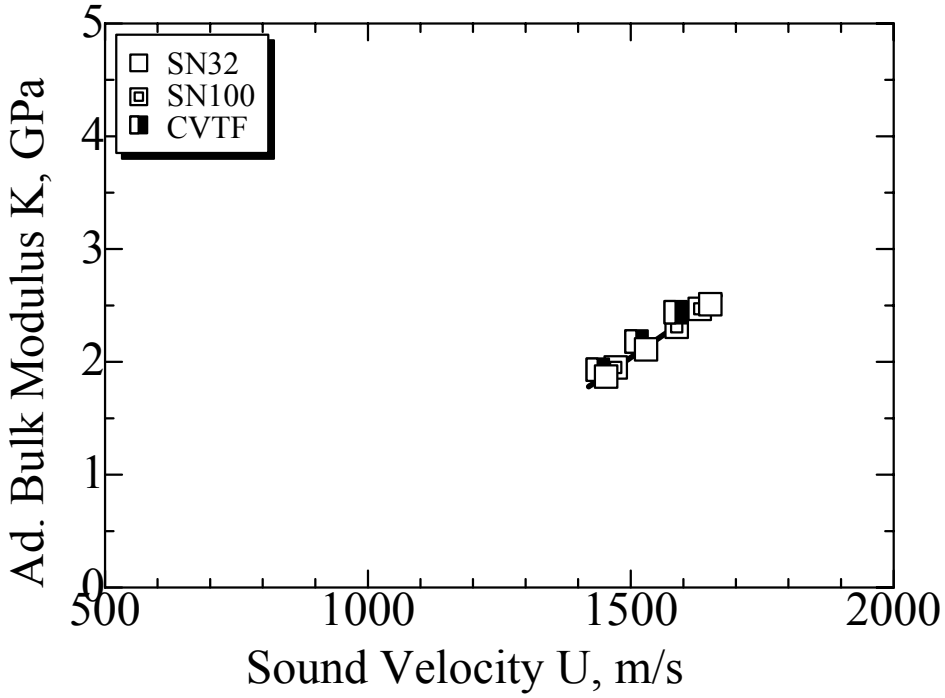


Fig. 4.9 Relation between adiabatic bulk modulus and sound velocity of traction oil

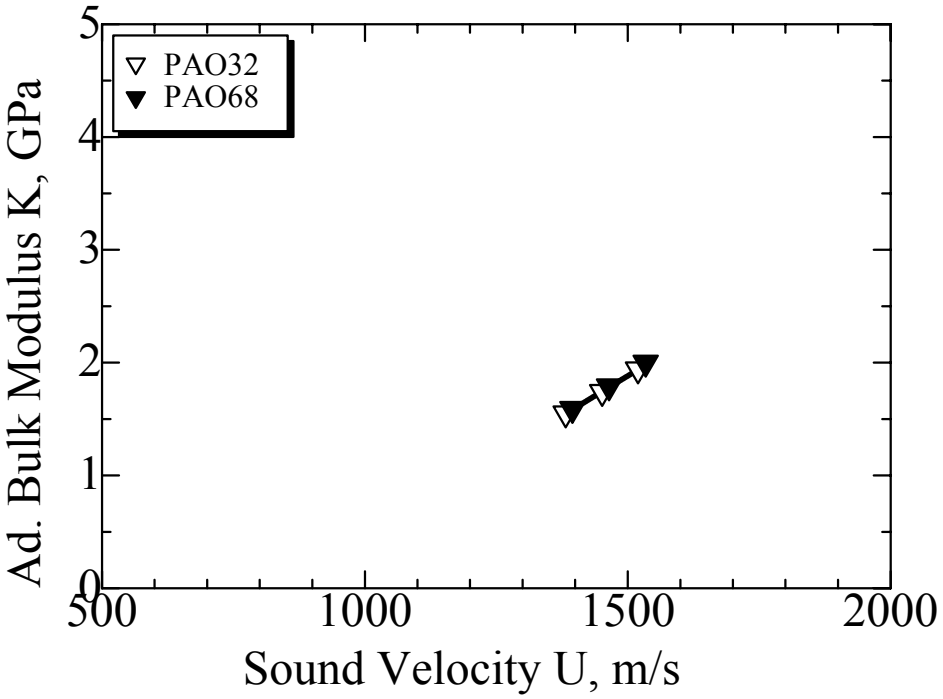


Fig. 4.10 Relation between adiabatic bulk modulus and sound velocity of PAO

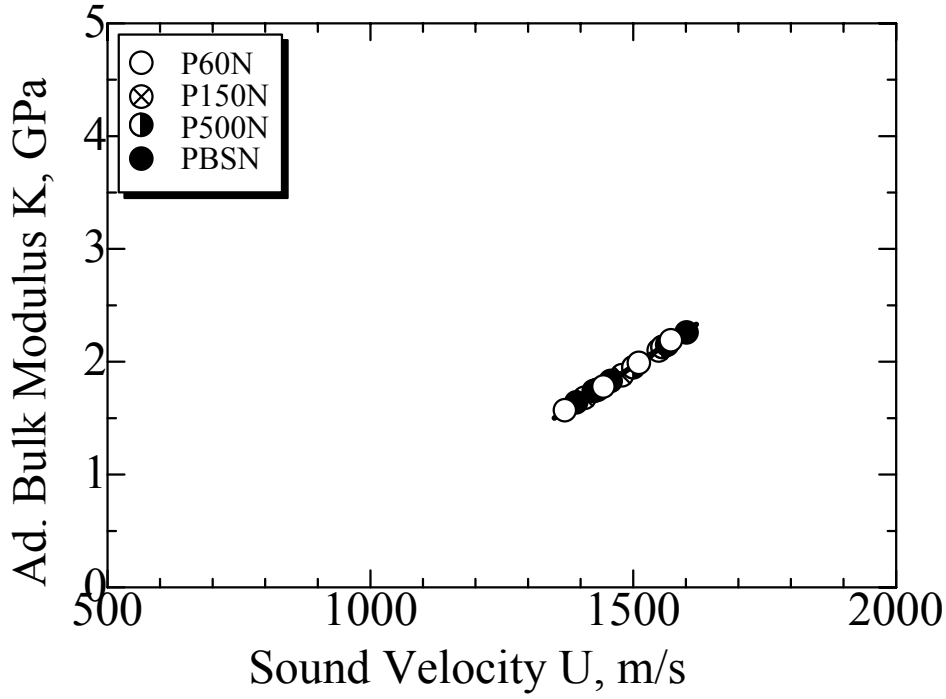


Fig. 4.11 Relation between adiabatic bulk modulus and sound velocity of paraffinic mineral oils

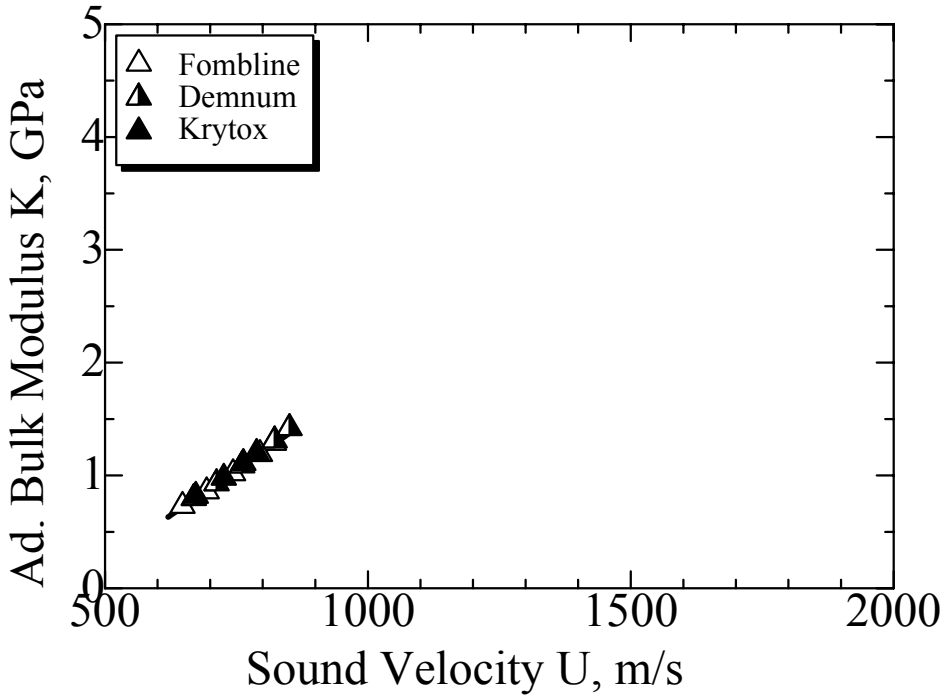


Fig. 4.12 Relation between adiabatic bulk modulus and sound velocity of PFPE oils

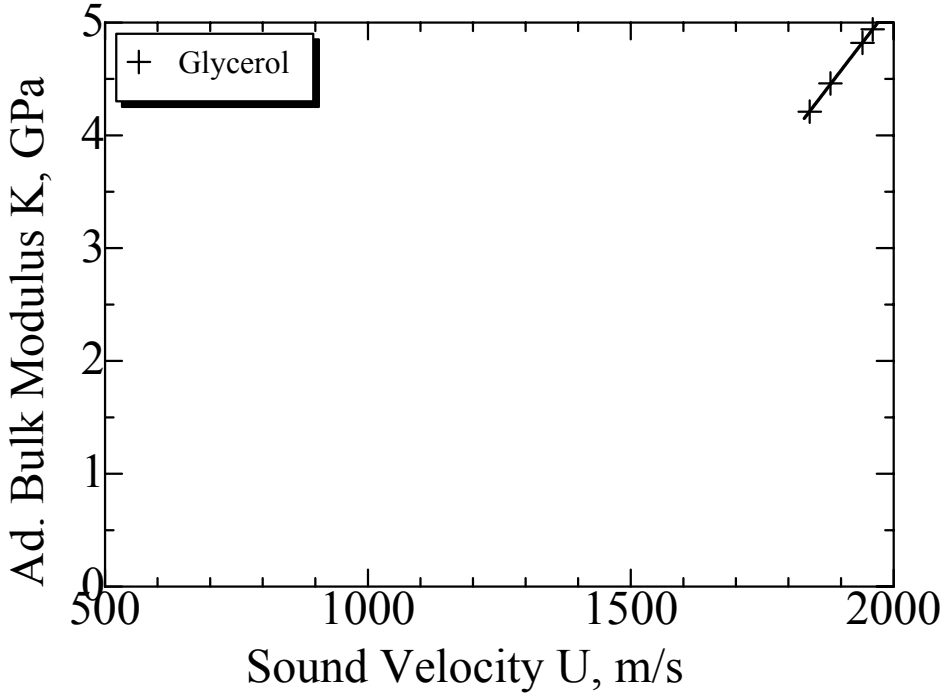


Fig. 4.13 Relation between adiabatic bulk modulus and sound velocity of glycerol

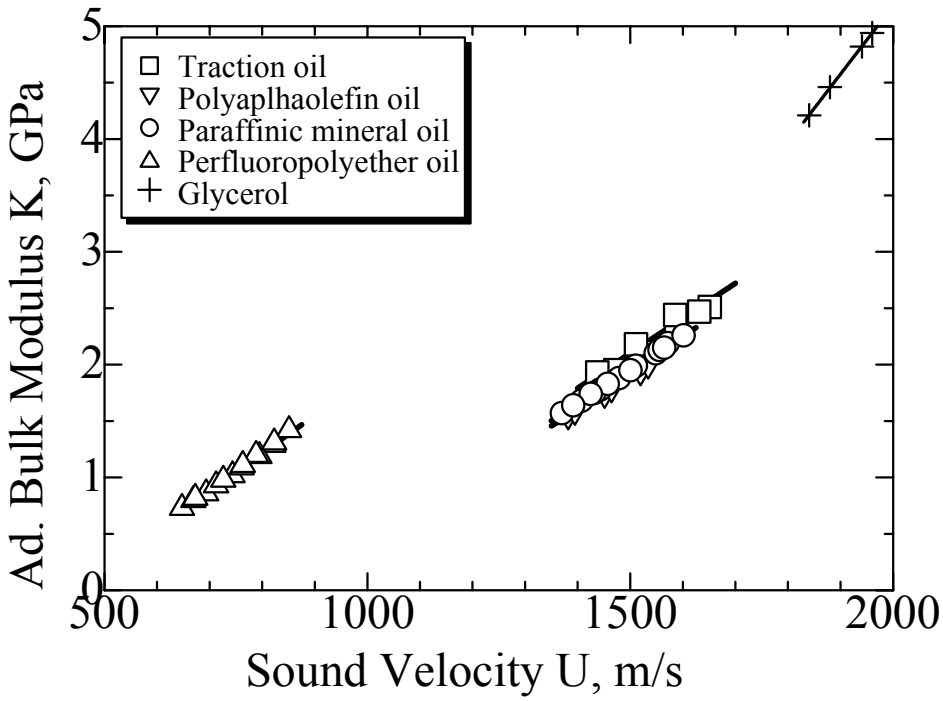


Fig. 4.14 Relation between adiabatic bulk modulus and sound velocity comprising all tested oils

In the Fig. 4.14, traction oils are shown at upper positions that of PAO oils and paraffinic mineral oils. PAO oils and paraffinic mineral oils are merged each other. On the other hand PFPE oil and glycerol placed at different position due to different molecular behaviors. Causes of these phenomena are the free volume and the intermolecular force of the liquid according to molecular structure, it influence directly on the sound velocity. The main molecular structure of traction oil SN32 and SN100 is cycloaliphatic hydrocarbon [61] and CVTF is bridged ring compound [62]. Therefore, for the closest results, it was divided into traction oil and mineral oil including PAO, for further analysis. Experimental values of pressure viscosity coefficient $\alpha$ and adiabatic bulk modulus $K$ calculated from sound velocity of lubricating oils are plotted in Fig. 4.15.

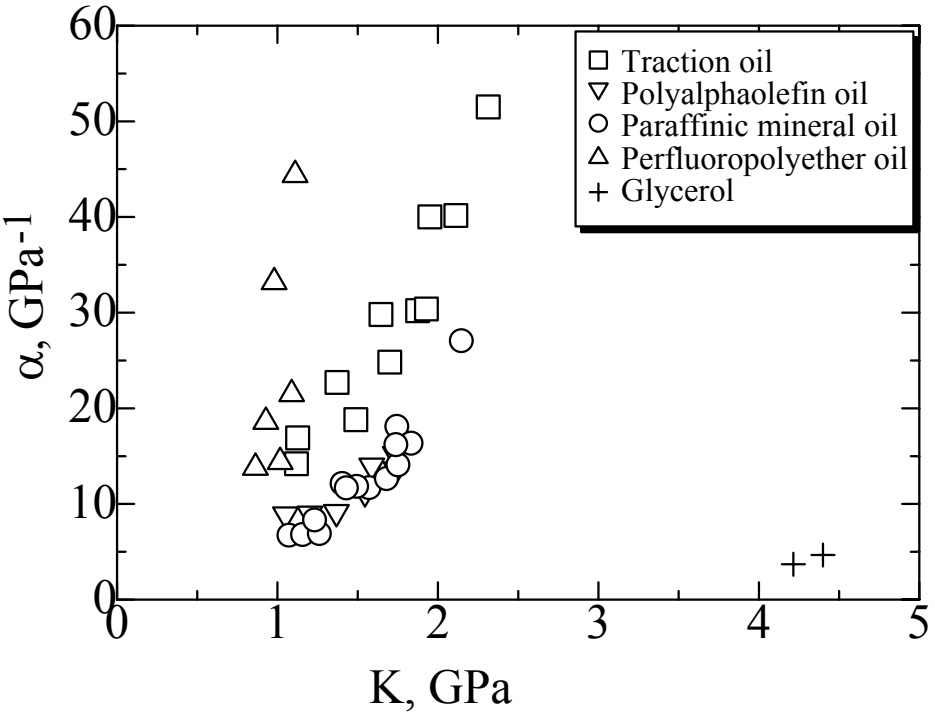


Fig. 4.15 Changes of α with respect to *K*

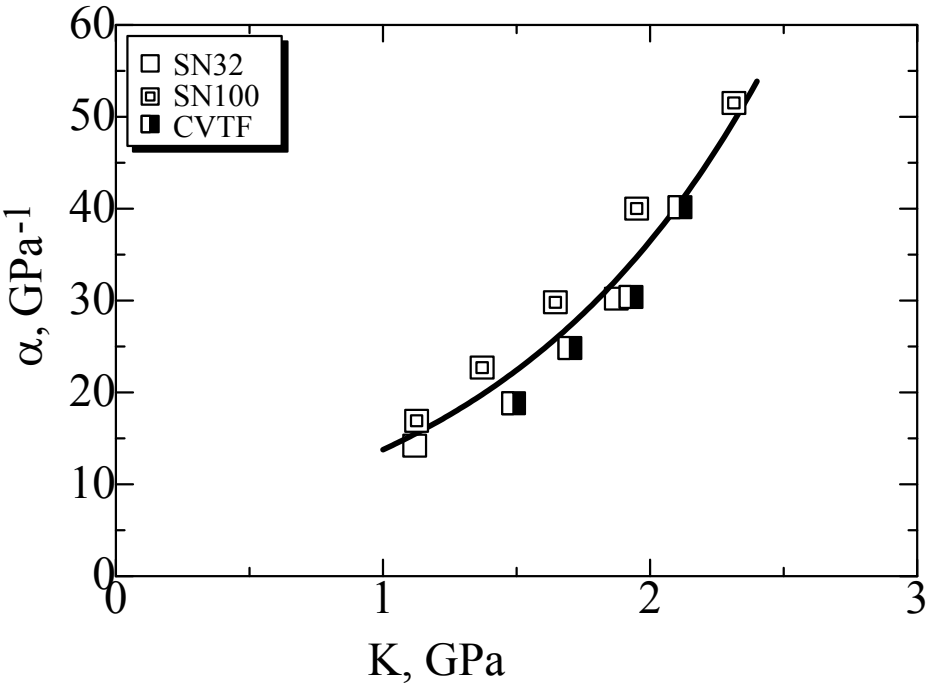


Fig. 4.16 Relation between α and *K* for traction oils

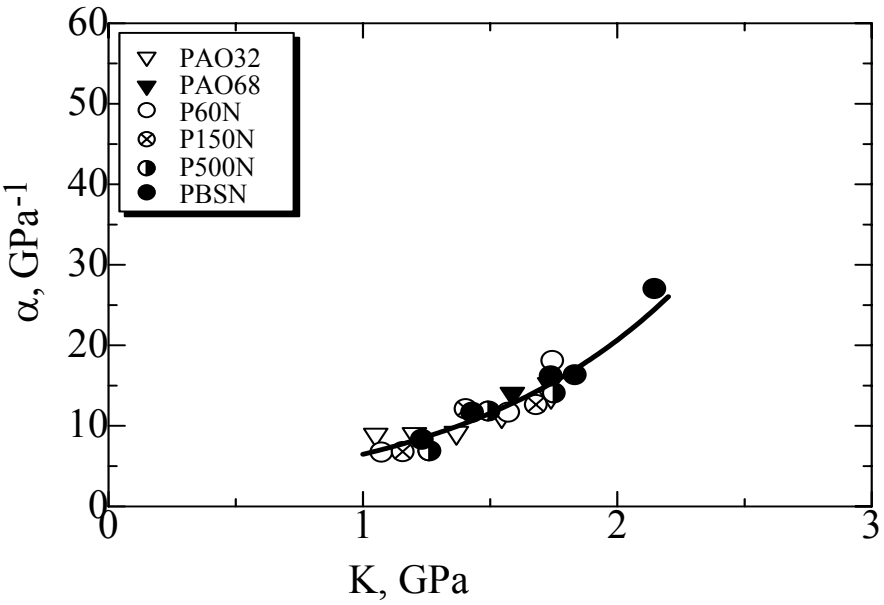


Fig. 4.17 Relation between α and *K* for PAO and paraffinic mineral oils

Figure 4.15 shows that the changes of pressure viscosity coefficient with adiabatic bulk modulus for traction oil increment is identifiable compared to others. Similarly the increment of polyalphaolefin oil and paraffinic mineral oils are considerably same and also identifiable from others. So, separated same behavior results to another graph. As a result, another two graph has found and can easily observed the changes of pressure viscosity coefficient with respect to adiabatic bulk modulus. Fig. 4.16 shows the relationship between pressure-viscosity coefficient and adiabatic bulk modulus for traction oils, and Fig. 4.17 demonstrates the relationship between pressure-viscosity coefficient and adiabatic bulk modulus for PAO and Paraffinic mineral oils

By the regression analysis for traction oil and also for PAO and paraffinic mineral oil, it has found that α increases exponentially with *K*. But in the methodology it was assumed that α is proportional to *K*. That was the assumption since in the liquid region both α and *K* increases proportionally with respect to pressure. In the Sing around sound velocity measurement, measured sound velocity was at liquid region. By analysis the relation between α and *K* for traction oils, it has found an excellent correlation. The relation is mentioned in Eq. 4.9.

$$\alpha = 5.20 \exp(0.974K) \tag{4.9}$$

Similarly, by the analysis of the relation between α and *K* for polyalphaolefin and paraffinic mineral oils, it has found that α increases exponentially with *K* following another excellent correlation. The relation for PAO and paraffinic mineral oils is shown in Eq. 4.10.

$$\alpha = 2.03 \exp(1.16K) \tag{4.10}$$

It was also calculated the predicted pressure-viscosity coefficient by the Eqs. 4.9 and 4.10 for corresponding oils. The predicted pressure-viscosity coefficient $\alpha_{cal}$ and the error with respect to experimental pressure-viscosity coefficient $\alpha_{exp}$ are mentioned in Table 4.6 and Table 4.7, where *T* is the temperature and *K* is the adiabatic bulk modulus. Error is shown as the deviation of calculated predicted pressure-viscosity coefficient from the experimental pressure-viscosity coefficient. Most of the error has found within ± 10 %, which was considered as permissible error for the prediction.

Table 4.6 Predicted pressure viscosity coefficient and error respect to experimental pressure viscosity coefficient for traction oil

| Sample oil | *T* | *K* | $\alpha_{exp}$ | $\alpha_{cal}$ | Error |
|---|---|---|---|---|---|
| | °C | GPa | $GPa^{-1}$ | $GPa^{-1}$ | % |
| SN32 | 40 | 1.87 | 30.2 | 32.3 | 6.8 |
| | 100 | 1.12 | 14.2 | 15.5 | 8.9 |
| SN100 | 20 | 2.31 | 51.5 | 49.5 | -3.8 |
| | 40 | 1.95 | 40.0 | 34.7 | -13.2 |
| | 60 | 1.65 | 29.8 | 25.8 | -13.3 |
| | 80 | 1.37 | 22.7 | 19.8 | -12.9 |
| | 100 | 1.13 | 16.9 | 15.6 | -7.9 |
| CVTF | 25 | 1.93 | 30.4 | 34.0 | 12.0 |
| | 40 | 2.11 | 40.2 | 40.7 | 1.3 |
| | 60 | 1.70 | 24.8 | 27.2 | 9.7 |
| | 80 | 1.49 | 18.8 | 22.2 | 17.9 |

Table 4.7 Predicted pressure viscosity coefficient and error respect to experimental pressure viscosity coefficient for PAO and paraffinic mineral oil

| Sample oil | *T* | *K* | $\alpha_{exp}$ | $\alpha_{cal}$ | Error |
|---|---|---|---|---|---|
| | °C | GPa | $GPa^{-1}$ | $GPa^{-1}$ | % |
| PAO32 | 20 | 1.74 | 13.6 | 15.3 | 12.2 |
| | 40 | 1.55 | 11.2 | 12.2 | 8.9 |
| | 60 | 1.37 | 9.1 | 9.9 | 8.5 |
| | 80 | 1.20 | 9.0 | 8.2 | -8.8 |
| | 100 | 1.05 | 8.9 | 6.9 | -22.9 |
| PAO68 | 25 | 1.59 | 14.0 | 12.8 | -8.6 |
| | 40 | 1.73 | 15.2 | 15.2 | -0.2 |
| P60N | 22 | 1.57 | 11.7 | 12.6 | 7.3 |
| | 40 | 1.74 | 18.1 | 15.4 | -15.2 |
| | 100 | 1.07 | 6.7 | 7.0 | 4.5 |
| P150N | 40 | 1.68 | 12.7 | 14.2 | 12.6 |
| | 70 | 1.40 | 12.1 | 10.3 | -14.8 |
| | 100 | 1.16 | 6.8 | 7.8 | 14.2 |
| P500N | 40 | 1.75 | 14.1 | 15.5 | 9.8 |
| | 70 | 1.49 | 11.8 | 11.5 | -3.0 |
| | 100 | 1.26 | 6.9 | 8.8 | 27.1 |
| PBSN | 20 | 2.15 | 27.1 | 24.5 | -9.6 |
| | 40 | 1.83 | 16.4 | 17.0 | 4.0 |
| | 50 | 1.74 | 16.2 | 15.2 | -5.9 |
| | 80 | 1.43 | 11.7 | 10.7 | -8.8 |
| | 100 | 1.23 | 8.3 | 8.5 | 1.7 |

These equations for prediction of pressure-viscosity coefficient were checked by testing some polymer-thickened oils as shown in Table 4.8. Viscosity index improver olefin copolymer (OCP) with $M_W=1.2x10^5$ added by different weight percent with PAO32 and TN32 oil. Tested results are shown in Table 4.9.

Table 4.8 Physical properties of PAO32 and TN32 with viscosity index improver OCP

| Oil name | Density ρ, g/mL | Kinematic viscosity ν, $mm^2/s$ | |
|---|---|---|---|
| | 15°C | 40°C | 100°C |
| PAO32 | 0.827 | 30.5 | 5.9 |
| +OCP 1% | 0.828 | 66.4 | 11.6 |
| +OCP 3% | 0.830 | 350.4 | 43.0 |
| +OCP 5% | 0.833 | 1595.0 | 144.9 |
| TN32 | 0.971 | 31.6 | 4.32 |
| +OCP 1% | 0.978 | 128.4 | 13.8 |

Table 4.9 Experimental results and comparison of the prediction equations at 40 °C

| Oil Name | *U* (m/s) | *K* GPa | $\alpha_{exp}$ $GPa^{-1}$ | $\alpha_{cal}$ $GPa^{-1}$ | Error (%) |
|---|---|---|---|---|---|
| PAO32 | 1382 | 1.55 | 11.2 | 12.2 | -8.9 |
| +OCP 1% | 1333 | 1.43 | 11.1 | 10.7 | 3.3 |
| +OCP 3% | 1334 | 1.44 | 11.2 | 10.8 | 3.3 |
| +OCP 5% | 1335 | 1.45 | 11.3 | 10.9 | 3.9 |
| TN32 | 1495 | 2.13 | 39.2 | 41.4 | -5.6 |
| + OCP 1% | 1500 | 2.14 | 38.2 | 41.8 | -9.4 |

In case of polymer thickened oils of PAO32 with OCP, it was calculated the prediction value of pressure-viscosity coefficient by Eq. 4.10, since the base oil was polyalphaolefin. Error has found within the accepted value. TN32 is usually produced from hydrogenation of the coal tar and then distillated under atmospheric pressure [63]. It is one kind of traction oil with condensed polycyclic naphthenic rings. The prediction value of pressure-viscosity coefficient of polymer thickened oil of TN32 was calculated by Eq. 4.9. It also shown acceptable error compared with experimental value.

## 4.6 Conclusion

The relationship between the pressure-viscosity coefficient and the bulk modulus is investigated in this study, being compared with those of several oils of different molecular structures. The following conclusion can be drawn from the study:

(1) Sound velocity in the lubricating oil is an important parameter, which is related to the molecular structure of lubricating oil.
(2) Adiabatic bulk modulus can be calculated from the sound velocity in lubricating oil.
(3) Pressure-viscosity coefficient is measured from the high-pressure viscosity measurement, which depends on free volume as well as the molecular structure of lubricating oil.
(4) From the study, it is found that the pressure-viscosity coefficient increases exponentially with the adiabatic bulk modulus. Hence, the relationship demonstrates that the pressure-viscosity coefficient can be predicted from the adiabatic bulk modulus. The prediction depends on the group of lubricating oil, due to their different molecular structure.
(5) This study proposes two equations to predict pressure-viscosity coefficient, one for the traction oil and another for the paraffinic mineral oil and polyalphaolefin oil. Using these equations, the pressure-viscosity coefficient can be predicted from the sound velocity in lubricating oil at atmospheric pressure.

Perfluoropolyether oil and Glycerol are not considered on the prediction due to inadequate experimental data. But in this study it has shown clearly that they have different behavior.

# Chapter 5

# Sound Velocity as an Indicating Parameter for Low Temperature Fluidity of Lubricating Oils

## 5.1 Introduction

Low temperature behavior of lubricating oil is essential for many applications such as at automobile cold start engine, aircraft or space mechanism, wind turbine etc. Low temperature fluidity is an important parameter for the selection of lubricating oil. The pour point is an indicating parameter of low temperature fluidity, which is defined in ASTM–D-97-39 as the lowest temperature at which the oil will pour or flow when it is chilled without disturbance under definite prescribed conditions. Bondi [7] reports that a large number of oils show glassy solidification due to higher viscosity at the pour point. Viscoelastic solid transition temperature $T_{VE}$ also represents the low temperature fluidity of lubricating oil. The physical and practical significance of viscoelastic solid transition temperature is much better than the pour point.

Recently, Sharma and Stipanovic [33] reported a process for predicting low temperature rheology using nuclear magnetic resonance spectroscopy and mass spectrometry. They found the effect of hydrocarbon base oil composition on the low temperature rheology of lubricants. Ohno [34] reported that the $T_{VE0}$ is related with free volume and free volume also related with tangential bulk modulus ($K_T$). There is a well-known relation between tangent bulk modulus $K_T$ and adiabatic bulk modulus $K$, which can be expressed as $K = \kappa K_T$, where $\kappa$ is the ratio of specific heat at constant pressure and constant volume [7]. From the study, it is found that there is a relation between sound velocity and the adiabatic bulk modulus. In this study, it is investigated experimentally to find out a relation between the viscoelastic solid transition temperature and the adiabatic bulk modulus of lubricating oils.

In the previous study, viscoelastic solid transition temperature is estimated from the occurrence of photo elastic effect by lowering the temperature using liquid nitrogen [62]. The same technique is applied in the current study. The measurement is quite difficult and requires low temperature apparatus for handling the liquid nitrogen. Again, Calculating the adiabatic compressibility or adiabatic bulk modulus from

sound velocity is a well-established practice [9-12]. The compressibility and density are combined using Urick equation [11], which was based on an idea suggested by Wood [12]. Kondo et al. [64] combines optical interferometry from ultrasonic pulse echo reflection coefficient techniques to determined bulk modulus of entrapped films. Recently, ultrasonic wave is also using for measuring viscosity of thin lubricant films [65]. It can conclude from the above studies that, sound velocity is directly related to the bulk properties of any substance. In this study, bulk modulus has been calculated from the sound velocity in the lubricating oil. It has been found experimentally that, viscoelastic solid transition temperature has relation with the adiabatic bulk modulus. The relation depends on the molecular structure of the lubricating oils and linear relation exhibits for same group of lubricating oil. Then, author studied about the blend oils of different group of lubricating oil and found that estimation of blend's low temperature fluidity can possible from their base oils $T_{VE0}$ and adiabatic bulk modulus [66].

## 5.2 Experimental

### *5.2.1 Sample Oils*

Several kinds of lubricating oils from different group were tested. List of tested oils and their physical properties are given in Table 3.1 to Table 3.6. Blends of disebacate (DOS), benzylbiphenylhydride (BBPH), a bridged ring compound (SNHV) and a paraffinic mineral oil (PBSN) are also considered in the study. Hayashi et al. [67] also used the same blend oils in their study.

### *5.2.2 Sound Velocity in Lubricating Oil*

Sound velocity is measured using the Sing around UVM-2 device (Cho-Onpa Kogyo Company, Japan). Details of the device and the measuring procedure of sound velocity have been given in chapter 2. The basic principle of this device is the ultrasonic wave pulse launches from the transmission oscillator. The wave pulse propagates in the sample, and then receives to the reception oscillator. The ultrasonic wave pulse converts into mono pulse after amplifying the auto gain control. Then it passes through the delay circuit and receives again the supersonic wave pulse. Sing around device displays total propagation time of the cycle including delay time. It also displays the delay time of the circuit. The propagation time of the sample inside is

calculated from the difference between the above mentioned times of a cycle when propagation becomes steady. A sing around software using PC 98 series computer check the steadiness of the propagation. Sound velocity in lubricating oil is measured from the propagation time in the sample oil and the distance between 2 ultrasonic transducers in the oil container.

Sound velocity $U$ in sample oils is measured at different temperatures. A temperature control bath is used to control the temperature. The change of sound velocity with temperature for one sample of each group of lubricating oil is shown in Fig.5.1. It shows that the sound velocity decreases with the increases of temperature. Relation between the sound velocity and temperature for ester oils is also shown in Fig 5.2.

Adiabatic compressibility or adiabatic bulk modulus of sample oils is calculated from the sound velocity using the Wood equation [6]:

$$U = \frac{1}{\sqrt{\rho\beta}} = \sqrt{\frac{K}{\rho}} \qquad (5.1)$$

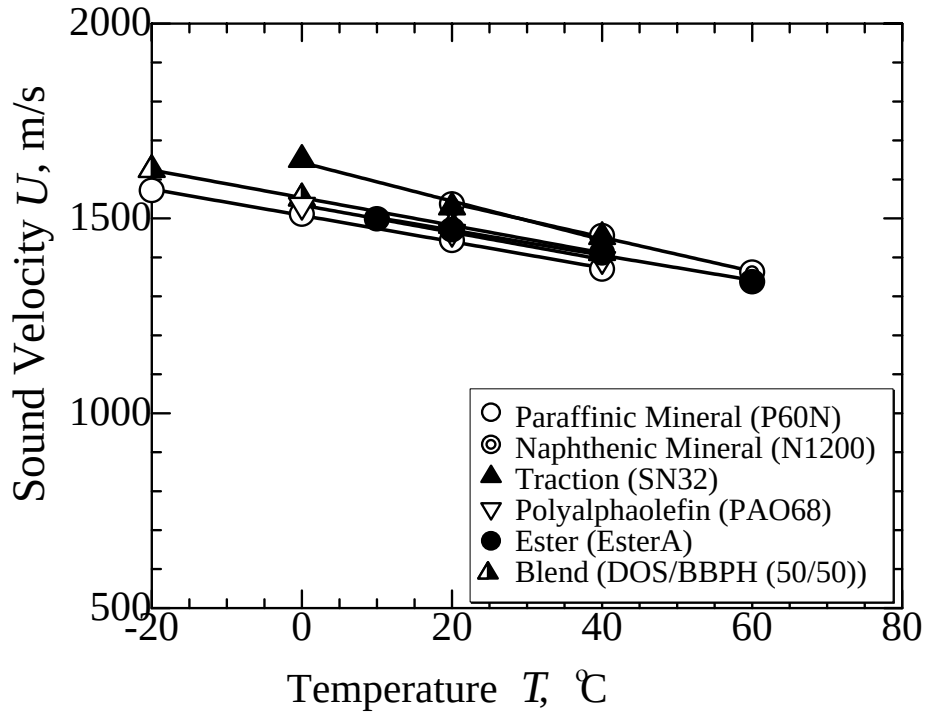


Fig. 5.1 Changes of Sound velocity with temperature of lubricating oils

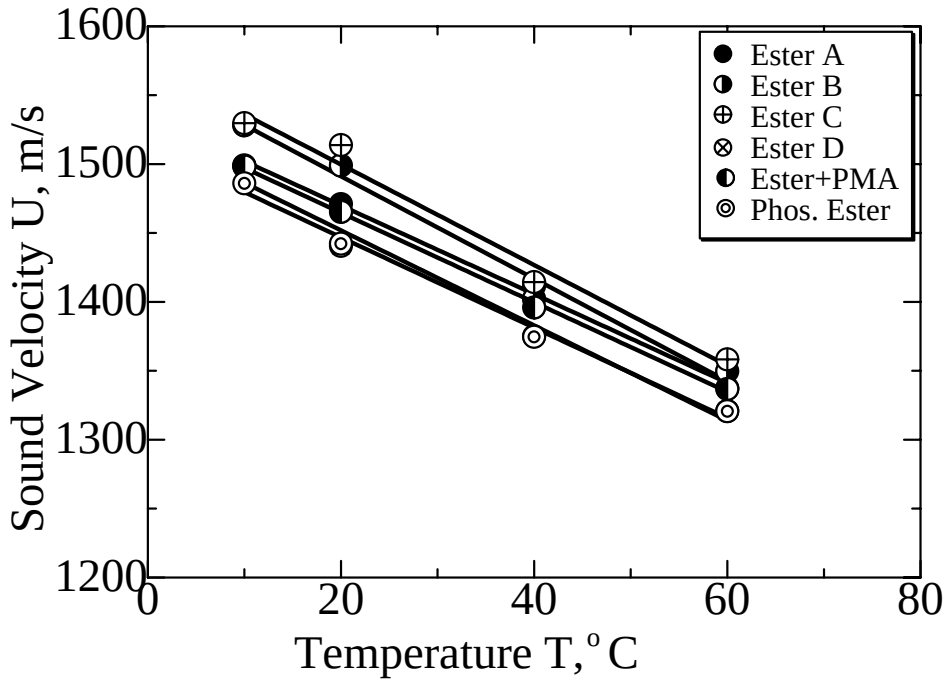


Fig. 5.2 Changes of Sound velocity with temperature for Ester oils

where $U$ is the sound velocity (m/s), β is the compressibility ($Pa^{-1}$) which is reverse of adiabatic bulk modulus $K$ (Pa) and ρ is the density ($kg/m^3$). The density of the sample oils is measured using a digital density meter (Model: DA-130, Kyoto Electronics Manufacturing Co. Ltd., Japan).

### *5.2.3 Low Temperature Fluidity*

Viscoelastic solid transition temperature at atmospheric pressure ($T_{VE0}$) is an indicating parameter of low temperature fluidity of lubricating oil. Details of the experimental devices, set up and measuring procedure have been discussed in chapter 3. In the experiment, an air bubble is inserted into the sample oil, which is covered by two glass plates. Fig.5.3 represents the experimental view of sample oil with air bubble at the beginning of measurement. The diameter of the air bubble apparently expands due to contraction of liquid by means of cooling. Thus expanded bubble generates tensile stresses along its interface of test oil under solidified condition. At the same time, the photoelastic effect appears at dark polarized field as shown in Fig. 5.4. This enables the stress analysis and estimation of mechanical properties of the

solidified fluid [68]. The temperature, when the photoelastic effect occurs, is identified as viscoelastic solid transition temperature ($T_{VE0}$) of the sample oil at atmospheric pressure. The expansion of air bubble diameter with temperature for ester A is presented in Fig. 5.5 with point out the $T_{VE0}$.

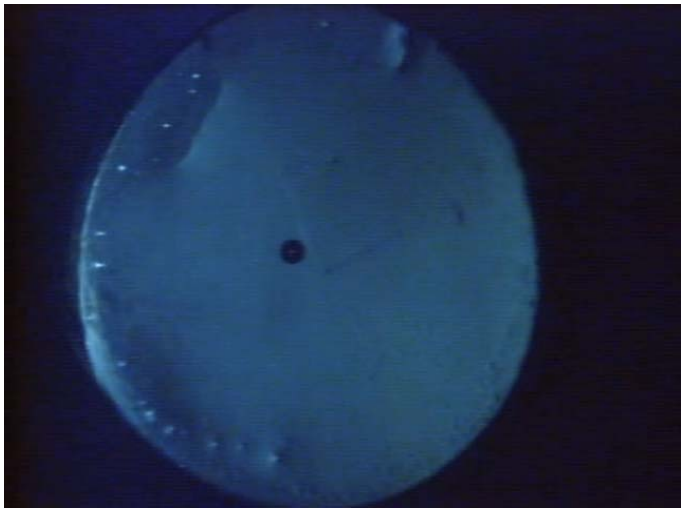

Fig. 5.3 Experimental views of $T_{VE0}$ measurement of Ester A oil at the 0 °C.

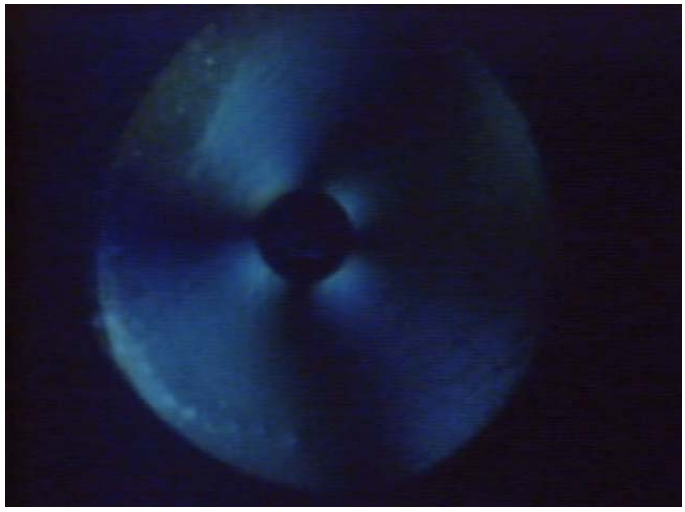

Fig. 5.4 Experimental views of $T_{VE0}$ measurement of Ester A oil at the -58 °C.

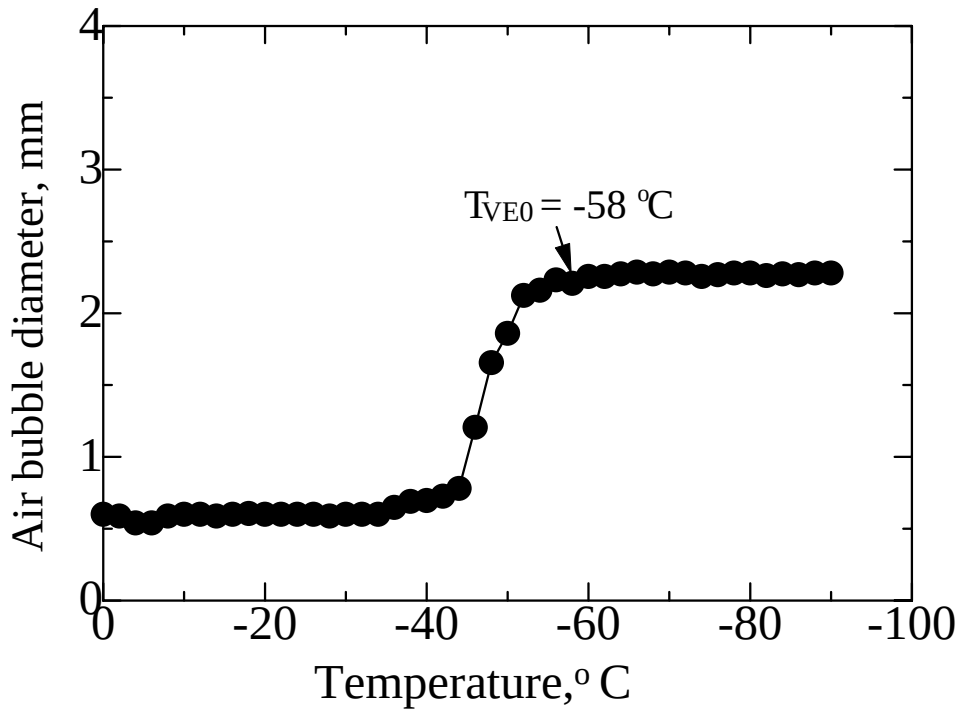


Fig. 5.5 Increases of air bubble diameter at $T_{VE0}$ measurement for Ester A.

## 5.3 Results & Discussion

Viscoelastic solid transition temperature of lubricating oil has physical significance on lubricant's rheology. Solidification as viscoelastic solid or an elastic-plastic solid occurs when the value of $T_{VE} - T$ exceeds the critical value $T_{VE} - T > 0$ (where $T_{VE}$ is the viscoelastic solid transition temperature at pressure $p$; and $T$ is the oil temperature) [69]. Viscoelastic solid transition temperature at pressure $p$ of oil can obvious from the tangent bulk modulus. Again, lubricant's liquid-solid phase behavior can be known from its viscoelastic solid transition temperature at different pressures [62]. Ohno et al. [70] showed the dependency of the squeeze out time of entrapped oil film at EHL experiment on the phase diagram parameter $T_{VE} - T$. In this study, all experiments are conducted at atmospheric pressure.

Table 5.1: Experimental results of tested oils

| Group | Oil name | Sound velocity *U*, m/s (at 40°C) | Adiabatic Bulk modulus *K*, GPa (at 40°C) | Viscoelastic solid transition temperature $T_{VE0}$, °C |
|---|---|---|---|---|
| Paraffinic Mineral | P60N | 1370 | 1.57 | -46 |
| | P150N | 1408 | 1.68 | -36 |
| | P500N | 1432 | 1.75 | -26 |
| | PBSN | 1457 | 1.83 | -36 |
| Naphthenic Mineral | N1200 | 1456 | 1.89 | -29 |
| Traction | SN32 | 1453 | 1.89 | -70 |
| | SN100 | 1472 | 1.95 | -56 |
| | CVTF | 1437 | 1.93 | -77 |
| | BBPH | 1476 | 1.98 | -62 |
| | SNHV | 1460 | 2.06 | -52 |
| Ester | EsterA | 1412 | 2.09 | -58 |
| | Ester B | 1402 | 2.37 | -32 |
| | Ester C | 1414 | 2.30 | -38 |
| | Ester D | 1375 | 2.14 | -54 |
| | Ester+PMA | 1396 | 2.03 | -58 |
| | Phos. Ester | 1375 | 2.19 | -52 |
| | DOS | 1361 | 1.66 | -99 |

Experimental results of viscoelastic solid transition temperature at atmospheric pressure $T_{VE0}$, Sound velocity *U* and calculated adiabatic bulk modulus *K* for all samples are presented in Table 5.1. $T_{VE0}$ of the sample oils and *K* at 40°C of corresponding oils are plotted in Fig. 5.6. It also represents the relation between them. The viscoelastic solid transition and the bulk modulus of oil are related with its molecular structure [71]. A linear relation exhibits between the $T_{VE0}$ and *K* for the same group of oils based on molecular structure. For the lower bulk modulus, viscoelastic solid transition temperature also shows the lower value. In the case of different molecular structure of sample oils, it is not merged the relation.

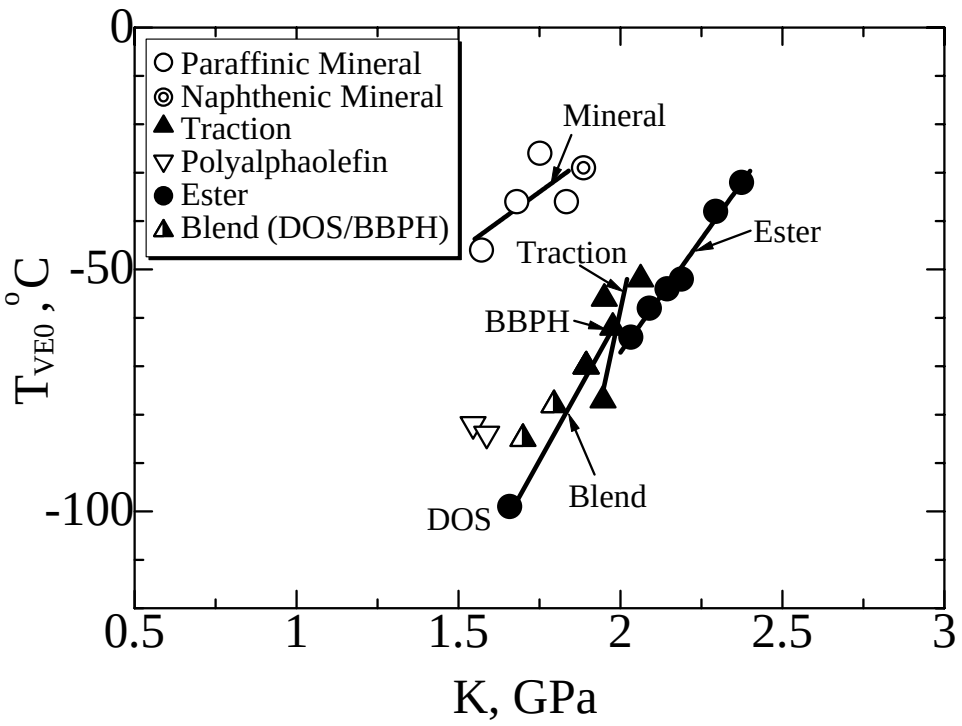


Fig. 5.6 Relation between viscoelastic solid transition temperature $T_{VE0}$ and adiabatic bulk modulus $K$ at 40°C.

Naphthenic and paraffinic mineral oils are almost similar molecular structure comparing with other and they follows almost the same relation in the figure. Considering individually, non-linearity found due to paraffinic chain and naphthenic ring compound in their molecular structure. Molecular structure of paraffinic mineral oil P60N, P150N and P500N is almost similar but different with PBSN and N1200 oil. Again, in case of traction oil, sample oil's molecular structure is different. CVTF belongs to bridge ring compounds, which differs from SN32 and SN100. Where as, a linear relation is found for the ester oils. The linear relation is also found for the two-oil blend (DOS/BBPH). Relation between viscoelastic solid transition temperature at atmospheric pressure and adiabatic bulk modulus of each group of oil is shown in Fig. 5.7 to Fig. 5.10.

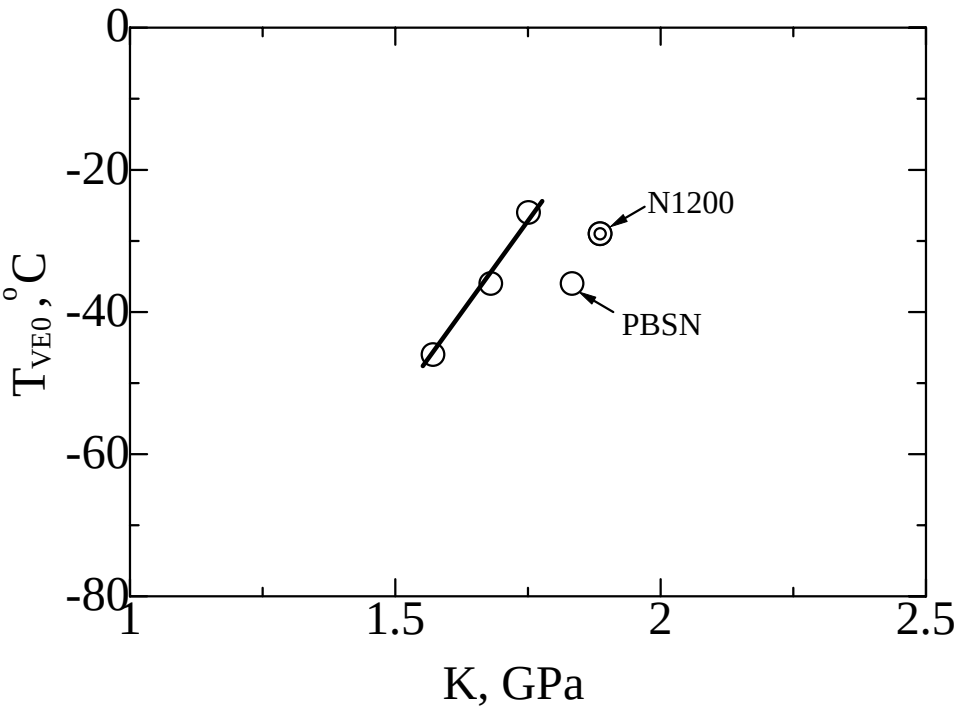


Fig. 5.7 Relation between viscoelastic solid transition temperature $T_{VE0}$ and adiabatic bulk modulus $K$ at 40°C for mineral oil.

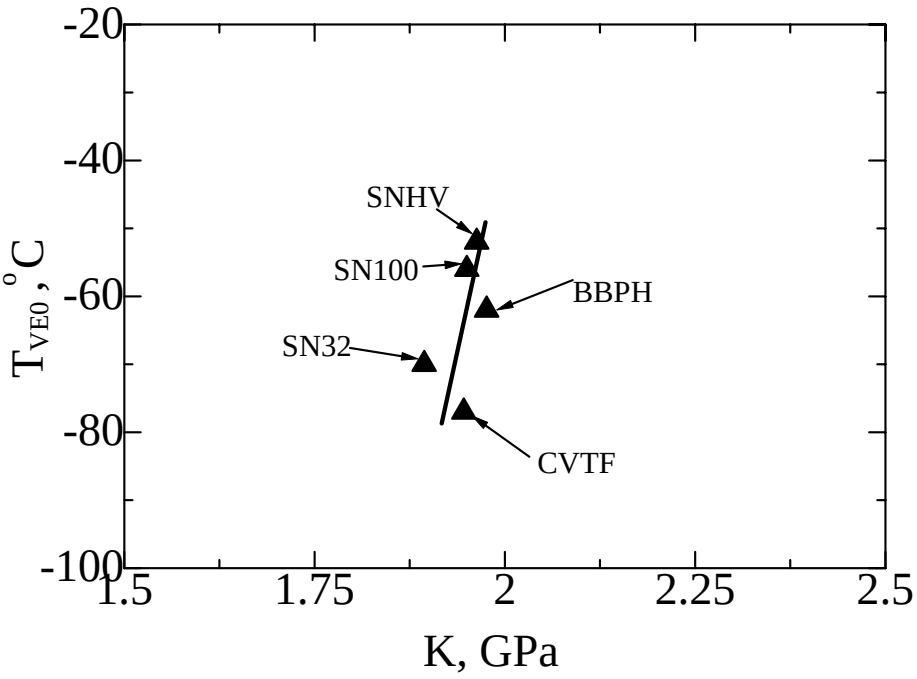


Fig. 5.8 Relation between viscoelastic solid transition temperature $T_{VE0}$ and adiabatic bulk modulus $K$ at 40°C for traction oil.

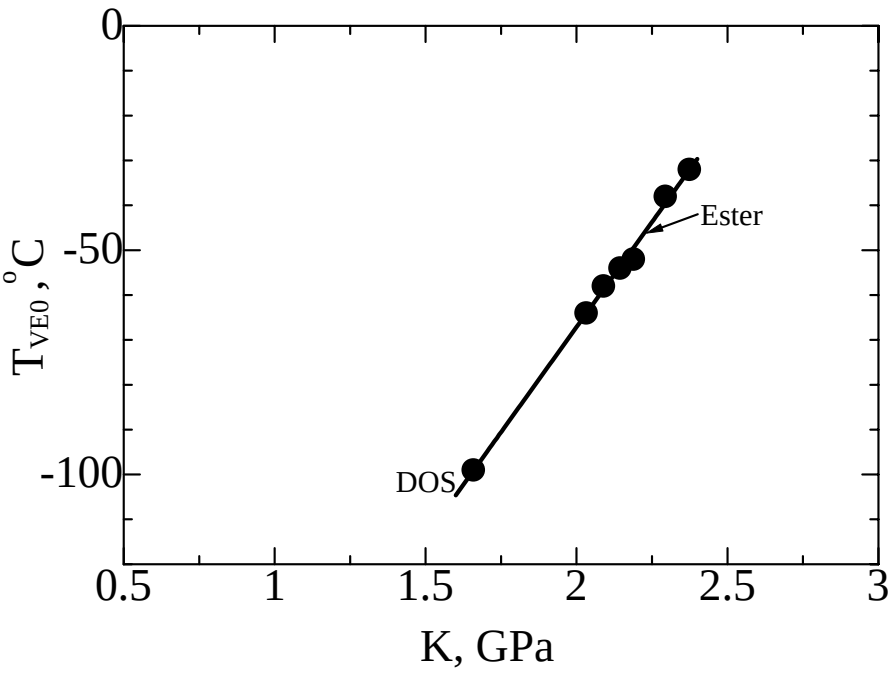


Fig. 5.9 Relation between viscoelastic solid transition temperature $T_{VE0}$ and adiabatic bulk modulus $K$ at 40°C for Ester oil.

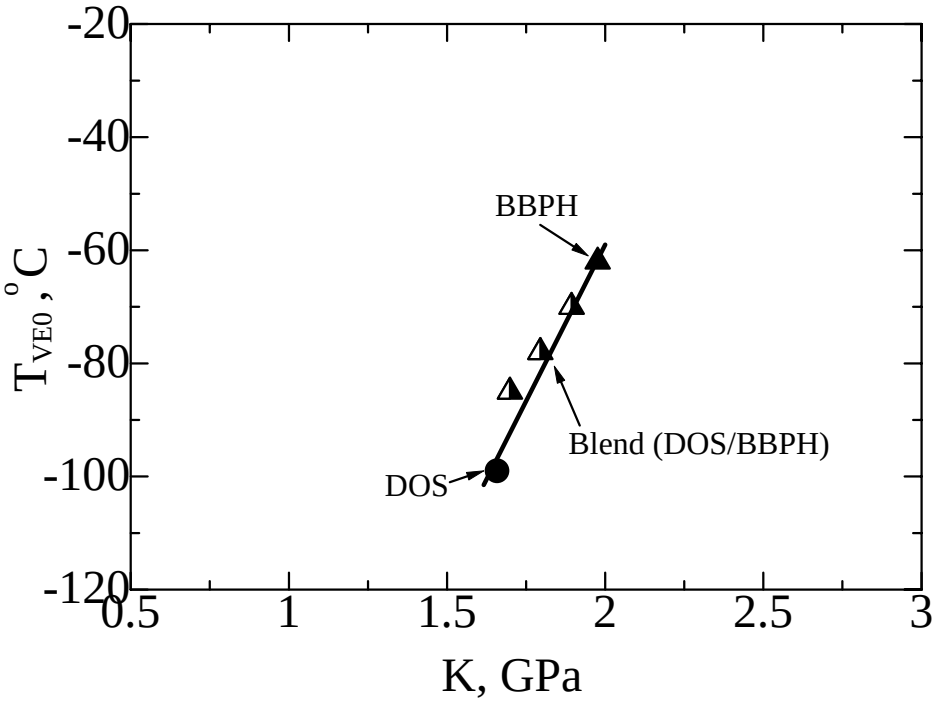


Fig. 5.10 Relation between viscoelastic solid transition temperature $T_{VE0}$ and adiabatic bulk modulus $K$ at 40°C for blend oil (DOS/BBPH).

The relation between the viscoelastic solid transition temperature $T_{VE0}$ and the adiabatic bulk modulus $K$ for blend oils is also observed in the study. Hayashi et al. [67] found the predicting relation of pressure viscosity coefficient of blend oils from the base oils' viscosity. The same blend oils are considered here for the prediction of viscoelastic solid transition temperature [66]. Figure 5.11 shows the graphical representation of $T_{VE0}$ and $K$ for the four base oils and two-oil [1:1] blend of each other. A quadrilateral is drawn from the four base oils data. Each side of the quadrilateral represents the relation for the blends of two oils.

The experimental values of two-oil [1:1] blend do not coincide the middle of respective side of quadrilateral but it shows almost similar values especially for the $T_{VE0}$. It also can predict the viscoelastic solid transition temperature $T_{VE0}$ of four-oil mixture. The estimation result for four-oil mixture [1:1:1:1] is shown in Fig. 5.12.

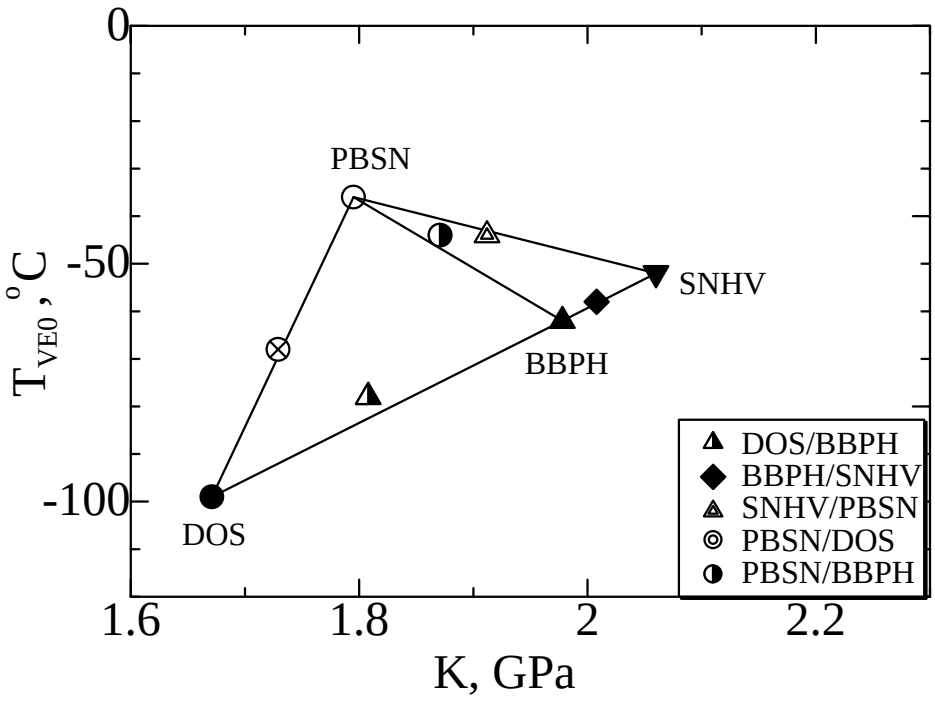


Fig. 5.11 Relation between Viscoelastic solid transition temperature $T_{VE0}$ and adiabatic bulk modulus $K$ at 40°C for the 4-blend oils.

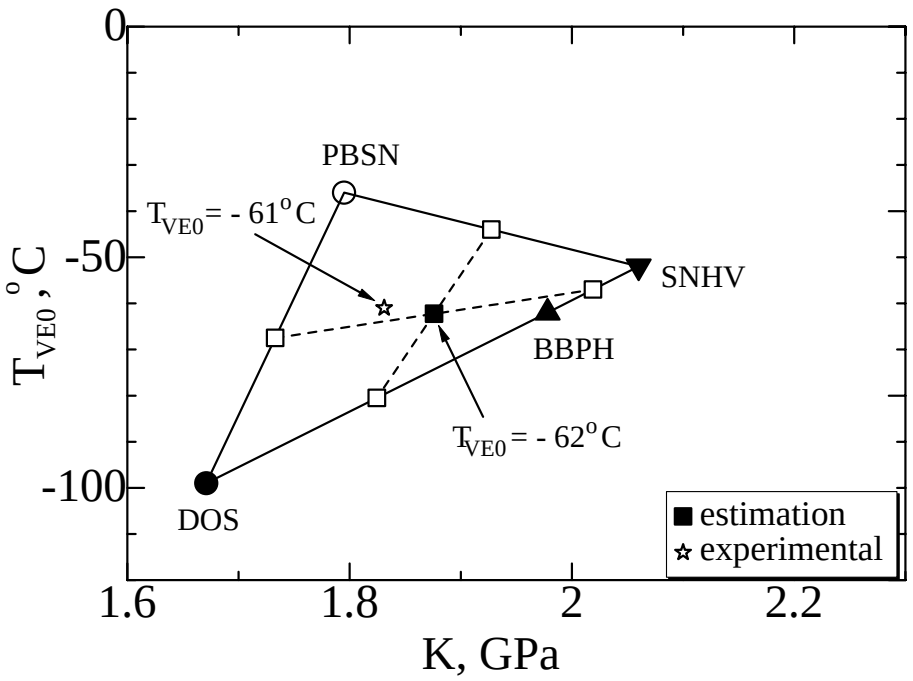


Fig.5.12 Estimation of viscoelastic solid transition temperature $T_{VE0}$ for 4-oil blend. K: adiabatic bulk modulus at 40°C.

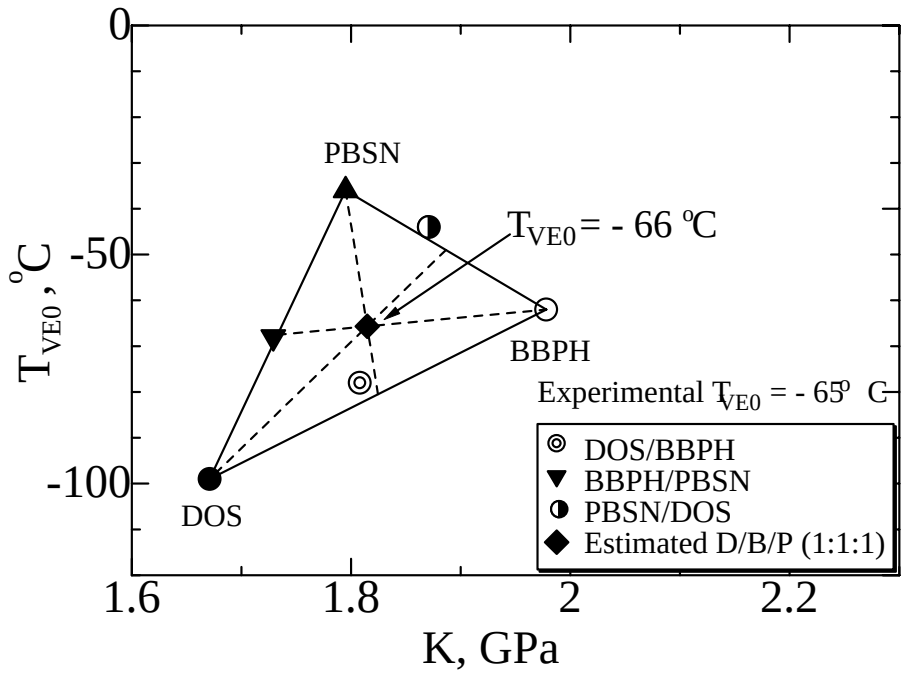


Fig. 5.13 Estimation of viscoelastic solid transition temperature $T_{VE0}$ for 3-oil blend. K: adiabatic bulk modulus at 40°C.

For the estimation, first pointed out the midpoint of each side of the quadrilateral and then connected the four midpoints. Two medians intersect at a point, which represents the estimation value. The corresponding value of $T_{VE0}$ represents the predicted viscoelastic solid temperature that corresponds to the low temperature fluidity of the blend. Estimation of the $T_{VE0}$ is found for the four-oil blend is -62°C, whereas experimentally it is at -61°C. Similar prediction can be possible for three-oil blend and any other proportion of blend. Figure 5.13 shows the prediction of viscoelastic solid transition temperature for three-oil blend from a triangular using the base oil's $T_{VE0}$ and $K$. According to the estimation, the $T_{VE0}$ for the three-oil blend is found at –66 °C whereas experimentally it is found at -65°C. Closer results of estimated value and experimental value express the possibility of prediction.

## 5.4 Conclusion

Low temperature fluidity is related to the bulk property as well as the sound velocity in lubricating oil. From the study, the following conclusions are drawn:

1. Adiabatic bulk modulus is a property that related to the molecular structure, which can be calculated from the sound velocity. Sound velocity can measure accurately by passing the sound wave through the sample.

2. For the lubricating oil of low adiabatic bulk modulus, good low temperature fluidity is found. Low adiabatic bulk modulus of oil indicates the lower viscoelastic solid transition temperature in case of the same group of oil.

3. In the case of blend oils, viscoelastic solid transition temperature can predict from the base oils' adiabatic bulk modulus and viscoelastic solid transition temperature. Hence, low temperature fluidity of blend oil can predict from the base oils' sound velocity.

# Chapter 6

# Effect of Molecular Structure of Lubricating Oil on the Sound Velocity

## 6.1 Introduction

Sound is the disturbance of molecules whose propagation is facilitated by the collisions between particles. This disturbance propagates in a longitudinal wave, one molecule hits the next molecule and that molecule hits the next, and so forth. So far, it is well known that sound velocity is an important criterion on the basis of molecular structure as well as elastic constant of any substance. Sound velocity is directly related with the bulk modulus and density of a substance. In case of liquid, the bulk modulus is known as adiabatic bulk modulus. First Laplace [10], then Wood [12] introduces the relation between sound velocity and bulk modulus of liquid. Povey et al. [15] showed that in mixtures of molecules, thermal scattering significantly affects the sound velocity, making the determination of molar sound velocity in the mixture of core complicated.

Pressure-viscosity coefficient $\alpha$ of lubricating oil is an important property to know the performance of lubricating oil under elastohydrodynamic lubrications. Mia and Ohno [60] showed the pressure-viscosity coefficient of lubricant could be predicted by measuring the sound velocity in lubricating oil. The investigation of the study is to identify on the basis of the group of lubricating oil. There are many group of lubricating oil. Here the groups are considered on the basis of the molecular structure as like traction oil, polyalphaolefin (PAO) oil, paraffinic mineral oil, perfluoropolyether (PFPE) oil, and glycerol. According to chemical structure, traction oils are naphthenic hydrocarbon, polyalphaolefin oils are synthetic branched hydrocarbon and paraffinic mineral oils are long chain hydrocarbon. Perfluoropolyether and glycerol consists of different molecular structure in where PFPE consists of Fluorine with carbon bonding and glycerol has hydroxyl group. The relation between low temperature fluidity and the adiabatic bulk modulus of lubricating oil also exhibited the dependency on the molecular structure.

In the previous chapters, author described the measuring procedure of Sound velocity using Sing around method and the prediction of rheological parameters from the measured sound velocity. In this chapter, the effect of molecular structure on

sound velocity of lubricating oil has been investigated. The property, density and surface tension are related to the molecular behavior of any substance. Density of the test lubricant was measured using an electronic density meter. Surface tension was measured by Pendant drop shape analysis method. Measuring procedure of surface tension is given in chapter 3. When compared these properties with sound velocity every group showed different behavior due to different molecular structure.

## 6.2 Chemical Structure of Lubricating Oil

Chemical structure of base oil of tested lubricating oils are shown in Fig. 6.1 to 6.3.

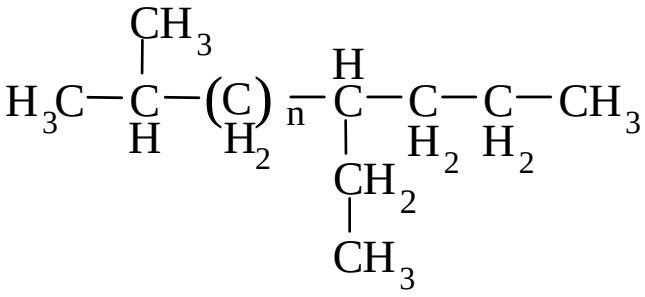

(a) Paraffinic mineral series

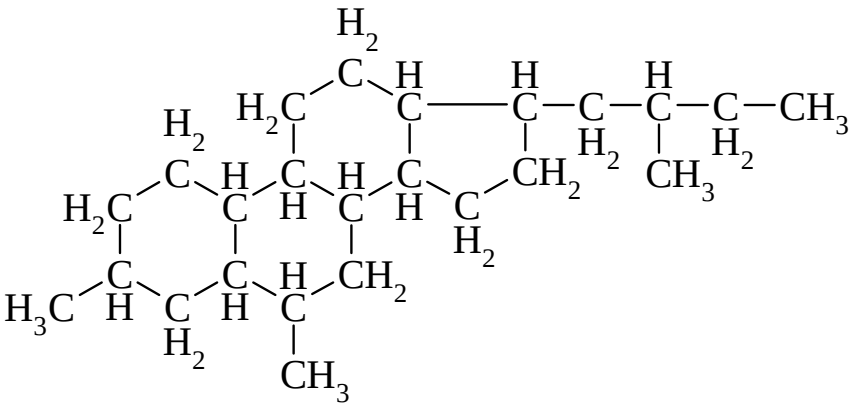

(b) Naphthene mineral series

Fig. 6.1 Chemical structure of mineral oil

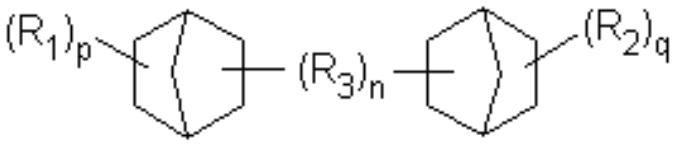


(a) Bridged ring compounds (CVTF)

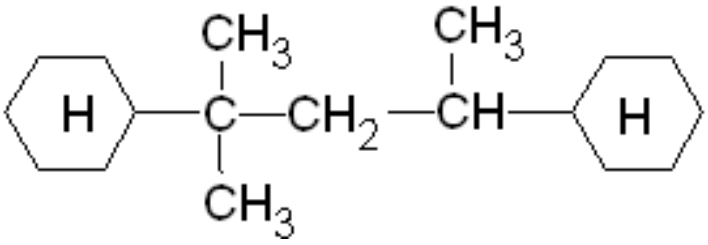


(b) Synthetic Cycloaliphatic Hydrocarbon (SN32, SN100)

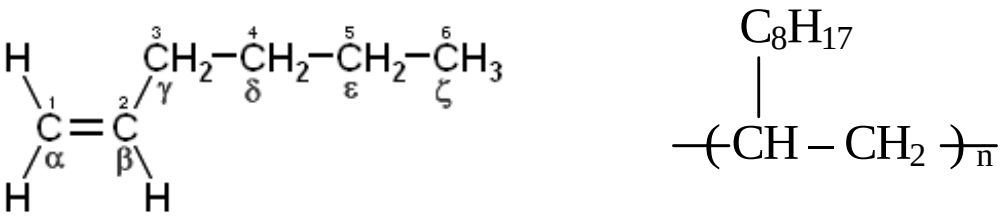


(c) Polyalphaolefin (PAO)

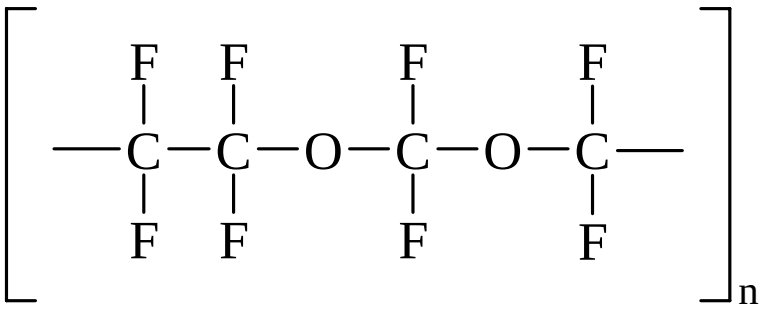


(d) Perfluoropolyether (PFPE) series

Fig. 6.2 Chemical structures of traction oil, PAO oil and PFPE oil

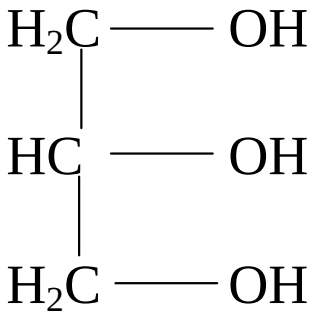


(a) Glycerol

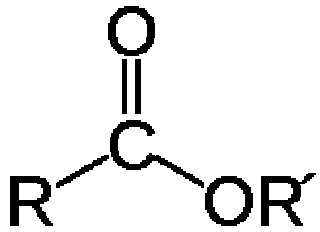


(b) A carboxylic acid ester. R and R' denote any alkyl ($C_nH_{2n+1}$)or aryl ($C_6H_5$) group.

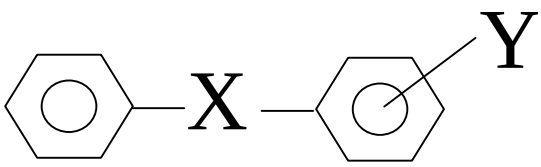


(c) Aromatic Ester
(tested sample ester oils)

Fig. 6.3 Chemical structures of glycerol and ester oils

## 6.3 Experimental Procedure

Sound velocity was measured by the Sing around UVM-2 apparatus. Apparatus consists of an oil container with 2 ultrasonic transducers. The Sing around device combines with the ultrasonic transducer and measures the supersonic wave spread time in a sample liquid. The basic principle of this device is the ultrasonic wave pulse launched from the transmission oscillator propagates in the sample and is received to the reception oscillator. The description of the Sing around device and the measuring procedure of sound velocity in lubricating oil are given in chapter 2.

Sound velocity U of tested lubricating oils was measured at different temperature. The change of sound velocity with temperature of all tested lubricating oils is shown in Fig. 6.4. Figure shows that sound velocity decreases proportionally with the temperature since the molecular bonding looses due to increasing of temperature.

Adiabatic bulk modulus *K* of a substance essentially measures the substances to uniform compression. It is also defined as the pressure increases needed to affect a given relative decrease in volume.

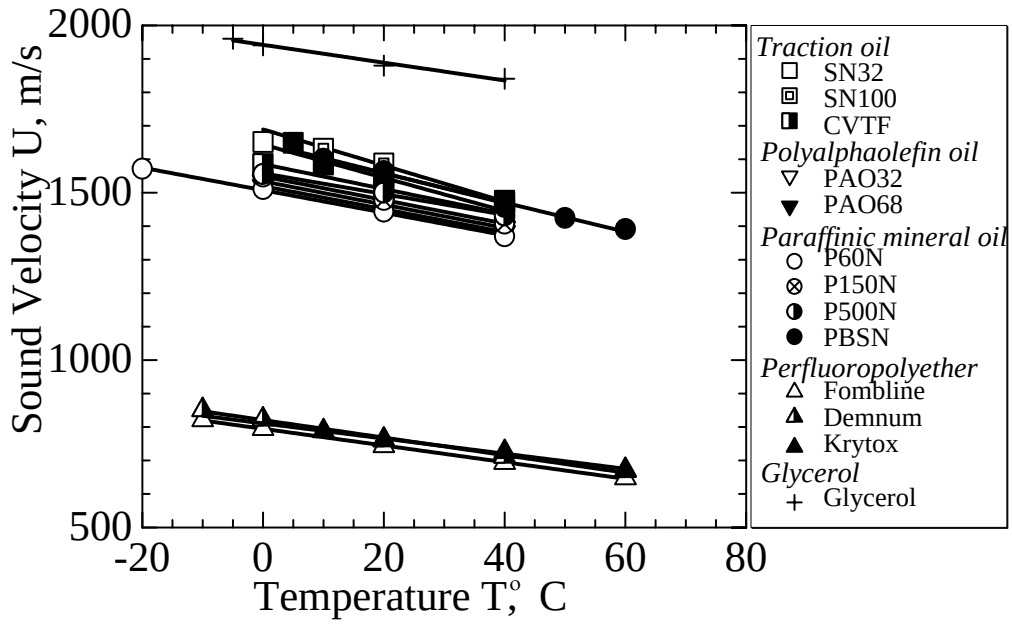


Fig. 6.4 Changes of sound velocity with temperature

This important property related to the molecular structure was calculated from the measured sound velocity. A digital density meter was used to measure the accurate density of tested oil. Another important property of liquid is surface tension. It is a measurement of the cohesive energy present at an interface. The molecules of a liquid attract each other. An equal attractive force in all directions balances the interactions of a molecule in the bulk of a liquid. Surface tension was measured at 20°C and 40°C by Pendant drop method. There are many relations between the surface tension and other physical and chemical properties [72]. Macleod relation is one of them. Macleod found that the fourth root of surface tension divided by the density is independent of temperature [73],

$$\gamma^{\frac{1}{4}}/(\rho_L - \rho_G) = const. \qquad (6.1)$$

where $\gamma$ is the surface tension, $\rho_L$ and $\rho_G$ refer to the densities of the liquid and the gas phase. $\rho_G$ can ordinarily be neglected. Other values of surface tension were calculated using Eq. 6.1.

Finally all these properties of the sample oils were compared with sound velocity in them.

## 6.4 Results and Discussion

Sound velocity is directly related to the molecular structure and the properties such as density, bulk modulus, surface tension etc. which are related with molecular structure. Here the relation between sound velocity and all these properties are shown graphically. Figure 6.5 shows the relation between density and sound velocity of tested fluids. It has been recognized for several decades that the density of liquid is closely related to its molecular composition. Comparison shows that the plots are positioned on group basis.

Kagathara and Parsania reported that the decrease in free length confirms the decreases in inter molecular distance, and the flexible structures are more compressible than rigid structures [35]. Since bulk modulus plays an important role on the molecular structure, the relation between adiabatic bulk modulus and sound velocity is also important. The relation between the adiabatic bulk modulus and sound velocity of all tested oils is shown in Fig. 6.6. PFPE lubricants demonstrate that of higher density but lower adiabatic bulk modulus, it situated in a separate position when compared with sound velocity. Glycerol shows a large variation of density and adiabatic bulk modulus, it is also taken different position with higher sound velocity.

Usually, sound velocity decreases with an increase of density, but sound velocity increases with an increase of bulk modulus. It is found that the value of bulk modulus impacts on the sound velocity in the lubricating oil. Here, density of PFPE oil is comparatively higher, but bulk modulus is lower. Sound velocity in the PFPE oil showed lower value. On the other hand, density of glycerol is lower than the PFPE oil but higher than that of the mineral oil, PAO oil and traction oil. But, bulk modulus of glycerol is greater than that of the other tested oils and belongs to higher sound velocity compare to others.

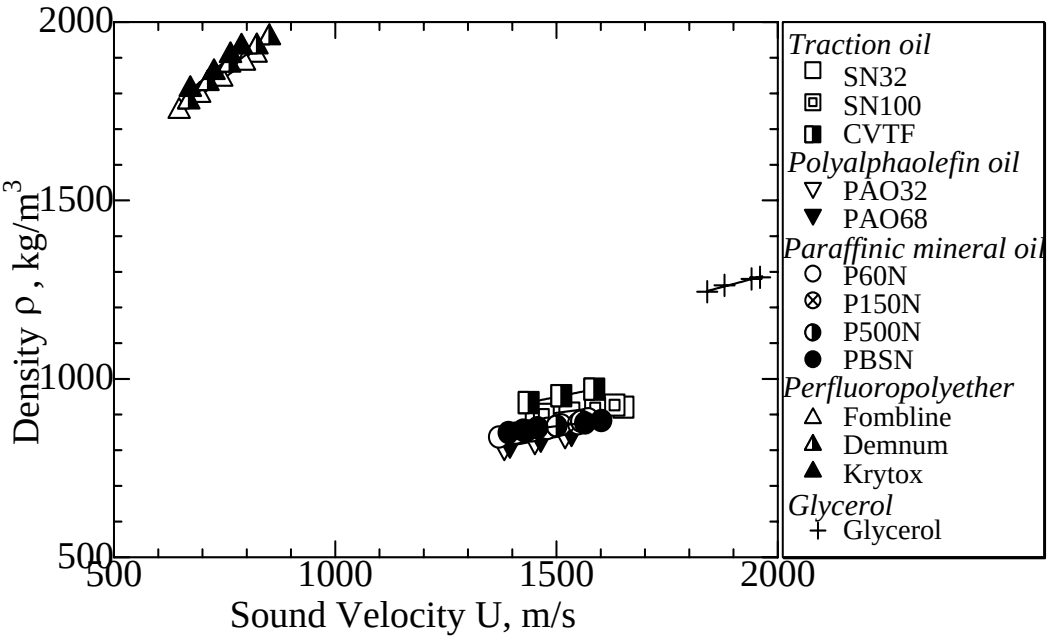


Fig. 6.5 Relation between density and sound velocity of lubricating oils

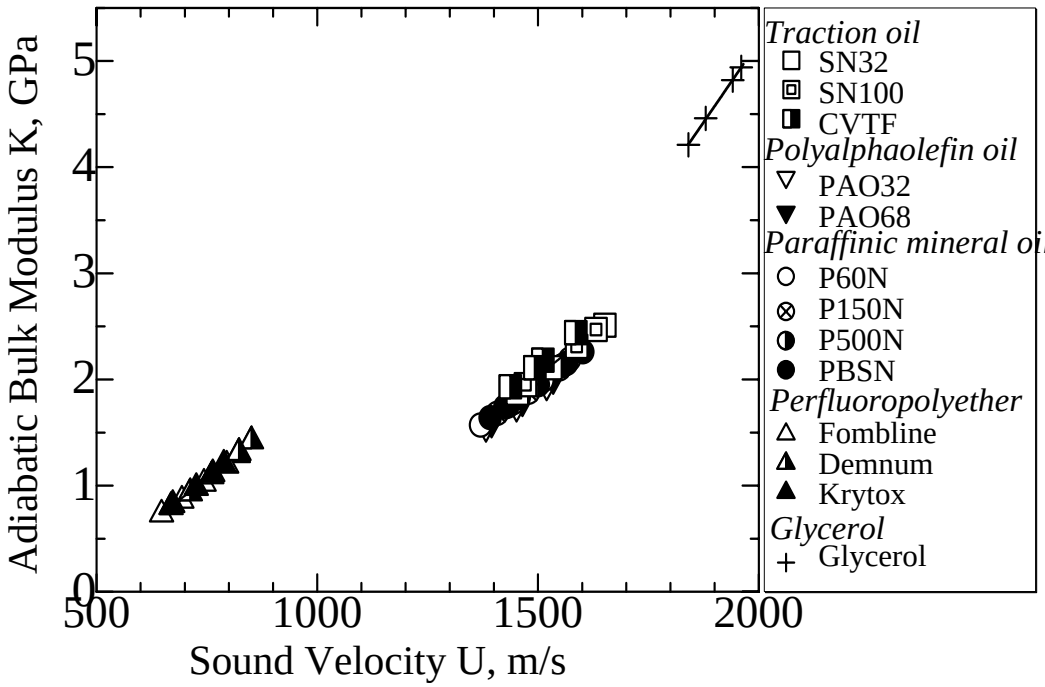


Fig. 6.6 Relation between adiabatic bulk modulus and sound velocity

Surface tension is another important property of liquid lubricant, which is related to the molecular structure. It is the difference between the molecular attraction between one fluid and that with another at the interface that results in what we measure as surface tension. A liquid with low surface tension would spread easily on the solid surface and provide good lubrication. The relation between the surface tension and the sound velocity is shown in the Fig. 6.7. The surface tension for the finished lubricants is sensitive to additives [3]. In the figure, for traction oil, PAO and paraffinic mineral oil, the relation is not uniform since additives are added to the base oil of tested oils. The relationship between surface tension and sound velocity has shown as group basis in Fig. 6.8 to Fig. 6.12.

It has found that sound velocity decreased with rise in temperature as shown in Fig. 6.4. The decrease in *U* with temperature indicated weakening of intermolecular forces due to thermal agitation. Usually sound velocity should decrease with an increase of density but due to an increase of the adiabatic bulk modulus, sound velocity is increased.

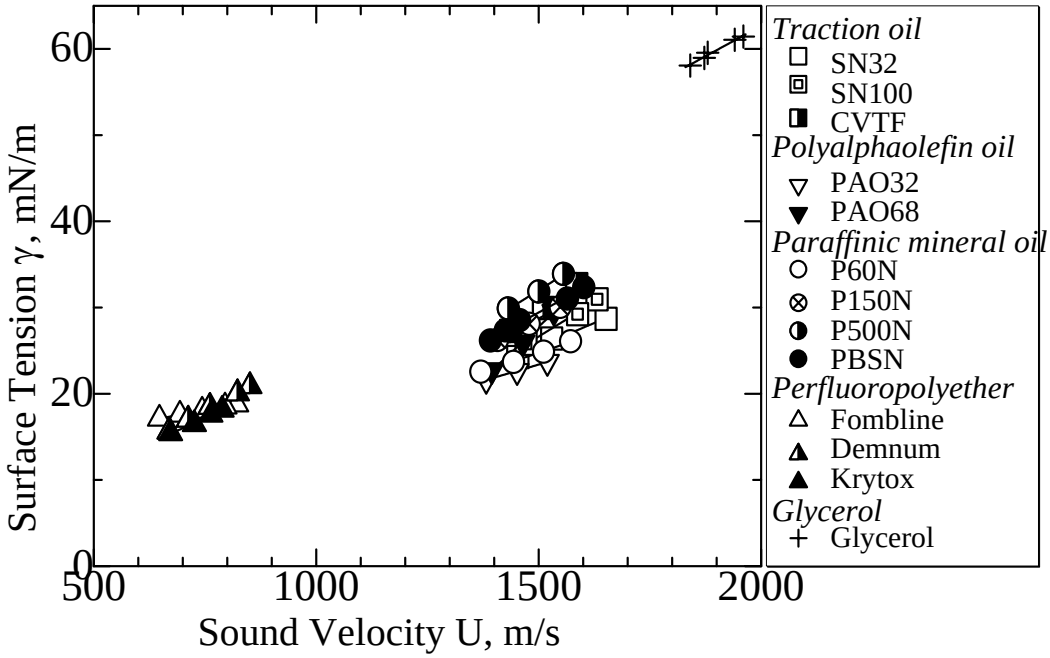


Fig. 6.7 Relation between surface tension and sound velocity

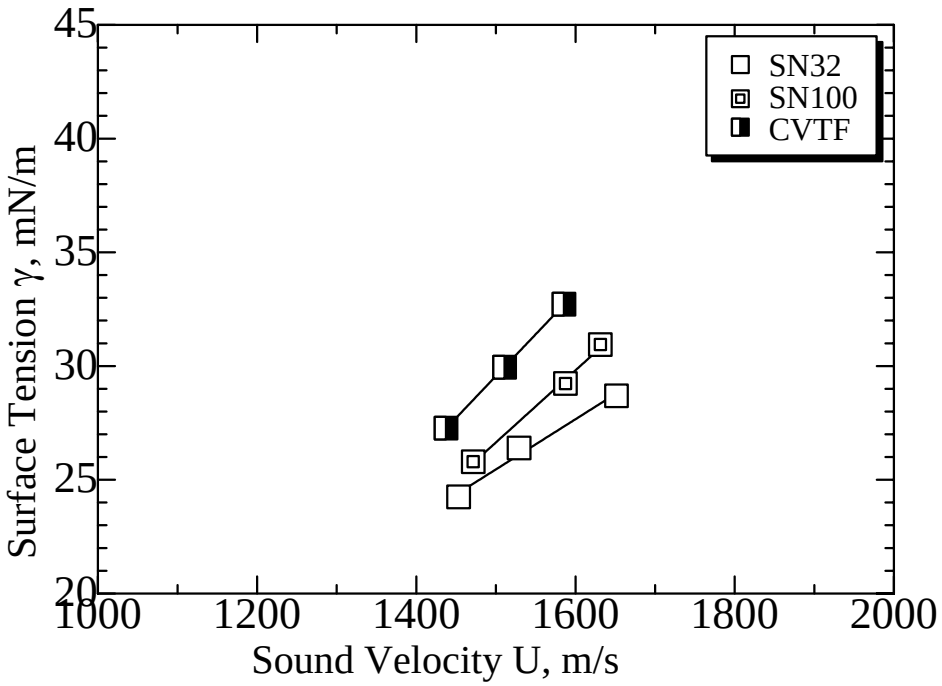


Fig. 6.8 Relation between surface tension and sound velocity for traction oils

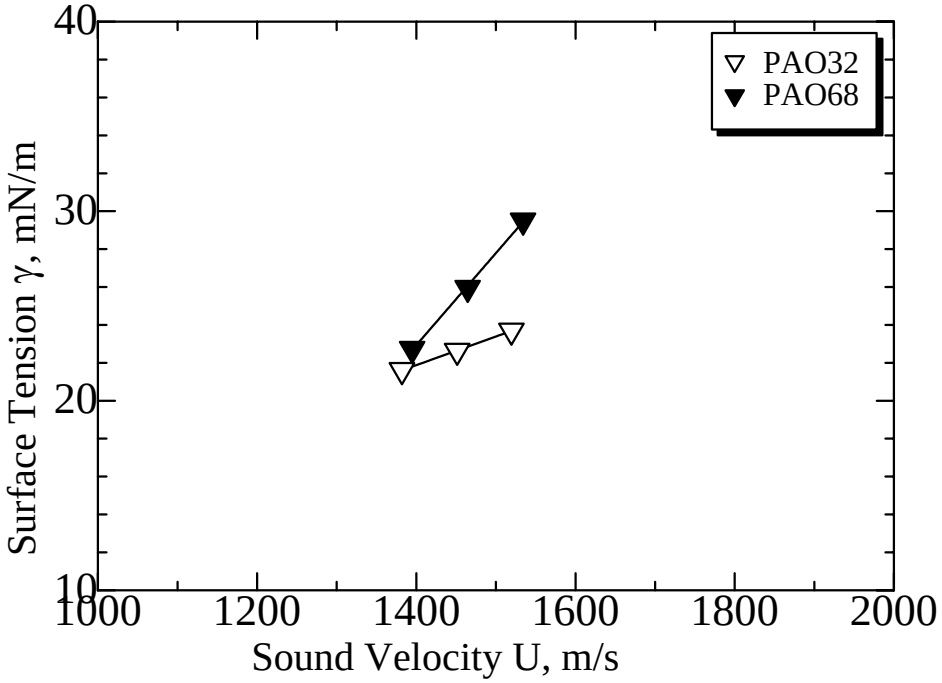


Fig. 6.9 Relation between surface tension and sound velocity for polyalphaolefin oils

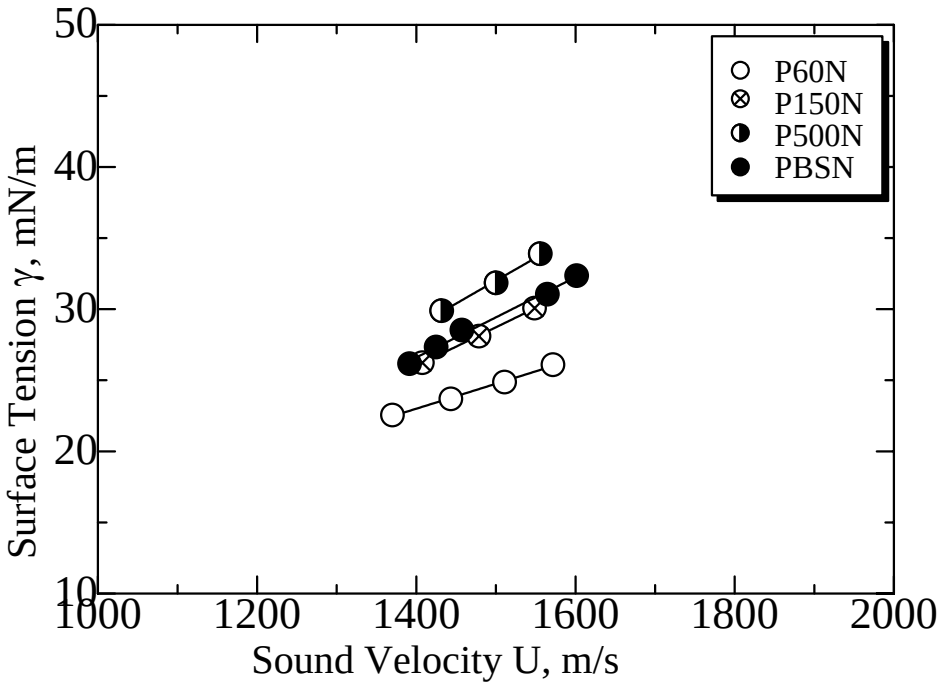


Fig. 6.10 Relation between surface tension and sound velocity for paraffinic mineral oils

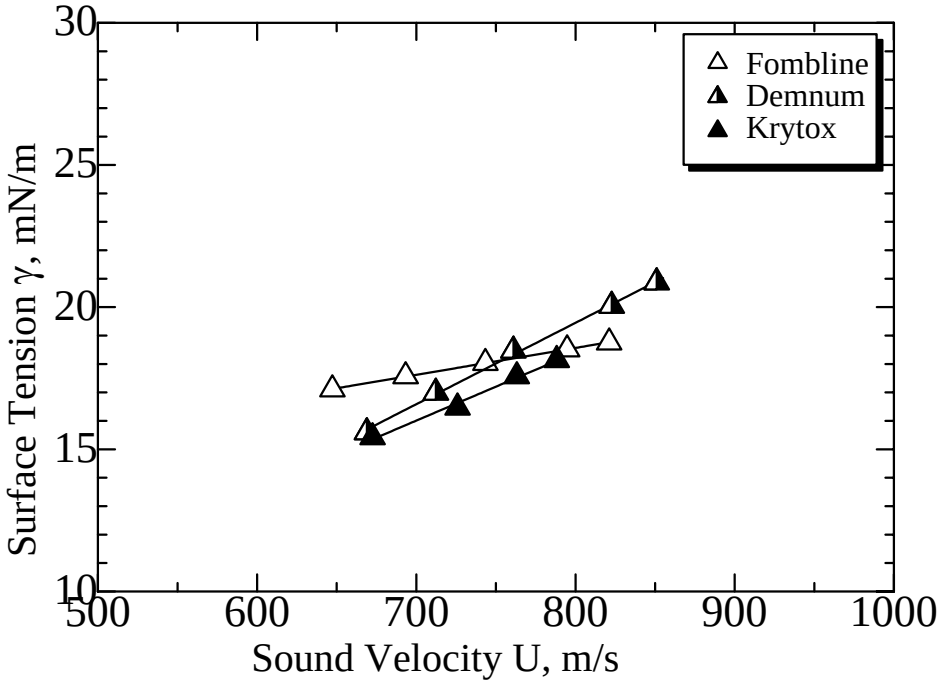


Fig. 6.11 Relation between surface tension and sound velocity of perfluoropolyether oils

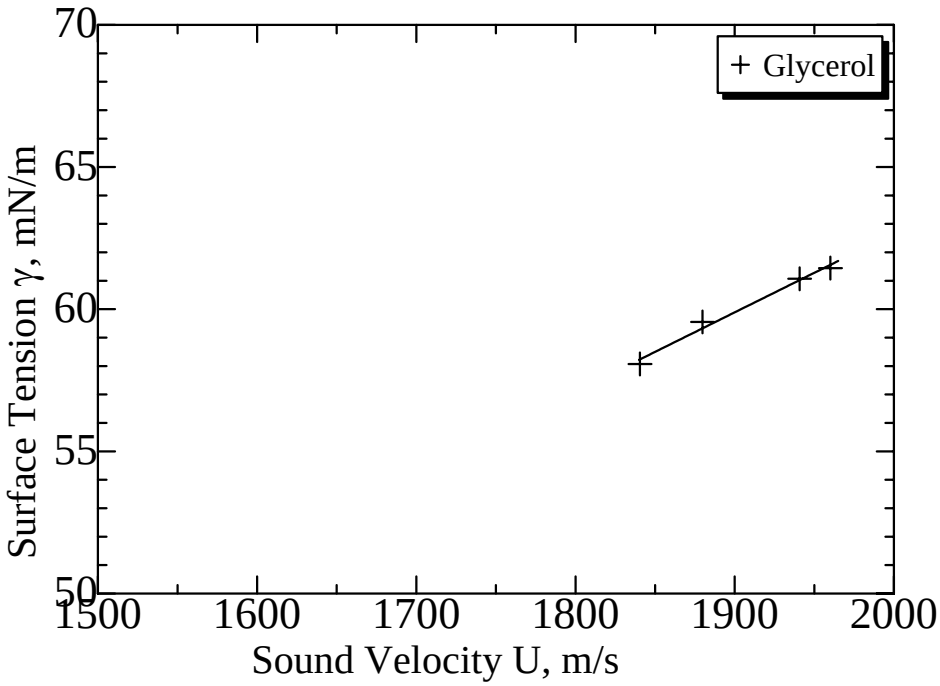


Fig. 6.12 Relation between surface tension and sound velocity of glycerol

By studying the above graphical relation, it is clear that PFPE oil and glycerol laid on the different position in the graph. But traction oil, PAO and paraffinic mineral oil have lain on almost at the same position. PFPE consists of C-F bond and glycerol consists of C-OH bond, where as traction, PAO and paraffinic mineral oils are hydrocarbon base that is why their position is almost similar. Though this three group's position is near to each other but their behavior is little bit distinguishable to observe the graph. Among them paraffinic mineral oils is chain like hydrocarbon with single bond between the carbons. These molecules can be linear. Whereas PAO is similar to paraffinic mineral oils except that they contain one or more double bonds between carbon atoms with branch carbon bonding. Mia and Ohno [60] considered paraffinic mineral oil and PAO in same group to predict the pressure viscosity coefficient by sound velocity. Traction oils are naphethenic hydrocarbon, which contains ring like molecule also known as cycloparaffin. Ring like molecules are stronger than the chain like molecule and bulk modulus and density is slightly higher on same condition. So, sound velocity also slightly higher on that condition. For the effect of molecular behavior, Mia et al. [66] found the linear relation between the

viscoelastic solid transition temperature at atmospheric pressure and the adiabatic bulk modulus for the same group of oil. For further analysis it should necessary to estimate organic chain length [15] or molecular analysis by chemically [36].

In this study, sometimes difficulties faced to measured the sound velocity by Sing around technique. Though the technique gives precision result, but sometimes it didn't found the propagation of sound wave through the lubricating oils. As a result, device didn't showed good sense. In the case of difficulty to measurement of sound velocity, author found an estimation relation of sound velocity from the properties related to molecular structure. The relation is found by mathematical analysis of the measured sound velocity, density and surface tension of lubricating oils. The relation is presented as the following equation,

$$U = C\rho^{a}\gamma^{b} \tag{6.2}$$

where sound velocity $U$ is in m/s, density ρ is in kg/m$^3$ and surface tension γ is in mN/m. The values of constant $C$ = 11060, $a$ = -0.58 and $b$ = 0.58 were found for all tested data. Error of this estimation formula is limited to ± 10%. Comparison of estimated results and experimental results is shown in Table 6.1 to Table 6.5.

Table 6.1 Comparison of estimated sound velocity with experimental sound velocity for traction oils.

| Sample Oil | Temp. $T$ | Density ρ | Surface Tension γ | Estimated Sound velocity $U_{est}$ | Experimental Sound velocity $U_{exp}$ | Error |
|---|---|---|---|---|---|---|
| | °C | kg/m$^3$ | mN/m | m/s | m/s | % |
| SN32 | 0 | 920.6 | 28.69 | 1488 | 1652 | 9.9 |
| | 20 | 904.0 | 26.40 | 1433 | 1529 | 6.3 |
| | 40 | 887.4 | 24.24 | 1378 | 1453 | 5.2 |
| SN100 | 10 | 926.5 | 30.94 | 1549 | 1631 | 5.0 |
| | 20 | 918.2 | 29.23 | 1507 | 1588 | 5.1 |
| | 40 | 900.4 | 25.79 | 1417 | 1472 | 3.7 |
| CVTF | 0 | 971.1 | 32.72 | 1557 | 1586 | 1.8 |
| | 20 | 952.6 | 29.94 | 1496 | 1511 | 1.0 |
| | 40 | 933.5 | 27.27 | 1433 | 1437 | 0.3 |

Table 6.2 Comparison of estimated sound velocity with experimental sound velocity for polyalphaolefin (PAO) oils.

| Sample Oil | Temp. $T$ | Density ρ | Surface Tension γ | Estimated Sound velocity $U_{est}$ | Experimental Sound velocity $U_{exp}$ | Error |
|---|---|---|---|---|---|---|
| | °C | kg/m$^3$ | mN/m | m/s | m/s | % |
| PAO32 | 0 | 842.2 | 23.69 | 1402 | 1520 | 7.7 |
| | 20 | 825.7 | 22.63 | 1381 | 1451 | 4.9 |
| | 40 | 809.3 | 21.61 | 1360 | 1382 | 1.6 |
| PAO68 | 0 | 848.6 | 29.50 | 1586 | 1534 | -3.4 |
| | 20 | 832.3 | 25.95 | 1488 | 1465 | -1.6 |
| | 40 | 816.0 | 22.73 | 1394 | 1395 | 0.1 |

Table 6.3 Comparison of estimated sound velocity with experimental sound velocity for paraffinic mineral oils.

| Sample Oil | Temp. $T$ | Density ρ | Surface Tension γ | Estimated Sound velocity $U_{est}$ | Experimental Sound velocity $U_{exp}$ | Error |
|---|---|---|---|---|---|---|
| | °C | kg/m$^3$ | mN/m | m/s | m/s | % |
| P60N | -20 | 888.3 | 26.09 | 1438 | 1572 | 8.5 |
| | 0 | 871.2 | 24.87 | 1414 | 1511 | 6.4 |
| | 20 | 854.1 | 23.69 | 1390 | 1443 | 3.7 |
| | 40 | 837.0 | 22.55 | 1367 | 1370 | 0.2 |
| P150N | 0 | 874.2 | 30.07 | 1576 | 1549 | -1.8 |
| | 20 | 861.0 | 28.10 | 1529 | 1479 | -3.4 |
| | 40 | 847.8 | 26.23 | 1482 | 1408 | -5.3 |
| P500N | 0 | 881.4 | 33.90 | 1682 | 1556 | -8.1 |
| | 20 | 867.7 | 31.85 | 1637 | 1500 | -9.1 |
| | 40 | 853.9 | 29.89 | 1592 | 1432 | -11.2 |
| PBSN | 10 | 883.1 | 32.36 | 1635 | 1602 | -2.1 |
| | 20 | 876.4 | 31.05 | 1603 | 1565 | -2.5 |
| | 40 | 862.9 | 28.53 | 1540 | 1457 | -5.7 |
| | 50 | 856.2 | 27.34 | 1509 | 1425 | -5.9 |
| | 60 | 849.4 | 26.17 | 1478 | 1392 | -6.2 |

Table 6.4 Comparison of estimated sound velocity with experimental sound velocity for perfluoropolyether (PFPE) oils.

| Sample Oil | Temp. $T$ | Density ρ | Surface Tension γ | Estimated Sound velocity $U_{est}$ | Experimental Sound velocity $U_{exp}$ | Error |
|---|---|---|---|---|---|---|
| | °C | kg/m$^3$ | mN/m | m/s | m/s | % |
| Fombline | -10 | 1907.4 | 18.76 | 761 | 821 | 7.3 |
| | 0 | 1884.9 | 18.52 | 761 | 795 | 4.2 |
| | 20 | 1839.8 | 18.04 | 760 | 743 | -2.2 |
| | 40 | 1794.7 | 17.57 | 759 | 693 | -9.5 |
| | 60 | 1749.7 | 17.11 | 759 | 647 | -17.2 |
| Demnum | -10 | 1956.2 | 20.87 | 799 | 851 | 6.2 |
| | 0 | 1930.5 | 20.05 | 786 | 823 | 4.5 |
| | 20 | 1879.2 | 18.47 | 761 | 761 | 0.0 |
| | 40 | 1827.9 | 16.99 | 737 | 712 | -3.4 |
| | 60 | 1776.5 | 15.60 | 713 | 669 | -6.5 |
| Krytox | 10 | 1930 | 18.14 | 742 | 788 | 5.9 |
| | 20 | 1906.2 | 17.57 | 733 | 763 | 3.9 |
| | 40 | 1858.7 | 16.47 | 717 | 726 | 1.3 |
| | 60 | 1811.3 | 15.43 | 700 | 673 | -4.1 |

Table 6.5 Comparison of estimated sound velocity with experimental sound velocity for glycerol.

| Sample Oil | Temp. $T$ | Density ρ | Surface Tension γ | Estimated Sound velocity $U_{est}$ | Experimental Sound velocity $U_{exp}$ | Error |
|---|---|---|---|---|---|---|
| | °C | kg/m$^3$ | mN/m | m/s | m/s | % |
| Glycerol | -5 | 1284.5 | 61.45 | 1911 | 1960 | 2.5 |
| | 0 | 1280.1 | 61.07 | 1908 | 1941 | 1.7 |
| | 20 | 1262.1 | 59.55 | 1896 | 1880 | -0.8 |
| | 40 | 1244.2 | 58.07 | 1884 | 1841 | -2.3 |

## 6.5 Conclusion

Sound velocity is an important property of lubricant. Since it is related to molecular structure, it has found the effect of sound velocity on the molecular structure of lubricant. Sound velocity decreases with increases the temperature and increases with increases the bulk modulus. So, sound velocity of lubricating oils can indicates roughly the molecular structure of that lubricating oil.

By measuring the sound velocity and compared with density, bulk modulus and surface tension, it can be possible to find out the group. Mainly it is easy to classify the hydrocarbon oil (traction oil, PAO and paraffinic mineral oil), perfluoropolyether oil and glycerol. Behavior of traction oil, PAO and paraffinic mineral oils are almost similar since the hydrocarbon oil's molecular structure is almost similar. So it could be possible to identify unknown oil roughly.

Sound velocity of lubricating oils can be estimate from the density and surface tension by the proposed estimation formula $U = C\rho^a\gamma^b$.

# Chapter 7

# Effect of Sound Velocity in Lubricating Oil to the Tribological Applications

## 7.1 Introduction

The branch of science and technology concerned with interacting surfaces in relative motion and with associated matters as friction, wear, lubrication and the design of bearing is known as tribology. Common tribological components which are used in industrial applications include sliding contact and rolling contact bearings, seals, gears, cams and tappets, piston rings, electrical brushes and cutting and forming tools. Some of the other common industrial applications include material processing, internal combustion engines for automotives applications, gas turbine engines for aerospace applications, railroads and magnetic storage devices. For a desired performance and life of a component, its friction and wear needs to be minimized or optimized for a given application. Relevant friction and wear mechanisms are dependent upon the device and the operating condition.

Some tribological components operate at low to moderate contact pressure. There are many components which operate at high Hertzian pressure include rolling element bearing. High-pressure tribological research is important on that respect. As like the component materials, lubricant should also have sustained the high pressure. Liquid lubricant phase also change to viscoelastic or solid under high Hertzian pressure. Ohno et al. [74] worked on some advanced base oil for space applications. They used PFPE 815Z oil, multiply alkylated cyclopentanes (MAC) 2001A and some greases using these as base oil. They found the general tendency of the base oils and the greases shows that the bearing life increases with the EHL film parameter. We know that EHL film parameter depends on the lubricants pressure viscosity coefficient. Again phase diagram of lubricant is important in case of high- pressure applications. Ohno et al. [75] then studied the effect of same base oils and greases on friction and wear behavior using Soda type four-ball tribometer. The highest wear scar was found for PFPE 815Z, but it showed lowest coefficient of friction. Authors also found the decomposition of bass oil 815Z containing acetal group (-$OCF_2O$-) occurred by mechanical shear at high shear rates in the elastic plastic solid. Mia et al. [76] found the permanent viscosity loss of PFPE 815Z oil, occurred rapidly with time

at a mean contact pressure of 1.95 GPa to 2.67 GPa. The viscosity loss at higher pressure may influence on the higher wear scar. Ohno et al. [77] also worked on newly developed thermo-reversible gel lubricants (TR-Gel Lube) and construct the phase diagram using diamond anvil cell (DAC). To construct the phase diagram they used viscoelastic solid transition temperature at atmospheric pressure for base oil polyalphaolefin, using the same technique of this study. They also mentioned the relation of viscoelastic solid transition temperature at high pressure from the viscoelastic solid transition temperature at atmospheric pressure. Although, sound velocity in lubricating oil is measured at atmospheric pressure at different temperature but have found the relation with pressure viscosity coefficient and with the viscoelastic solid transition temperature. Mia et al. [78] showed the effect of high-pressure rheology of different lubricating oils on boundary lubrication. In the study, they used bridge ring compound of base oil for traction (SN-LV, SN-MV and SN-HV), polybutenes (PB-LV, PB-MV and PB-HV), a synthetic diester DOS, a Tricyclic compound BBPH and blended oils of DOS and BBPH. Phase diagram was drawn performing several high-pressure rheological experiments and then frictional and wear behavior were examined. They reported that the bridge ring compound exhibits minimum wear due to solidification, which occurs at high pressure. They also reported that the anti wear action of the oil in sliding concentrated contact is related to the oil molecular packing parameter $T_{VE} - T$. The greater the oil molecular packing parameter indicates the smaller wear scar. The oil molecular packing parameter also related with the adiabatic bulk modulus. Adiabatic bulk modulus, which is calculated from the measure sound velocity is then compared with the frictional and wear behavior of the lubricating oils.

This chapter also discussed the effect of sound velocity on the wind turbine gear oil. Lubrication of gear and bearing in the gearbox are important to improve the performance of a wind turbine. Frictional and wear behavior, low temperature fluidity and high load carrying capacity are important for wind turbine gear oil. Measuring the sound velocity in wind turbine gear oil, we can calculate the adiabatic bulk modulus. Then compared the adiabatic bulk modulus with the viscoelastic solid transition temperature, it has found that the low adiabatic bulk modulus of oil indicates better low temperature fluidity and better frictional and wear behavior for wind turbine gear oil [79].

## 7.2 Relation between sound velocity and wear behavior

Friction and wear experiments were carried out using a conventional four-ball wear tester. The experimental apparatus is shown in Fig. 7.1 and the arrangement of the test balls is shown in Fig. 7.2. Bearing steel balls of 19.05 mm in diameter and 5.7 nm in mean surface roughness were used. All experiments were conducted at load 1.39 kN and at upper rotating ball speed 60 rpm, corresponding to a sliding speed of 0.035m/s. Duration for each experiment was 1 h, and thus total sliding distance was 124.6 m. Load of each pair was 564 N, corresponding mean Hertzian pressure = 2.6 GPa, and Hertzian diameter $d_H$ = 0.521 mm. Friction was measured by means of a torsion bar to which the bottom of the oil container was clamped. Experiments were carried out at room temperature.

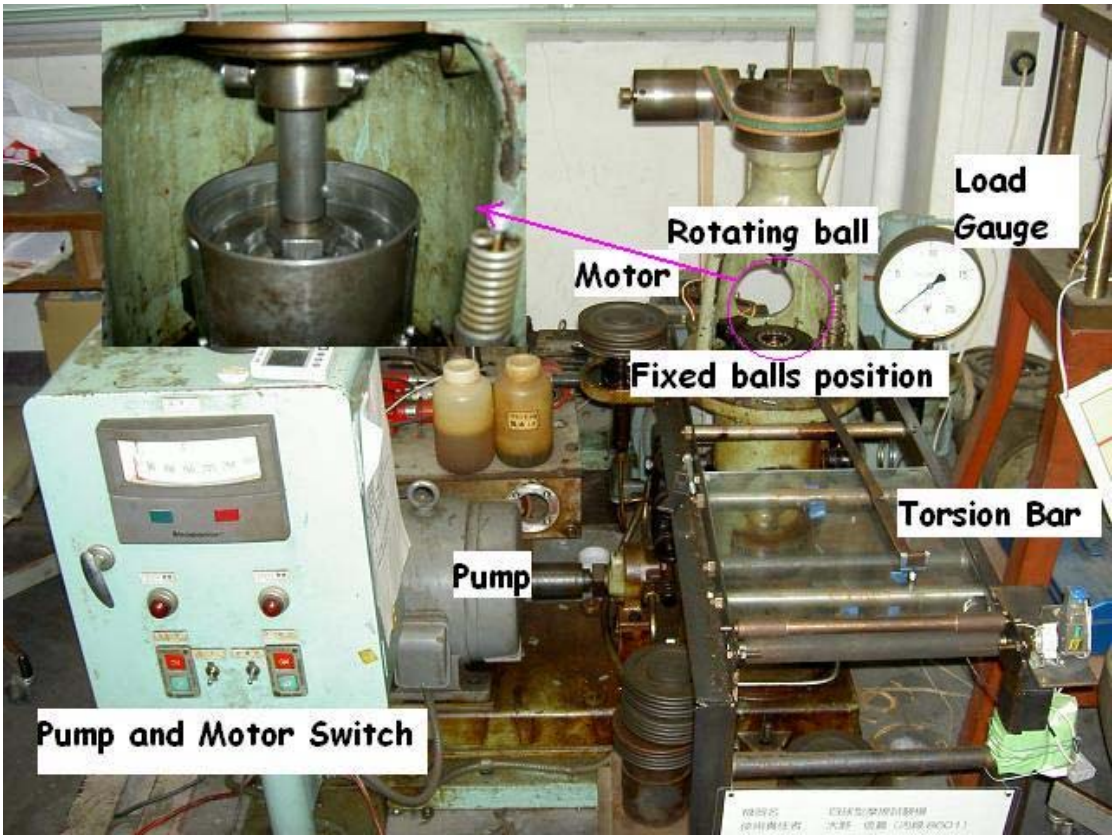


Fig. 7.1 Experimental Apparatus of the Four-ball Wear Test.

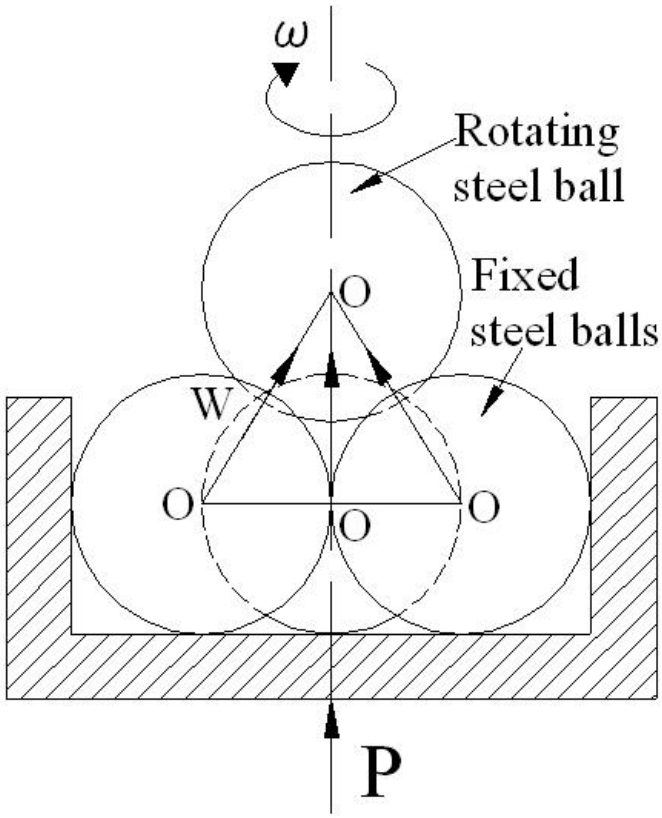


Fig. 7.2 The arrangement of the four steel balls in the 4-ball wear test experiment.

After an hour, released the load and removed the fixed balls from the ball holder and rotating ball from the rotor shaft. The four balls were clean using ultrasonic cleaner. Then photograph of the wear scar was taken using a microscope at 10X zooms. Photographs of traction oil CVTF have shown in Fig. 7.3. Wear scar diameter of each fixed ball was calculated from the photograph. Area of wear scar was calculated from the average data and then compared with the adiabatic bulk modulus at 40 °C. Similar calculation was done for other samples. Comparison between wear scar area and adiabatic bulk modulus is shown in Fig. 7.4. Figure showed, larger wear scar area found for low adiabatic bulk modulus. Again, the friction coefficient was recorded during the 1-hour wear test.

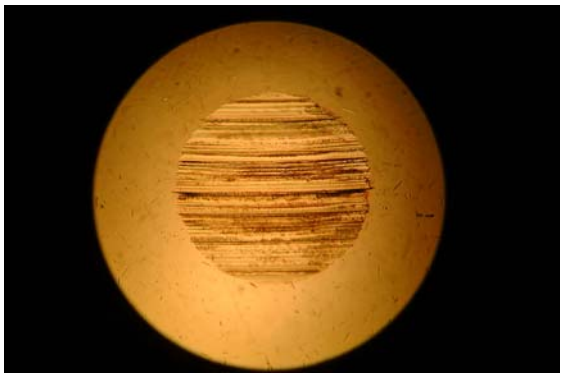

(a) Fixed ball 1, $A_1 = 0.3127$ mm$^2$

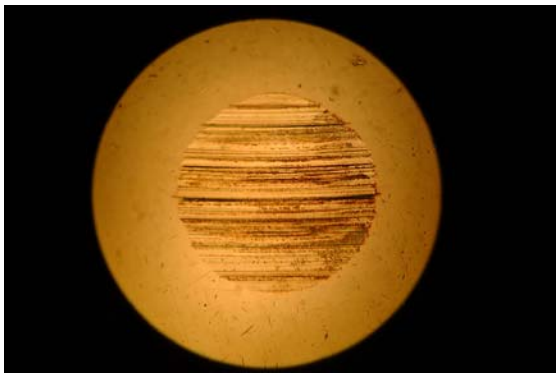

(b) Fixed ball 2, $A_2 = 0.3380$ mm$^2$

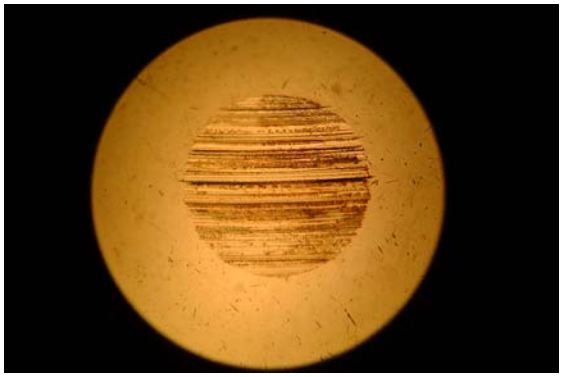

(c) Fixed ball 3, $A_3 = 0.2846$ mm$^2$

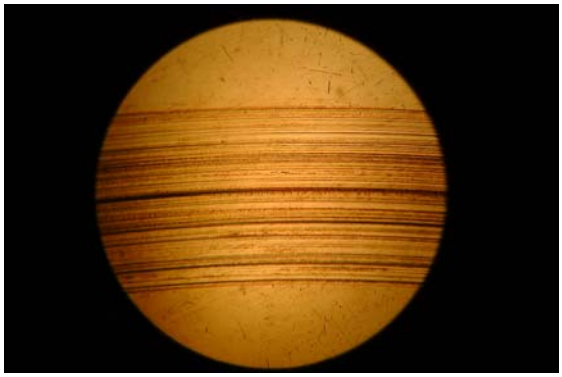

(d) Rotating ball

Fig. 7. 3 Photographs of wear scar area for traction oil CVTF

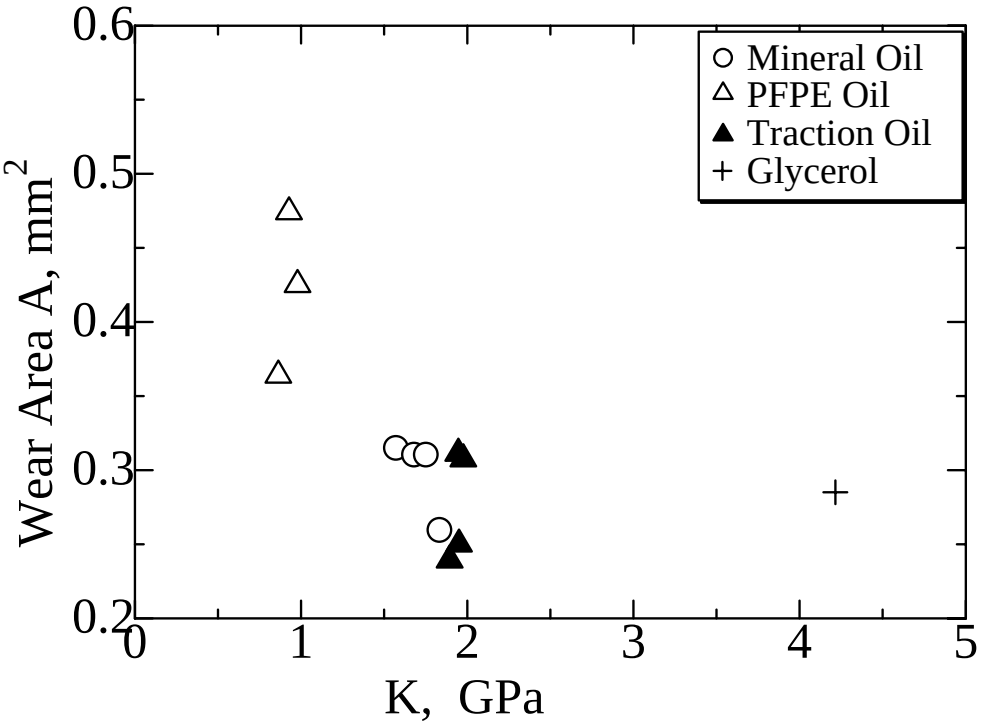


Fig. 7.4 Relation between the adiabatic bulk modulus and wear scar area

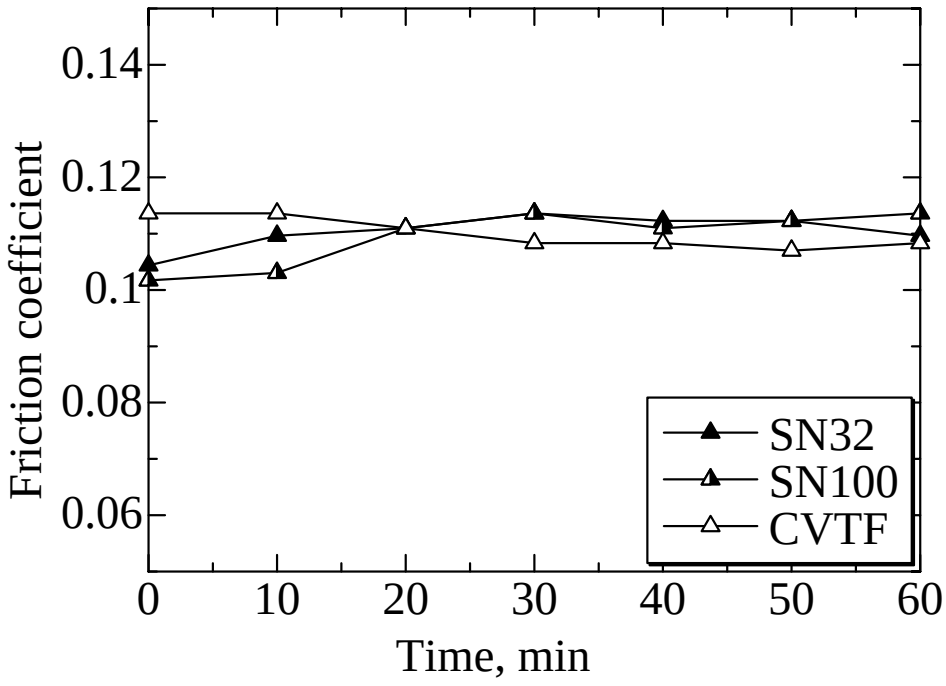


Fig. 7. 5 Change of friction coefficient in 1-hour 4-ball wear test.

## 7.3 Relation between sound velocity and Friction Coefficient

Frictional behavior of lubricating is another important term for boundary lubrication [75]. This study also tried to find out the influence of adiabatic bulk modulus on friction coefficient of lubricating oil. Friction coefficient was observed in 4-ball wear test using a torsion bar as shown in the 4-ball experimental device. A sample of the change of friction coefficient in 1-hour test is given in Fig. 7.5. Again, for the static friction, soda type pendulum test is necessary. For that Friction coefficient has been measured using pendulum test.

***Experimental apparatus and methods***

Soda pendulum test machine is fixed on a column of steel with the T-pattern pendulum in the center. Photograph of the apparatus is shown in Fig. 7.6. The pendulum is supported on four bearing steel balls by a roller pin. It is the device, which measures the frictional coefficient from the degree of decline in the free swing of the pendulum. Steel ball diameter was 4.75 mm and roller pin diameter is 3.0 mm with hardness number RC 60-66. Other parts are base stand with a leveler, weight, roller pin holder, V-ring and oil container. Prior to each test, all these parts were carefully cleaned by immersion in an ultrasonic cleaner, rinsed out in hexane and dried in hot air. The base stand has a curvature like scale from where pendulum reading was taken for calculation.

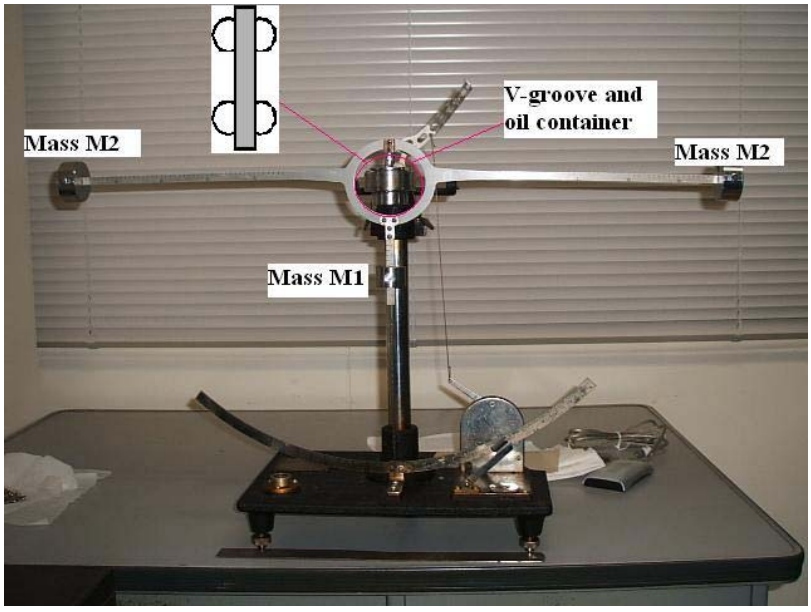

Fig. 7.6 Pendulum test machine for static friction measurement

First, the V-ring was set on the oil container and four steel balls were placed in the V-groove. The roller pin was inserted into the pin holder attached with pendulum and placed between the balls as shown in the figure. And it was put on the oil container. Oil was poured into the container up to the steel balls immersed. Three kinds of mass were placed in the pendulum, two of them were the same mass of $M_2$ = 240 gm and the other one was $M_1$ = 120 gm as shown in the photograph. The experiment was done at the atmospheric condition and at room temperature.

Experiment has started from setting the pendulum at 0.5 by pushing a lever and let the device swing freely till it stopped at 0 of curvature like scale. The number of pendulum swings and the scale reading of each swing were taken for calculation. This reading was different for different oils and thus gave different frictional coefficients. The experiment was repeated twenty times with the same conditions for same sample oil.

The coefficient of the static friction μ was calculated in this study by the following formula:

$$\mu = C \cdot \frac{A_0 \cdot n - (A_1 + A_2 + A_3 + \cdots\cdots\cdots + A_n)}{1 + 2 + 3 + \cdots\cdots\cdots + n} \qquad [7.1]$$

where, μ: friction coefficient

$A_0$: start amplitude of swing ($A_0$ = 0.5 radian)

$A_n$: every single time angle (radian, n = 1, 2, 3, …..n)

C: constant (standard no. in this experiment, C = 3.2)

n: number of swing revolution

Measured friction coefficient is then compared with the adiabatic bulk modulus of lubricating oil. The relation between them is shown in Fig. 7.7. PFPE oil has lower adiabatic bulk modulus, which showed low friction. Mineral oil has variation due to different type of mineral oil were used. PBSN has higher viscosity, which showed the low friction, other oils showed comparatively higher friction coefficient.

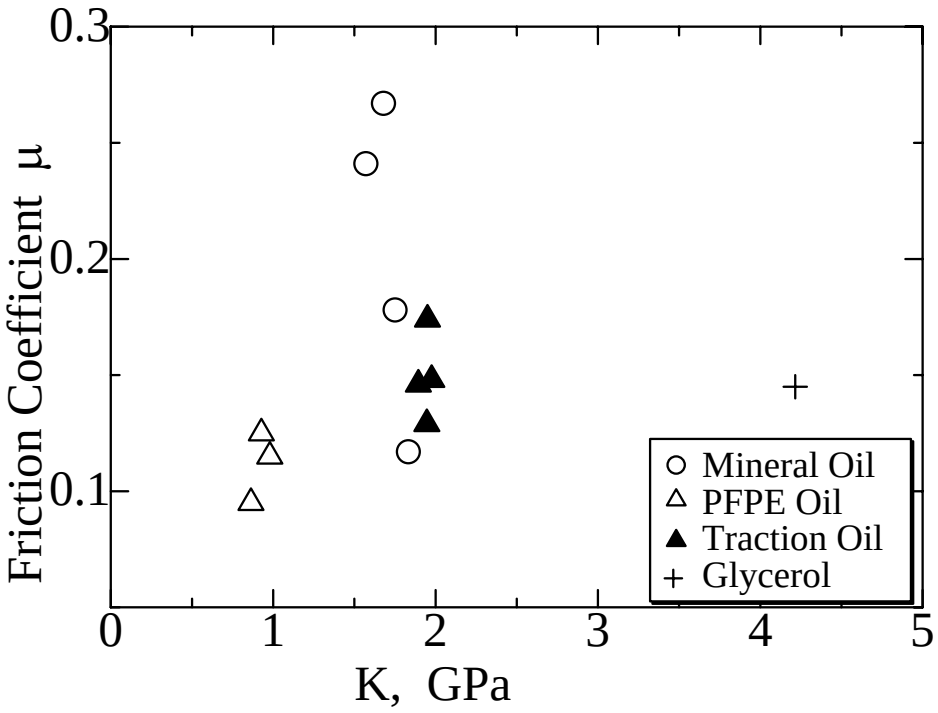


Fig. 7.7 Relation between adiabatic bulk modulus and friction coefficient.

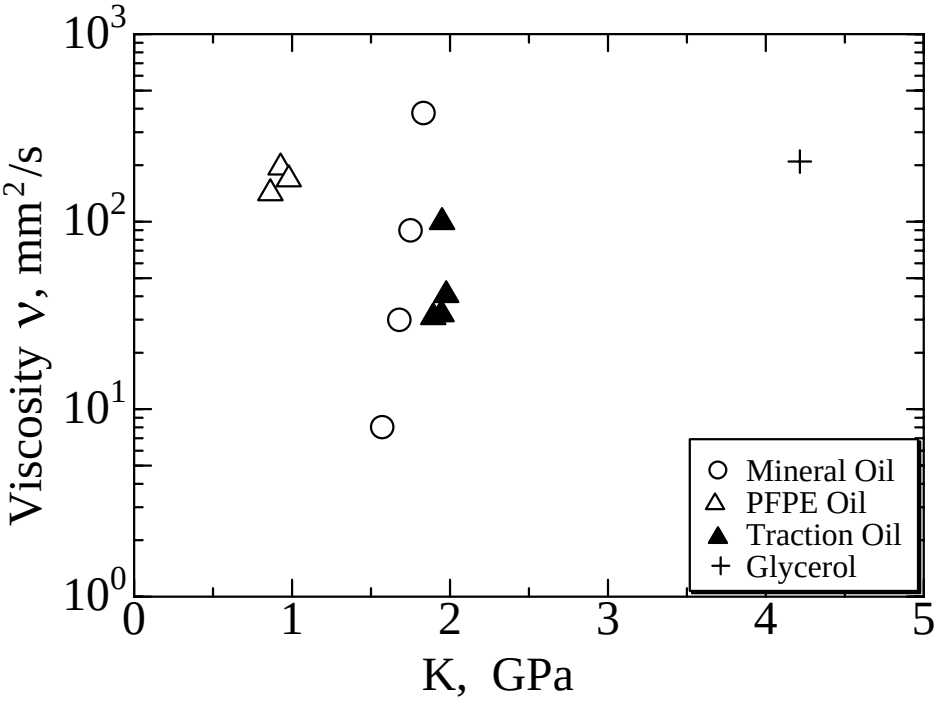


Fig. 7.8 Relation between the adiabatic bulk modulus and viscosity

## 7.4 Relation between sound velocity and viscosity

Viscosity is the most common and important property of lubricating oil. This study also compared between the adiabatic bulk modulus and the kinematic viscosity of lubricating oil. The relation between them for few oils is shown in Fig. 7.8. These samples were also considered for friction and wear test as shown in Fig. 7.4 and Fig.7.7.

Author again investigated about the relation between viscosity and bulk modulus of lubricating oil and plotted for many samples which is shown in Fig. 7.9. From the relation, it has been found that some samples have higher bulk modulus with low viscosity. This study also distinguished these samples. Fig. 7.10 represents the relation only for high adiabatic bulk modulus having low viscosity lubricating oil at 40°C temperature. High bulk modulus having low viscosity fluid is suitable for hydraulic system. The adiabatic bulk modulus of the fluids is also compared with the pressure viscosity coefficient and with the low temperature property to ensure the applications.

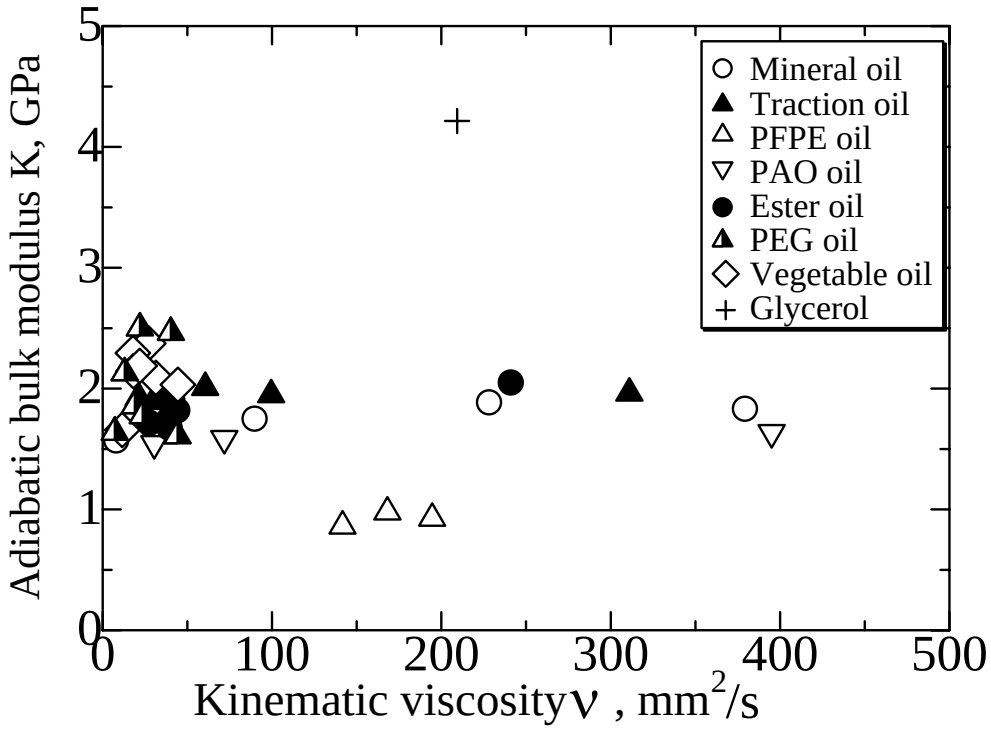


Fig. 7.9 Comparison of adiabatic bulk modulus with viscosity at 40°C temperature

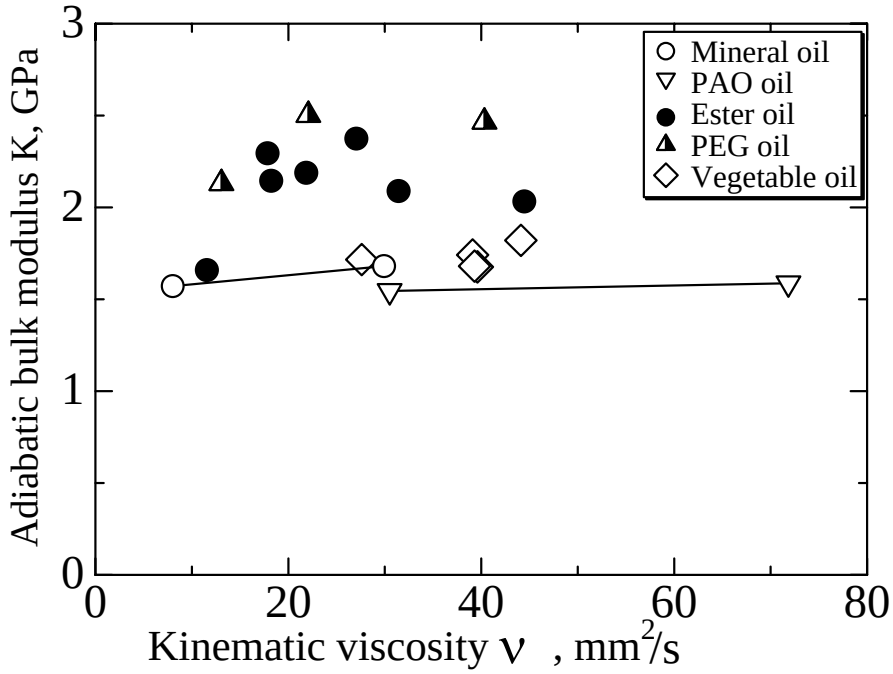


Fig. 7.10 Relation between high adiabatic bulk modulus and viscosity at 40°C temperature

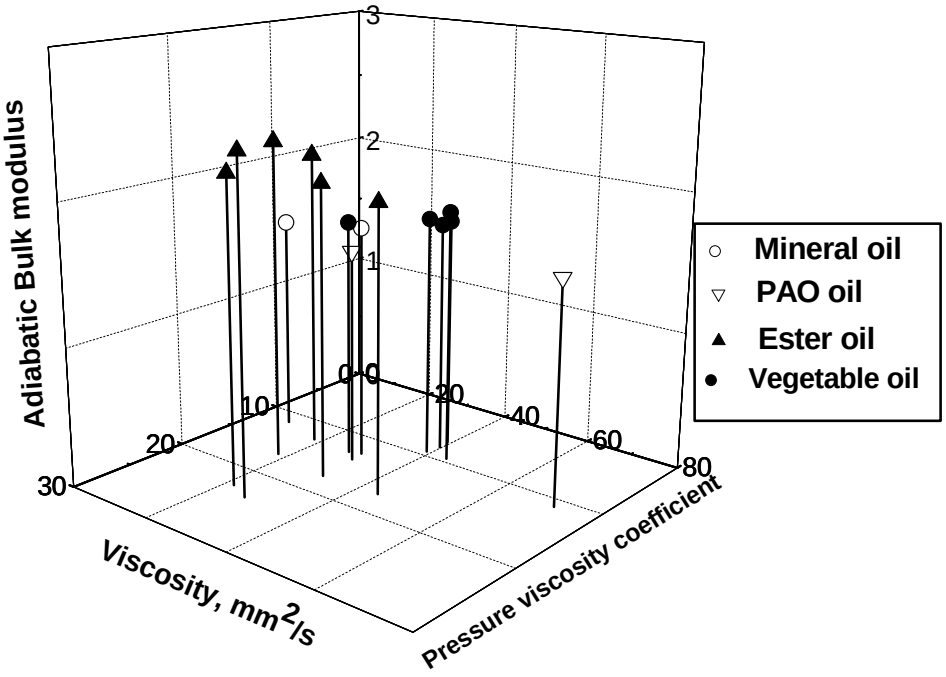


Fig. 7.11 K-ν-α relation of the tested oil at 40°C temperature

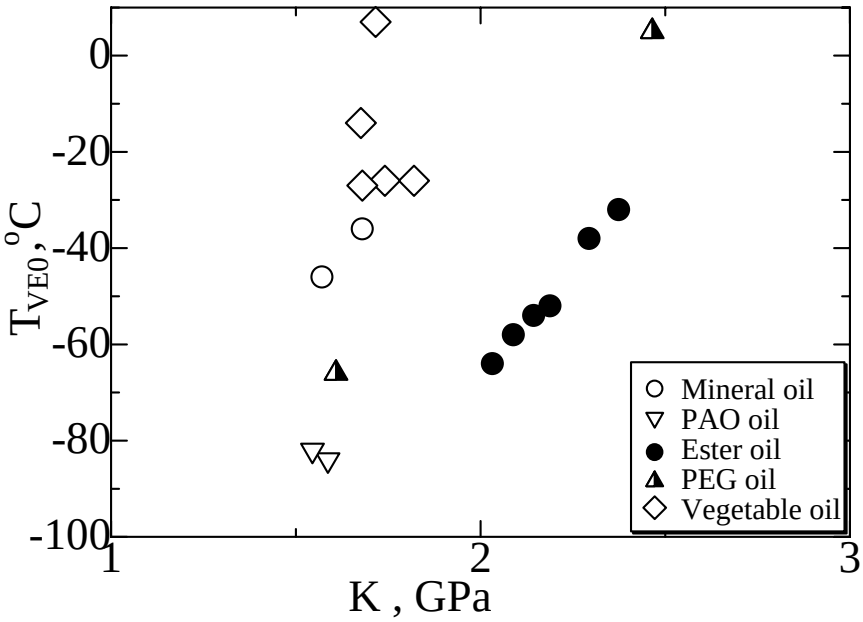


Fig. 7.12 Relation between Viscoelastic solid transition temperature $T_{VE0}$ and adiabatic bulk modulus $K$

Figure 7.10 represents that the ester oils, polyethylene glycol (PEG) oil and vegetable oils have higher adiabatic bulk modulus compare to the mineral oils and polyalphaolefin oils due to its different molecular structure. Synthesized ester oil and PEG oil have the strong intermolecular force with low free volume. So, the density of atom in the oil molecule is high. The relation between adiabatic bulk modulus, kinematic viscosity and pressure-viscosity coefficient has shown in Fig.7.11. Vegetable oils exhibit low viscosity with low pressure-viscosity coefficient but the tested ester oils have comparative higher pressure-viscosity coefficient with low viscosity. Again, to know the flow behavior we have compare the relation between viscoelastic solid transition temperature at atmospheric pressure and the adiabatic bulk modulus as shown in Fig. 7.12. Relation showed the ester oils have the better low temperature fluidity than the mineral oil and vegetable oils. PEG also has higher bulk modulus with low viscosity but one PEG oil found wax content during low temperature test, which is not suitable for the application. Other samples having high bulk modulus with low viscosity can apply as hydraulic fluid. Ester oils, PEG oils and Vegetable oils can be used in hydraulic systems for better performances.

## 7.5 Effect of sound velocity on wind turbine gear oils

Gearbox is a fundamental mechanical part of a wind turbine to generate electricity. Lubrication of the gear and bearings in the gearbox are important to improve the performance of a wind turbine. Gresham [80] reported that, at present, the weak spot in the overall design of wind turbine are its gearboxes. Low performance occurs due to poor lubrication in the gearbox and also for improper selection of lubricant. Since it is very difficult to monitor and replace the lubricant in case of wind turbine gear oil, it is very necessary to identify such lubricant, which will perform better and increase the efficiency and life of wind turbine gearbox. Usually, different types of gear oils are using for the lubrication in the gearbox. Mineral-based oils are mainly used as gear oil as they show comparatively low performance. Currently, synthetic lubricants are mostly used due to high viscosity index and low volatility. Polyalphaolefin (PAO) and Polyalkylene glycol (PAG) are newly applied lubricant in wind turbine [81]. Rudnick [82] mentioned that synthetic gear lubricants would play an increasing roll in future lubrication of high-performance gears of new processes, materials, and techniques. In this study authors considered several PAO oils in comparison to a mineral- based wind turbine oil. Physical properties of tested oils are given in Table 7.1. Mia et al. [79] described the high-pressure rheological analysis of these wind turbine gear oils.

Pressure-viscosity coefficient $\alpha$ is important parameter for wind turbine gear oil. Pressure-viscosity coefficient $\alpha$ was measured using high-pressure viscosity test. This $\alpha$ also can predict from the measured sound velocity in the oil using the predicting equation (Eq. 4.10). In addition, lubricant has some other important properties such as frictional property, low-temperature fluidity and others to get better performance, as

Table 7.1 Physical properties of wind turbine gear oils

| Oil name | Density $\rho$, g/cm$^3$ | Kinematic Viscosity $\nu$, mm$^2$/s | |
|---|---|---|---|
| | 15° C | 40° C | 100° C |
| Mineral-A | 0.8987 | 315.2 | 24.1 |
| PAO-A | 0.8607 | 336.1 | 38.05 |
| PAO-B | 0.8574 | 333.2 | 40.76 |
| PAO-C | 0.8603 | 313.1 | 32.84 |

Table 7.2 Experimental results of tested gear oils

| Oil name | $U_{40}$ [m/s] | $K_{40}$ [GPa] | $\alpha_{exp}$ at 40°C [$GPa^{-1}$] | $\alpha_{pred}$ at 40°C [$GPa^{-1}$] | $T_{VE0}$ [° C] |
|---|---|---|---|---|---|
| Mineral-A | 1433 | 1.813 | 21.6 | 16.6 | -9 |
| PAO-A | 1405 | 1.667 | 15.2 | 14.0 | -44 |
| PAO-B | 1413 | 1.608 | 14.2 | 13.1 | -57 |
| PAO-C | 1405 | 1.667 | 13.3 | 14.0 | -48 |

well as increase the efficiency of wind turbine. Considering these phenomena, the authors investigated the range of operating temperature especially found the viscoelastic solid transition temperature $T_{VE0}$ to know the low-temperature behavior. Moreover, Sound velocity in the wind turbine gear oil was measured using the same technique described in chapter 2. The experimental results for wind turbine gear oils are given in Table 7.2 where $U_{40}$ is the sound velocity in 40°C temperature, $K_{40}$ is the adiabatic bulk modulus in 40°C temperature, $\alpha_{exp}$ is the experimental pressure viscosity coefficient, $\alpha_{pred}$ is predicted pressure viscosity coefficient using Eq.4.10 and $T_{VE0}$ is the viscoelastic solid transition temperature. Predicted pressure-viscosity coefficient of Mineral-A oil has a large difference compared with experimental pressure-viscosity coefficient.

This difference may occur due to wax content in the Mineral-A oil. This can be obvious from the photo elastic effect in low temperature viscoelastic solid transition temperature measuring test. The photoelastic effect is shown in Fig. 7.13. Again, the adiabatic bulk modulus and the viscoelastic solid transition temperature both depend on the samples bulk property. The relation between $T_{VE0}$ and $K$ are shown in Fig. 7.14. Low adiabatic bulk modulus indicates better low-temperature fluidity. PAO oils show lower $K$ as well as the lower $T_{VE0}$ than the mineral-based oils. PAO oils also exhibit better low-temperature fluidity since wind turbine lubrication the temperature range should be -30 to 100° C [80]. Among the PAOs, $T_{VE0}$ for PAO-B is lowest (-57° C), with the lowest $K$. Investigating this phenomena, the authors observed the molecular weight distribution from the Gel Permeation Chromatography (GPC) analysis in Fig. 7.15. Analysis showed the different behavior of the three PAO oils. The peak top at $M_w$=742 for PAO-A indicates straight polyalphaolefin. Whereas for PAO-B, two peaks were found: $M_w$=528 for polyalphaolefin and $M_w$=1869 for polymethakrylate

(PMA). PAO-B is a lower-viscosity grade base blended oil than PAO-A and PMA. In case of PAO-C, peak occurred at $M_w$=683 for base polyalphaolefin and another peak at $M_w$=267 for any synthetic oil. Presence of PMA in PAO-B caused the lowest $T_{VE0}$.

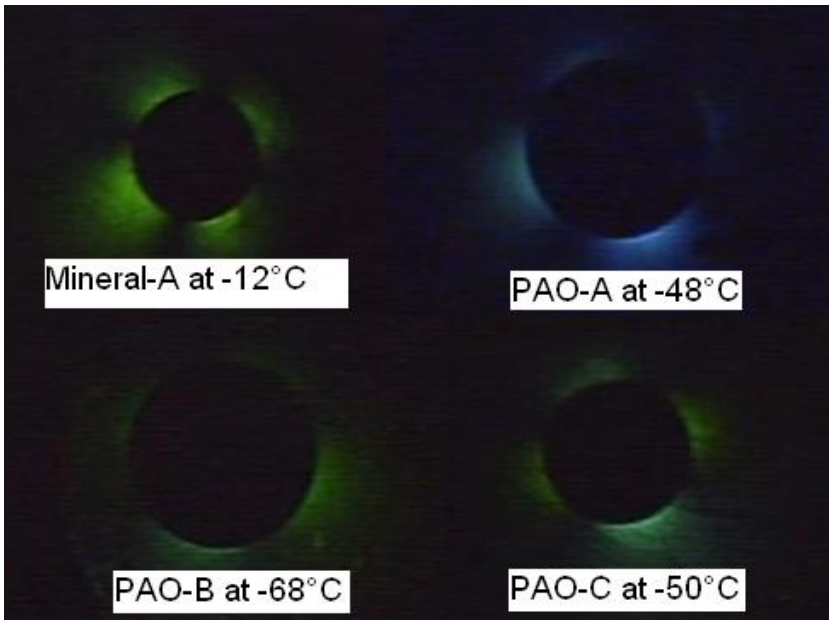


Fig. 7.13 Photoelastic effect in low temperature $T_{VE0}$ measurement

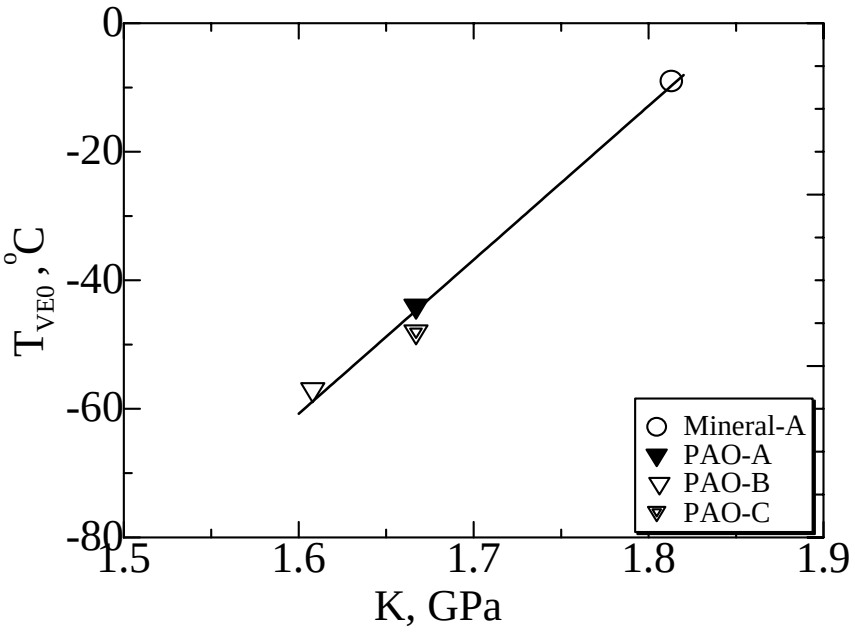


Fig. 7.14 Relation between viscoelastic solid transition temperature and adiabatic bulk modulus of wind turbine gear oils

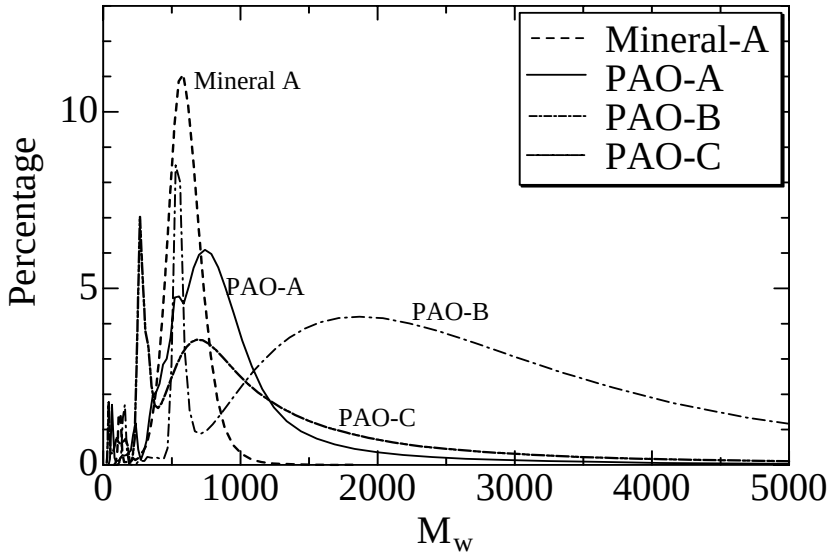


Fig. 7.15 Molecular distributions of wind turbine gear oils from GPC test

## 7.6 Conclusion

From the above study, it can be concluded that the sound velocity in lubricating oil is an important property of lubricating oil. Adiabatic bulk modulus can calculated from the measured sound velocity. Adiabatic bulk modulus has relation with the lubricant various properties, such as wear behavior, friction, viscosity etc. Larger wear scar area has been found for low adiabatic bulk modulus of lubricating oil but they depend on molecular structure. Perfluoropolyether oils have low adiabatic bulk modulus, which showed comparatively higher wear but lower friction coefficient. But, in case of same group of oil, relation can be changed. Again, from the viscosity and bulk modulus relation, some samples have been found which can be used as hydraulic fluid, since high-bulk modulus fluid having low viscosity is suitable for hydraulic systems. Ester oils, PEG oils and Vegetable oils having high adiabatic bulk modulus with low viscosity compare to mineral oil and PAO oil. Ester oils having comparatively high pressure-viscosity coefficient with low viscosity can be used in some high-pressure applications, as like autofrettege system, and having low pressure-viscosity coefficient is suitable for hydraulic system. This study also found that the pressure-viscosity coefficient and the low temperature fluidity of wind turbine gear oil can predict from the adiabatic bulk modulus which can be calculated from the measured sound velocity.

# Chapter 8

# Application of Sound Velocity in Environment Friendly Lubricating Oils

## 8.1 Introduction

It is well known that mechanical systems often employ lubricants, the majority of which are petroleum based, to decrease component friction and surfaces wear. Now a days, due to rising of petroleum based oil prices, the diminishing supplies of natural resources, global climate change and increased environmental sensitivity, various alternatives to petroleum based lubricants are currently being explored. Such alternatives include synthetic lubricants and vegetable based lubricants. Oils and fats of vegetable and animal origin were extensively used as lubricants till the middle of the $19^{th}$ century. In general, vegetable oils are highly attractive substitutes for petroleum based oils because they are environmentally friendly, renewable, less toxic and readily biodegradable.

Vegetable oils exhibit positive production trends and show good potential for a variety of industrial applications. The worldwide production of oilseed is increasing day by day, but at present it is costly compared to petroleum based oils. Economic losses are justified when considering the life cycle advantages of vegetable based lubricants [83]. From both production and life cycle standpoints, the future seems optimistic for vegetable oils as a viable replacement for petroleum based lubricants.

In general, when compared with mineral oil base stokes, vegetables oils have the following advantages: higher viscosity index, lower evaporation loss and enhanced lubricity, which leads to improved energy efficiency [84]. However, vegetable oils have performance limitations, particularly in thermal, oxidative and hydrolytic stability [85]. Vegetable oils typically contain about 80-95% fatty acids, which are one of the main performance improvers in lubricants [86]. On the other hand, mineral oil typically contains saturated aliphatic compounds, namely paraffinic and naphthenic, and small amount of aromatics [87]. Thereby, mineral oils are more stable than vegetable oils through their chemical nature, but they have poorer lubricity [88].

In this study, I have measured sound velocity of the vegetable oils. Sample vegetable oils are: castor oil, olive oil, rapeseed oil, coconut oil, mustard oil and

camellia oil. Among them, mustard oil was collected from directly pressed mustard seed. The sound velocity is measured by Sing around sound velocity measuring technique. From the measured sound velocity, calculated the adiabatic bulk modulus. Measured sound velocity was compared with other properties of vegetable oils.

Pressure viscosity coefficient $\alpha$ of vegetable oils was calculated from the high-pressure viscosity measurement. I have tried to find out a relation for pressure viscosity coefficient and adiabatic bulk modulus of vegetable oils as like traction oil, polyalphaolefin oil and paraffinic mineral oil.

## 8.2 Sample oil

In this study, six kinds of vegetable oils were tested. Tested vegetable oils are: castor oil, olive oil, rapeseed oil, coconut oil, mustard oil and camellia oil. Mustard oil was the directly pressed oil from mustard seed. Physical properties of tested vegetable oils are given at Table 8.1.

## 8.3 Chemical Composition of Vegetable Oils

Vegetable oils are primarily composed of triglycerides with various long-chain hydrocarbon fatty acids. The fatty acid content of lubricant heavily influences its tribological performance, with larger concentration of fatty acids leading to increased lubricity. There are a number of carboxylic acids that are referred to as being fatty acids. The fatty acids constitution of vegetable oils is given in Table 8.2.

Table 8.1 Physical properties of vegetable oils

| Oil name | Density $\rho$, g/cm$^3$ | Kinematic Viscosity $\nu$, mm$^2$/s | |
|---|---|---|---|
| | at 15 °C | at 40 °C | at 100 °C |
| Castor oil | 0.9666 | 241.0 | 17.5 |
| Olive oil | 0.9137 | 39.62 | 8.24 |
| Rapeseed oil | 0.9456 | 39.10 | 8.30 |
| Coconut oil | 0.9260 | 27.55 | 5.89 |
| Mustard oil | 0.9180 | 44.11 | 9.41 |
| Camellia oil | 0.9168 | 39.32 | 8.28 |

## 8.4 Experimental Procedure

Sound velocity of vegetable oils was measured by Sing around technique. The detail of the sound velocity measuring technique is explained in chapter 2 at experimental details section. Sound velocity was measured at different temperature. The relation between sound velocity and the temperature of vegetable oils is shown in Fig. 8.1.

Table 8.2 Fatty acid compositions of vegetable oils

| Constituent of fatty acids | Carbon ratio | Castor oil | Olive oil | Rape seed oil | Coco-nut oil | Mustar-d oil | Camel lia oil |
|---|---|---|---|---|---|---|---|
| | | % | % | % | % | % | % |
| Caproic | 6:0 | - | - | - | 0.4 | - | - |
| Caprylic | 8:0 | - | - | - | 7.7 | - | - |
| Capric | 10:0 | - | - | - | 6.2 | - | - |
| Lauric | 12:0 | - | - | - | 47 | - | - |
| Myristic | 14:0 | - | - | - | 18 | - | - |
| Palmitic | 16:0 | 1.1 | 9.8 | 3.9 | 9.5 | 3.5 | 8.2 |
| Palmitoleic | 16:1 | - | 0.6 | - | - | 0.4 | - |
| Stearic | 18:0 | 1 | 3.2 | 1.8 | 2.9 | 1.6 | 2.1 |
| Oleic | 18:1 | 4.1 | 73.8 | 57.9 | 6.9 | 19.7 | 85 |
| Ricinoleic | 18:1 (mono) | 87.8 | - | - | - | - | - |
| | 18:1 (poly) | 0.3 | - | - | - | - | - |
| Linoleic | 18:2 | 4.8 | 11.1 | 21.8 | 0.2 | 22.2 | 4.1 |
| Linolenic | 18:3 | 0.5 | 0.4 | 11.3 | - | 13.4 | 0.6 |
| Garoleic | 20:1 | - | - | 1.7 | - | 13.8 | - |
| Eicosadienoic | 20:2 | - | - | - | - | 1.2 | - |
| Behenic | 22:0 | - | - | - | - | 0.7 | - |
| Erucic | 22:1 | - | - | 1 | - | 21.4 | - |
| Nervonic | 24:1 | - | - | - | - | 1.5 | - |

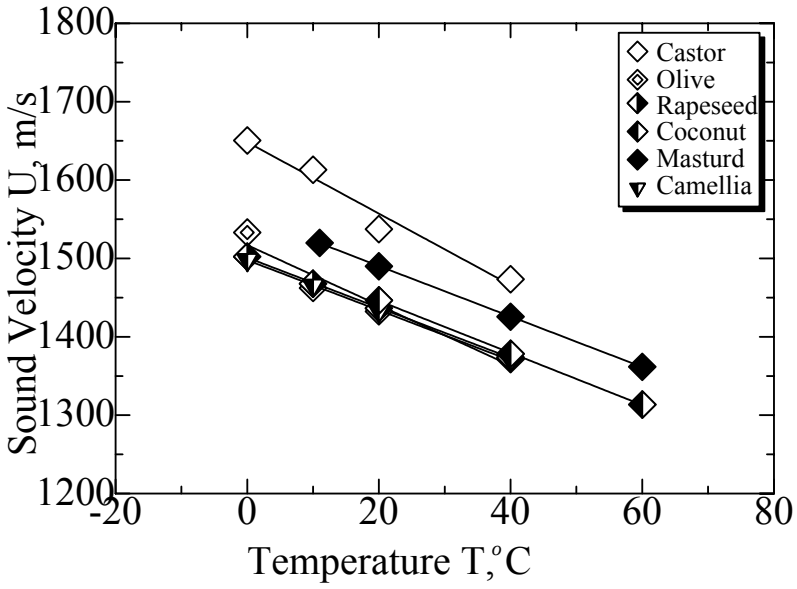


Fig. 8.1 Change of sound velocity with temperature of lubricating oil

It has been already explained about the importance of adiabatic bulk modulus of lubricating oil. The adiabatic bulk modulus of vegetable oils was calculated from the measured sound velocity. Since sound velocity of any substance is related to its bulk modulus and the density. Density of the tested vegetable oils was measured by a digital densitometer. From the measuring data, tried to find out the relation between each of property and sound velocity.

Pressure-viscosity coefficient $\alpha$ was calculated from the high pressure viscosity measurement. Measuring procedure is explained in chapter 3 at experimental details section. High pressure viscosity was measured by falling ball viscometer at 20 °C to 100 °C. This measuring temperature varied on different type of vegetable oils. High pressure viscosity of castor oil measured at that range but for mustard oil it was up to 60 °C. For coconut oil measured at 40 °C and 60 °C. the actual measurement value of high-pressure viscosity for mustard oil in the range to the pressure of 0.35 GPa is shown in Fig. 8.2. From that way pressure viscosity coefficient at different temperature was calculated. As like the previous study of traction oil, polyalphaolefin oil and paraffinic mineral oil using the experimental value of pressure-viscosity coefficient, I have tried to find out a relation to predict the pressure viscosity coefficient of vegetable oils.

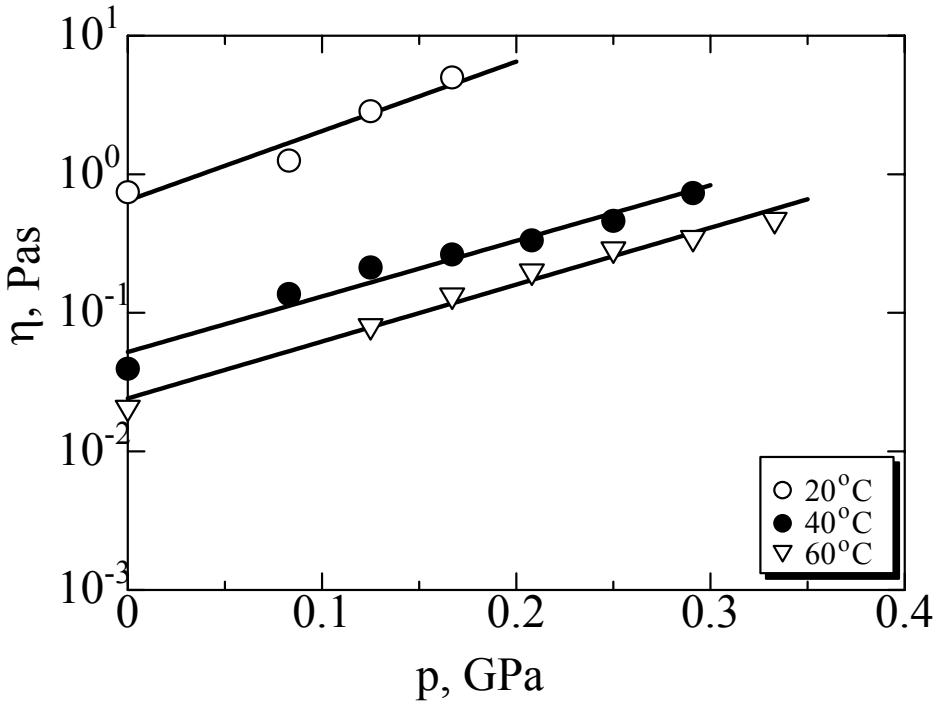


Fig. 8.2 Pressure-viscosity – temperature relation of Mustard oil

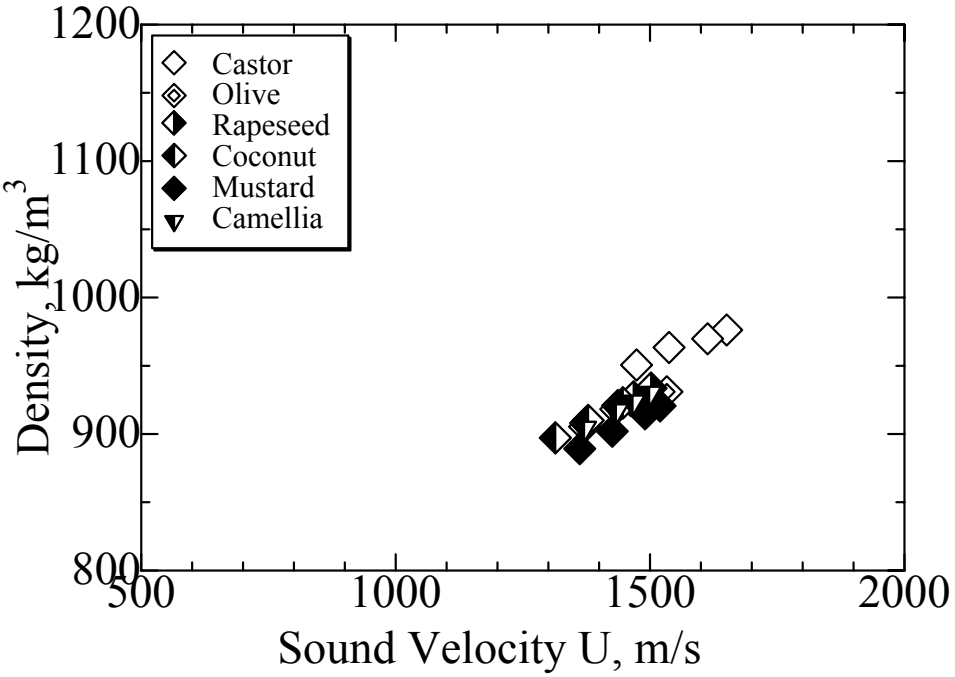


Fig. 8.3 Relation between the density and the sound velocity of vegetable oil

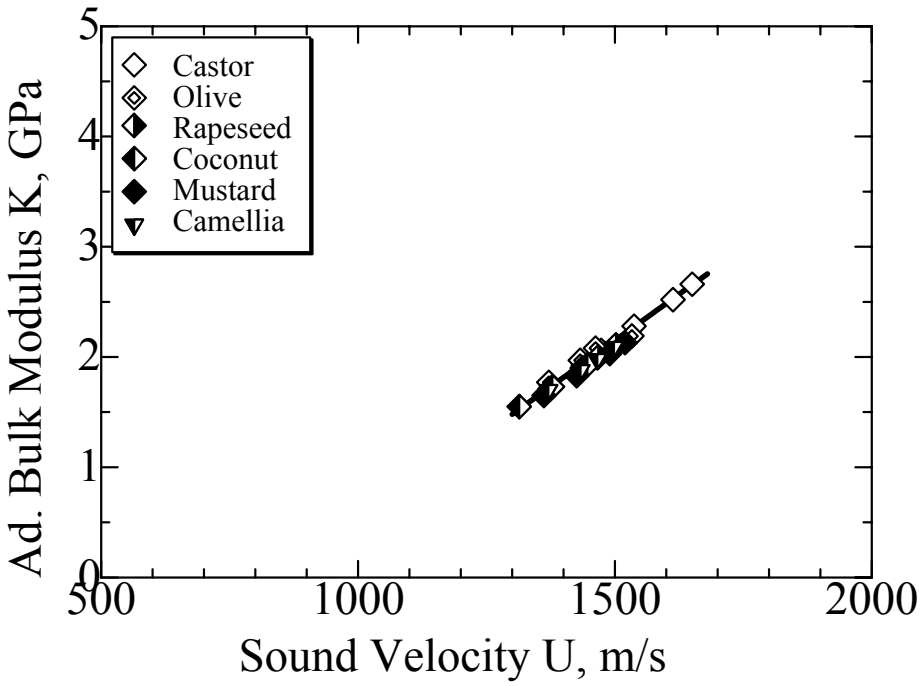


Fig. 8.4 Relation between adiabatic bulk modulus and sound velocity of lubricating oil

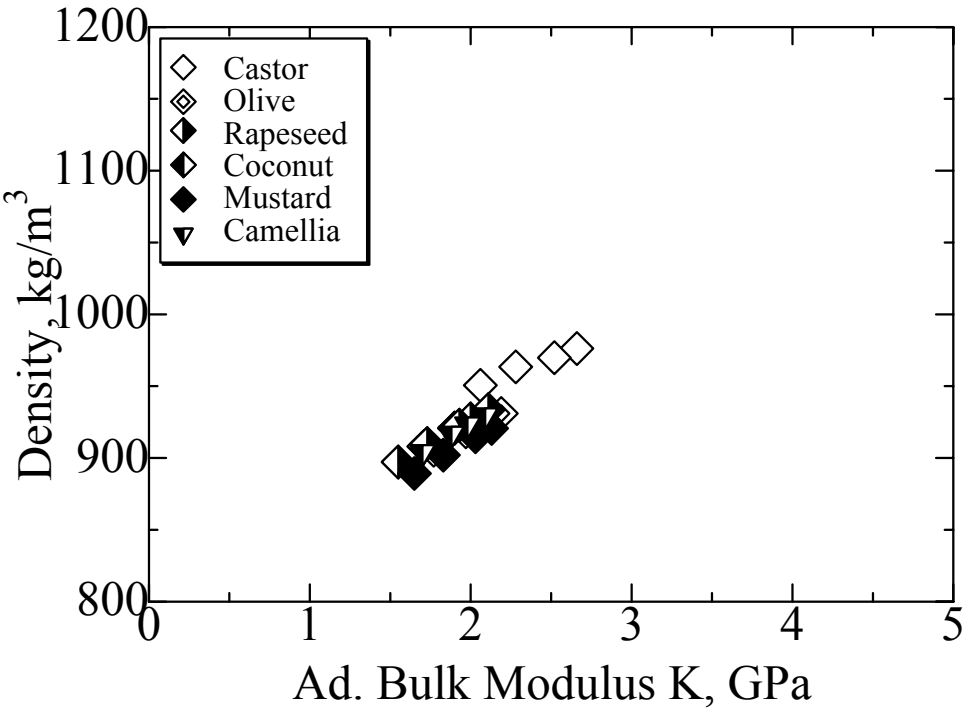


Fig. 8.5 Relation between density and adiabatic bulk modulus of vegetable oils

## 8.5 Results and Discussion

Sound velocity of lubricating oil is also an important property. Sound velocity is the disturbance of molecules, so it has effect on the molecular structure of the lubricating oil. Increasing the temperature the bond of the molecule becoming loose and sound velocity decreasing correspondingly. Figure 8.1 shows the changes of sound velocity with temperature. Decreasing rate of sound velocity through the vegetable oil indicates same of all vegetable oil except for castor oil. The relation between sound velocity and the density of vegetable oils is shown in Fig. 8.3.

Castor oil shows the higher density and sound velocity as well. Figure 8.4 shows the relation between adiabatic bulk modulus and the sound velocity. Among the tested vegetable oils castor oil has the higher sound velocity. So it exhibited the higher bulk modulus compared to other vegetable oils. Castor oil is widely used vegetable oil as lubricant. It has an unusual composition and chemistry, which makes it quite valuable. Eighty eight percent of fatty acid existed in castor oil. Ricinoleic acid, a monounsaturated, 18-carbon fatty acid, has a hydroxyl functional group at the twelfth carbon, a very uncommon property for a biological fatty acid. Figure 8.4 also shows, the bulk modulus increases proportionally to the sound velocity of the vegetable oils. Since both the bulk modulus and density of castor oil are higher than other vegetable oils, sound velocity of castor oil also given higher value. Figure 8.5 represent the relation between the density and adiabatic bulk modulus of vegetable oils.

The vegetable oils are environmentally friendly lubricant. The awareness and application of vegetable oils increases day by day. Siniawski et al. [89] has investigated the tribological characteristics of two vegetable oils and compared with a base mineral oil. They found the influence of fatty acid composition on tribological performance with lower abrasion rate and friction when compared to the mineral oil. Pressure-viscosity relationship is important parameter of lubricating oil to understand its performance. Mia. et al. [90] studied the high-pressure rheology of same vegetable oils and calculated the pressure-viscosity coefficient and low temperature fluidity and drawn the phase diagram. In this research I have also investigated the pressure viscosity relation and correlates with the sound velocity for vegetable oils. The experimental results are given in Table 8.3 for vegetable oils.

Table 8.3 Experimental results for Vegetable oils

| Sample oil | Temperature *T* | Sound velocity *U* | Ad. bulk modulus *K* | Experimental pressure viscosity coefficient $\alpha_{exp}$ |
|---|---|---|---|---|
| | °C | m/s | GPa | $GPa^{-1}$ |
| Castor | 20 | 1537 | 2.28 | 14.0 |
| | 40 | 1473 | 2.06 | 11.3 |
| | 60 | 1385 | 1.77 | 8.5 |
| | 80 | 1296 | 1.52 | 7.7 |
| | 100 | 1208 | 1.29 | 7.6 |
| Olive | 25 | 1449 | 1.92 | 9.2 |
| | 40 | 1397 | 1.77 | 8.1 |
| Rapeseed | 20 | 1437 | 1.90 | 11.0 |
| | 40 | 1374 | 1.71 | 9.3 |
| | 70 | 1278 | 1.45 | 8.3 |
| Coconut | 40 | 1378 | 1.73 | 13.1 |
| | 60 | 1314 | 1.55 | 9.8 |
| Mustard | 20 | 1490 | 2.03 | 11.5 |
| | 40 | 1426 | 1.83 | 9.2 |
| | 60 | 1362 | 1.65 | 9.5 |
| Camellia | 28 | 1410 | 1.81 | 8.5 |
| | 40 | 1370 | 1.70 | 7.0 |

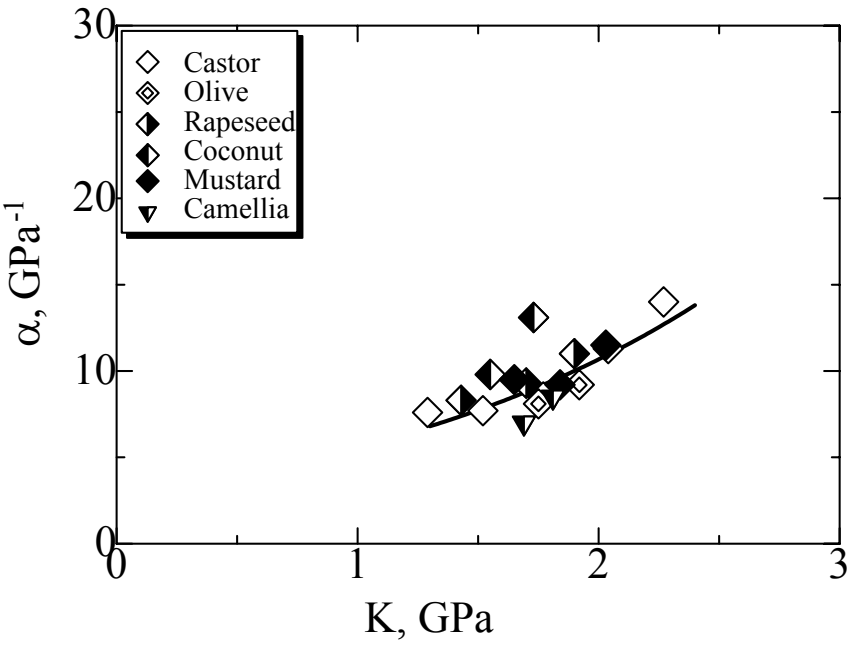


Fig. 8.6 Relation between pressure viscosity coefficient and bulk modulus

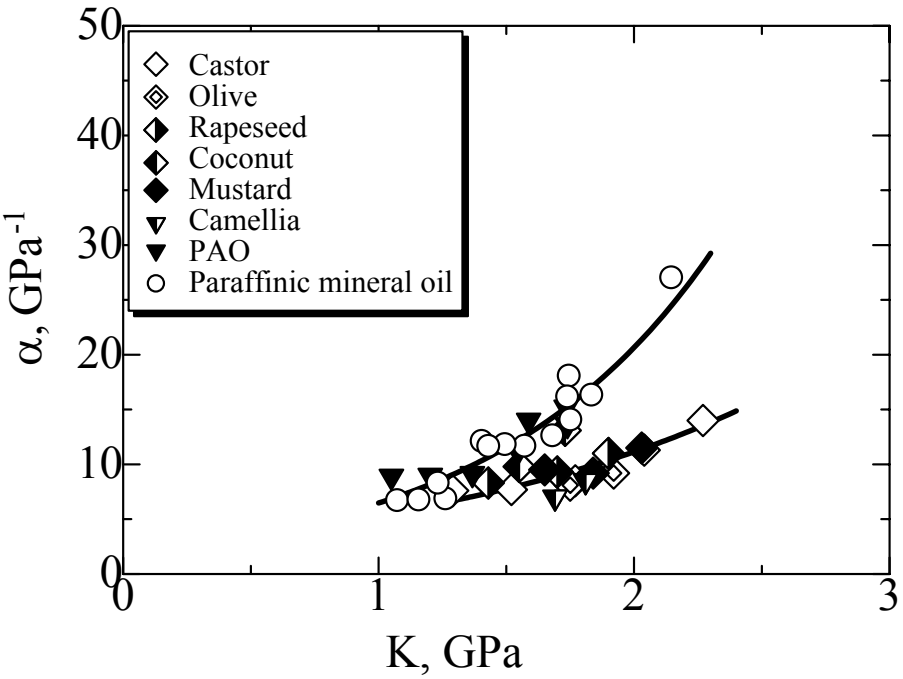


Fig. 8.7 Comparison of pressure viscosity coefficient-bulk modulus relation with paraffinic mineral oil and PAO

In chapter 4, I have explained the relation between the bulk modulus and the pressure viscosity coefficient. Figure 8.6 shows the relation between the pressure viscosity coefficient and the bulk modulus for vegetable oils. Bulk modulus was calculated from the measured sound velocity. In this figure, it was found that coconut oil exhibited different behavior considering other vegetable oil.

Then this relation was compared with the relation between pressure viscosity coefficient and bulk modulus of polyalphaolefine and paraffinic mineral oil as shown in Fig. 8.7. Among the vegetable oils coconut oil's behavior of pressure viscosity has found as like the polyalphaolefin and paraffinic mineral oil. From the chemical composition of vegetable oils, it has found that coconut oil has huge amount of saturated fatty acid which are straight chain single bonded carbon. Jayadas et al. [91,92] has shown in their various researches that coconut oil can be the alternative of mineral oil for many applications as industrial lubrication, as an automobile lubricant etc through some modifications.

So, except the coconut oil, I have tried to find out a correlation of pressure viscosity coefficient for other vegetable oils of unsaturated fatty acids. Correlation

obtained as like previous correlation for traction, PAO and paraffinic mineral oils. Pressure viscosity coefficient of vegetable oil also can be predicted from its bulk modulus K. The relation for the prediction is mentioned as below:

$$\alpha = 2.94\exp(0.644K) \tag{8.1}$$

Pressure viscosity coefficient α of the sample vegetable oils except coconut oil was calculated by the above equation (Eq. 8.1). The comparative results with experimental values are mentioned in Table 8.4. Error is shown as the deviation of calculated pressure viscosity coefficient $\alpha_{cal}$ from the experimental pressure viscosity coefficient $\alpha_{exp}$. Most of the error is within ± 10%, but also it has found some error exciding the limit. For the prediction ± 10% error is considered as precision prediction. But due to different chemical composition of different vegetable oils some error exhibited over the limit. So, for unsaturated fatty acid based vegetable oils, we can predict the pressure viscosity coefficient α by Eq. 8.1 from its adiabatic bulk modulus *K*.

Table 8.4 Predicted pressure viscosity coefficient and error respect to experimental pressure viscosity coefficient for vegetable oils

| Sample oil | *T* | *K* | $\alpha_{exp}$ | $\alpha_{cal}$ | Error |
|---|---|---|---|---|---|
| | °C | GPa | $GPa^{-1}$ | $GPa^{-1}$ | % |
| Castor oil | 20 | 2.27 | 14.0 | 12.7 | 9.29 |
| | 40 | 2.04 | 11.3 | 10.9 | 3.10 |
| | 60 | 1.77 | 8.5 | 9.2 | -8.25 |
| | 80 | 1.52 | 7.7 | 7.8 | -1.72 |
| | 100 | 1.29 | 7.6 | 6.8 | 11.14 |
| Olive oil | 25 | 1.92 | 9.2 | 10.1 | -10.16 |
| | 40 | 1.75 | 8.1 | 9.1 | -12.14 |
| Rapeseed oil | 20 | 1.9 | 11.0 | 10.0 | 9.04 |
| | 40 | 1.7 | 9.3 | 8.8 | 5.43 |
| | 70 | 1.43 | 8.3 | 7.4 | 10.95 |
| Mustard oil | 20 | 2.03 | 11.5 | 10.9 | 5.40 |
| | 40 | 1.84 | 9.2 | 9.6 | -4.63 |
| | 60 | 1.65 | 9.5 | 8.5 | 10.35 |
| Camellia oil | 28 | 1.81 | 8.5 | 9.4 | -11.08 |
| | 40 | 1.69 | 7.0 | 8.7 | -24.84 |

## 8.6 Conclusion

Vegetable based lubricants are primarily composed of triglycerides with various long chain hydrocarbon fatty acids. They are environment-friendly lubricant and renewable. Their tribological performance is investigated day by day. In this research also investigated some performance through measuring the sound velocity of vegetable oils.

Sound velocity of vegetable oils also an important property. It has measured by Sing around technique. Adiabatic bulk modulus was calculated from the measured sound velocity and studied the relations of sound velocity and other properties of vegetable oils. Sound velocity in vegetable oils increases with the increasing of bulk modulus and adiabatic bulk modulus depends on the fatty acid composition of the vegetable oils.

Pressure viscosity relation is very important parameter of lubricating oil in elastohydrodynamic and boundary lubrication. A prediction equation of pressure-viscosity coefficient for vegetable oil is proposed based on sound velocity of unsaturated fatty acids leading vegetable oils.

# Chapter 9

# Summery and Future Recommendations

## 9.1 Summery of the Thesis

Sound velocity is one of the essential parameter of lubricating oil. The effect of sound velocity has been found on the tribological and rheological behavior of lubricating oil. Sound velocity is related with the other properties of lubricating oil. Adiabatic bulk modulus was calculated from the measured sound velocity. The study also considered the pressure-viscosity coefficient and low temperature fluidity as important property of lubricating oil in the field of tribology and high pressure rheology. The pressure viscosity coefficient is key property to know the performance of lubricating oil in Elastohydrodynamic and boundary lubrication. Adiabatic bulk modulus was compared with the tribological and rheological properties of lubricating oils. From the comparison, it has been found some prediction relation of the property to know the lubricant behavior. In this research sound velocity of lubricating oils was measured using Sing around technique. The summary of the research can be concluded as follows:

- Sound velocity in the lubricating oil was measured accurately by Sing around technique.
- Sound velocity in lubricating oil is an important parameter, which is related to the molecular structure of the lubricating oil.
- Adiabatic bulk modulus of lubricating oil can be calculated from the measured sound velocity.
- Adiabatic bulk modulus was compared with the experimental pressure-viscosity coefficient which was measured from the high pressure viscosity measurement. From the comparison, it has been found that the pressure-viscosity coefficient increases exponentially with the adiabatic bulk modulus.
- An excellent relation between the pressure viscosity coefficient and the bulk modulus has been found. The relationship demonstrates that the pressure-viscosity coefficient can be predicted from the adiabatic bulk

modulus. The prediction depends on the group of lubricating oil, due to their different molecular structure.

- This study proposed three equations to predict pressure-viscosity coefficient, one for the traction oil, one for the mineral oil and polyalphaolefin oil, and another for the unsaturated fatty acid type vegetable oil. Using these equations, the pressure-viscosity coefficient can be predicted from the sound velocity in lubricating oil at atmospheric pressure.
- Adiabatic bulk modulus was also compared with the viscoelastic solid transition temperature at atmospheric pressure which is an identifying parameter of low temperature fluidity of lubricating oil.
- For the lubricating oil of low adiabatic bulk modulus, good low temperature fluidity can found. Low adiabatic bulk modulus of oil indicates the lower viscoelastic solid transition temperature in case of the same group of oil.
- The study also considered the prediction of low temperature fluidity for blend oil from the base oils' properties. In case of blend oils, viscoelastic solid transition temperature can predict from the base oils' adiabatic bulk modulus and viscoelastic solid transition temperature. Hence, low temperature fluidity of blend oil can predict from the base oils' sound velocity.
- Sound velocity of lubricating oils is directly related to the molecular structure and it decreased with increases the temperature by loosing the bond energy and increases with the increases of the bulk modulus.
- It can be possible to find out the group of lubricating oils by measuring the sound velocity and compared with density, bulk modulus and surface tension. It can be easily identified the group of hydrocarbon oil (traction, PAO and paraffinic mineral oil), perfluoropolyether oil and glycerol. Behavior of traction oil, polyalphaolefin (PAO) oil and paraffinic mineral oils is almost similar since the hydrocarbon oil's molecular structure is almost similar.

- Sound velocity of the lubricating oil can be estimated from the properties related to the molecular structure. An estimated formula for sound velocity from the density and surface tension has proposed in this research.
- This study also found some relation of sound velocity as well as the adiabatic bulk modulus to the tribological applications and with the boundary lubrication. Adiabatic bulk modulus influence on the wear and frictional behavior of lubricating oil. Low adiabatic bulk modulus fluid indicated the higher wear scar on materials. It also found that low adiabatic bulk modulus fluid indicates lower friction coefficient.
- From the relation between adiabatic bulk modulus and the sound velocity, application of the fluid can be identified. Higher adiabatic bulk modulus fluid having low viscosity is suitable as hydraulic fluid.
- Low temperature fluidity of wind turbine gear oil can also predict from the sound velocity in it. Low adiabatic bulk modulus indicates better low temperature fluidity, and better wears behavior of the gear oil.
- Vegetable oils are renewable and environment-friendly lubricant. In this research also investigated some performance through measuring the sound velocity of vegetable oils. Adiabatic bulk modulus depends on the fatty acid composition of the vegetable oils.
- Vegetable oils in general have excellent properties such as high viscosity index, high lubricity, high flash point, high bio-degradability etc. So, the important parameter pressure-viscosity coefficient also has been investigated and finally a prediction equation of pressure viscosity coefficient has been proposed for the vegetable oils based on sound velocity measurement.

## 9.2 Limitations and Future Recommendations

There are many researches on sound velocity measurement in different field but the measurement of sound velocity in lubricating oil and correlation with tribological and rheological behavior of lubricating oil is not available. In this research, I have proposed several prediction equations for pressure viscosity coefficient. For few sample and operating condition, errors exceeded the limit. So it should necessary to consider adequate experimental data for the prediction. Specially, due to lack of

sufficient experimental data I did not mention the prediction equation but showed the relation for the perfluoropolyether (PFPE) oils. PFPE is the most important lubricant in the modern lubrication such as magnetic recording media, aerospace industry and satellite instruments, hydraulic fluids, high temperature liquid lubricants in turbine engines etc. The study also showed the effect of sound velocity in PFPE oil on the frictional and wear behavior. Vegetable oils have a good prospect as lubricant and base oil of lubricant. In this research, a prediction equation has proposed for pressure viscosity coefficient for the unsaturated fatty acids based vegetable oils. By the measuring of sound velocity and other properties related to molecular structure, it will be possible to identify the nature of vegetable oils and classified on saturated and unsaturated fatty acids based vegetable oils. In this research, I have measured the sound velocity of liquid lubricant at atmospheric pressure. But, high pressure is applied in most of the tribological and the rheological application. Though, the data of sound velocity in lubricating oil at atmospheric pressure was compared with some properties involved high pressure. It can be possible to measure the sound velocity in lubricating oil at high pressure. It can be also possible to measure the sound velocity in grease and gel lubricant by studying the behavior of sound wave propagation through them and design oil container and select the appropriate sound velocity sensor in transducers. Behavior of grease and gel lubricant can be known from the sound velocity in it.

## References:


1. Ludema, K. C. (1996), *Friction, Wear, Lubrication: a text book in tribology*, CRC Press Inc., New York, USA.
2. Halling, J. (1976), *Introduction to Tribology*, Wykeham Publications (London) Ltd., London
3. Bhushan, B. (1999), *Principles and Applications of Tribology*, John Wiley & Sons, Inc., New York, USA.
4. Schowalter, W. R. (1978), *Mechanics of non-Newtonian Fluids*, ISBN-0-08021778-8.
5. Lansdown, A. R. (1982), *Lubrication: A practical guide to lubricant selection*, Pergamon Press Ltd., Oxford, England.
6. Barus, C. (1893), Isothermal, Isopiestics and Isometrics Relative to Viscosity, *American Journal of Science*, Vol. 45, pp. 87-96.
7. Bondi, A. (1951), *Physical Chemistry of Lubricating Oils*, Reinhold Publishing Corporation, New York, USA.
8. *The American Heritage Dictionary of English Language*, Fourth Edition, (2006), Houghton Mifflin Company, Boston, MA, USA.
9. Strutt, J.W. and Rayleigh, B. (1896), *The Theory of Sound*, Third Edition, Macmillan, London.
10. Laplace, P.S. (1816), *Analytical Chemistry*, Vol. 3, pp. 238-241.
11. Urick, R.J. (1947), A Sound Velocity Method for Determining the Compressibility of Finely Divided Substances, *Journal of Applied Physics*, Vol.18, pp. 983-987.
12. Wood, A.B. (1964), *A Text Book of Sound*, Third Edition, Bell and Sons, London.
13. Nichita, D. V., Khalid, P. and Broseta, D. (2010), Calculation of Isentropic Compressibility and Sound Velocity in Two-phase Fluids, *Fluid Phase Equilibria*, Vol. 291, No. 2, pp. 95-102.
14. Okazaki, N. (2000), Temperature Rule for the Speed of Sound in Water: A Chemical Kinetics Model, *Chem. Eur. Journal*, Vol.6, No.18, pp. 3339-3343.

15. Povey, M. J. W. et al. (2005), Estimating Organic Chain Length through Sound Velocity Measurements, *Ultrasonics*, Vol. 43, pp. 219-226.
16. Bell, J. C. and Kannel, J. W. (1971), Interpretations of the thickness of Lubricant Films in Rolling Contact II-Influence of Possible Rheological Factors, *Journal of Lubrication Tech. Trans. of ASME*, Vol. 93, No. 4, pp. 485-497.
17. Cheng, H. S. (1972), Isothermal Elastohydrodynamic Theory for the Full Range of Pressure-Viscosity coefficient, *Journal of Lubrication Tech. Trans. of ASME*, Vol. 94, No.1, pp. 35-43.
18. Fresco, G. P., Klaus, E.E. and Tewksbury, E. J. (1969), Measurement and Prediction of Viscosity-Pressure Characteristics of Liquids, *Journal of Lubrication Tech. Trans. of ASME*, Vol. 91, pp. 451-458.
19. Appeldoorn, J. K. (1963), A Simplified Viscosity-Pressure-Temperature Equation, *SAE Paper 630709*
20. Roelands, C. J. A., Vlugter, J. C. and Waterman, H. I. (1963), The Viscosity-Temperature-Pressure Relationship of Lubricating Oils and Its Correlation with Chemical Constitution, *ASME Journal of Basic Engineering*, December, pp. 601-608.
21. Johnston, W. G. (1981), A Method to Calculate the Pressure-Viscosity Coefficient from Bulk Properties of Liquids, *ASLE Transaction*, Vol. 24, No. 2, pp. 233-238.
22. So, B. Y. C. and Klaus, E. E. (1980), Viscosity-Pressure Correlation of Liquid, *ASLE Transaction*, Vol. 23, No. 4, pp. 409-421.
23. Wu, C. S., Klaus, E. E. and Duda, J. L. (1989), Development of a Method for the Prediction of Pressure-Viscosity Coefficients of Lubricating Oils Based on Free-Volume Theory, *Journal of Tribology, Trans. of ASME*, Vol.111, pp. 121-128.
24. Bair, S. and Kottke, P. (2003), Pressure-Viscosity Relationships for Elastohydrodynamics, *STLE Tribology Transaction*, Vol. 46, No. 3, pp. 289-295.
25. Leeuwen, H. V. (2009), The Determination of the Pressure-Viscosity coefficient of a Lubricant through an Accurate Film Thickness Formula and

Accurate Film Thickness Measurements, *Proc. ImechE Part J: Journal of Engineering Tribology*, Vol. 223, No. 8, pp. 1143-1163.

26. Roelands, C. J. A. (1966), Correlational Aspects of the Viscosity-Temperature-Pressure Relationship of Lubricating Oils, *Ph. D Thesis*, University Microfilms, Ann Arbor, Michigan, USA.
27. Bair, S. (2004), Roelands' Missing Data, *Proc. ImechE Part J: Journal of Engineering Tribology*, Vol. 218, No. 1, pp. 57-60.
28. Bair, S. (2001), The Variation of Viscosity with Temperature and Pressure for various Real Lubricants, *Journal of Tribology, Trans. of ASME*, Vol.123, No. 2, pp. 433-436.
29. Bair, S., Jarzynski, J., Winer, W. O. (2001), The Temperature, Pressure and Time Dependence of Lubricant Viscosity, *Tribology International*, Vol. 34, No. 7, pp. 461-468.
30. Bair, S. (2000), Pressure-Viscosity Behavior of Lubricants to 1.4 GPa and Its Relation to EHD Traction, *STLE Tribology Transaction*, Vol. 43, No. 1, pp. 91-99.
31. Yukhno, T. P., Vvdenski, Y. V., Sentyurikhina, L. N. (2001), Low Temperature Investigations on Frictional Behavior and Wear Resistence of Solid Lubricant coatings, *Tribology International*, Vol. 34, No. 4, pp. 293-298.
32. Matveevsky, R. M. (1958/1959), Influence of Low Temperatures on the Lubricating Capacity of Mineral Oils, *Wear*, Vol. 2, pp.315-317
33. Sharma, B. K., Stipanovic, A. J. (2004), Predicting of low temperature lubricant rheology using nuclear magnetic resonance spectroscopy and magnetic spectroscopy, *Tribology Letters*, Vol.16, No. 1-2, pp. 11-19.
34. Ohno, N, Hattori, N, Kuwano, N, Hirano, F. (1988), Some Observations on the Relationship between Rheological Properties of Lubricants at High Pressure and Regimes of Traction (Part 1), *Journal of Japan Society of Lubrication Engineers*, Vol. 33, No.12, pp. 56-62.
35. Kagathara, V. M. and Parsania, P. H. (2001), Sound velocity and thermodynamic parameters of chloro epoxy resins of bisphenol-C solutions in chlorinated and aprotic solvents at 35°C and 40°C, *European Polymer Journal*, Vol. 37, No. 7, pp. 1373-1377.

36. Hsu, S. M. (2004), Molecular basis of lubrication, *Tribology International*, Vol. 37, pp. 553-559.
37. Jones, W. R. Jr. and Hady, W. F. (1970), The effect of humidity and a Wettability Additive on Polyphenyl Ether Boundary Lubrication of Steel in Air and Nitrogen to 350 °C, *NASA TN D-6055*
38. Prahl, J. M. and Hamrock, B. J. (1984), The Mechanism of a Gaseous Film Barrier to Lubricant Wetting of Elastohydrodynamically Lubricated Conjunctions, *11th Leeds-Lyon Symposium on Tribology*, Leeds, UK.
39. Guangteng, G. and Spikes, H. A. (1996), The Role of Surface Tension and Disjoining Pressure in Starved and Parched Lubrication, *Journal of Engineering Tribology*, Vol. 210, J6, pp 113-124.
40. Borruto, A., Crivellone, G. and Marani, F. (1998), Influence of Surface Wettability on Friction and Wear Tests, *Wear*, Vol. 222, pp. 57-65.
41. Jones, W. R. (1986), Contact Angle and Surface Tension Measurements of a Five-Ring Polyphenyl Ether, *ASLE Trans*. Vol. 29, No. 3, pp. 276-282.
42. Wills, J. G. (1980), *Lubrication Fundamentals*, Marcel Dekker, New York.
43. Winer, W. O. (1982), *Lubricants, Tribological Technology – Volume II*, Senholzi, P.B., Eds., Martinus Mijhoff Publishers, The Hegue, pp 407-467.
44. Bhushan, B. (1990), *Tribology and Mechanics of Magnetic Storage Devices*, Springer, New York.
45. Jones, W. R. Jr. (1995) Properties of Perfluoropolyethers for Space Applications, *Tribology Transaction*, Vol. 38, pp. 557-564.
46. Liang, J. C. and Helmick, L. S. (1996), Tribochemistry of a PFPAE fluid on M-50 Surfaces by FTIR Spectroscopy, *Tribology Transaction*, Vol. 39, pp. 705-709.
47. Chemical Society of Japan (1975), *Handbook of Chemistry*, Maruzen, Tokyo, Japan, pp. 609.
48. Ohno, N. (1998), High Pressure Rheology of Lubricants and Liquid/Solid Transition Lubrication at High Pressure EHD Contacts, *Japanese Journal of Tribology*, Vol. 43, No. 6, pp. 699-708.
49. Bair, S. (2007), *High Pressure Rheology for Quantitative Elastohydrodynamics*, Elsevier, London, UK.

50. Bridgman, P. W. (1931), *The Physics of High Pressure*, Dover, New York, USA, pp. 330-340.
51. Ivring, J. B. and Barlow, A. J. (1971), An automatic High Pressure Viscometer, *Journal of Physics E*, Vol. 4, pp. 232-236.
52. Bair, S. and Winer, W. O. (1980), Some observations on the relationship between Lubricant Mechanical and Dielectric Transition under Pressure, *Journal of Lubrication Technology*, Vol.102, pp. 229-235.
53. Ohno, N. and Hirano, F. (2001), High Pressure Rheology Analysis of Traction Oils Based on Free Volume Measurements, *Lubrication Engineering*, Vol. 57, No.7, pp. 16-22.
54. Ohno, N., Kuwano, N. and Hirano, F. (1993), Effect of Bulk Modulus of Solidified Oils Under High Pressure on Tractional Behavior, *Japanese Journal of Tribology*, Vol. 38, No. 10, pp. 1361-1372.
55. Bair, S. and Qureshi, F. (2002), Accurate Measurement of Pressure-Viscosity Behavior in Lubricants, *STLE Tribology Transaction*, Vol. 45, No. 3, pp. 390-396.
56. Block, H. (1963), Inverse Problems in Hydrodynamic Lubrication and Design Directives for Lubricated Flexible Surfaces, *Proc. of International Symp. Lubrication and Wear*, Muster and Stemlicht, Eds., p. 74.
57. Cohen, M. H. and Turnbull, D. (1959), Molecular Transport in Liquids and Glasses, *Journal of Chem. Physics*, Vol. 31, No. 5, pp. 1164-1169.
58. Cutler, W. G., McMickle, R. H., Webb, W. and Schiessler, R. W. (1958), Study of the Compressions of Several High Molecular Weight Hydrocarbons, *Journal of Chem. Physics*, Vol. 29, No. 4, pp. 727-741.
59. Wright, W. A. (1967), Prediction of Bulk Moduli and Pressure-Volume-Temperature Data for Petroleum Oils, *ASLE Transactions*, Vol. 10, pp. 349-356.
60. **Mia, S.** and Ohno, N. (2009), Prediction of Pressure-Viscosity Coefficient of Lubricating Oils Based on Sound Velocity, *Lubrication Science*, Vol. 21, No. 9, pp. 343- 354.
61. Bair, S. and Winer, W. O. (1979), Shear Strength Measurements of Lubricants at High Pressure, *ASME Journal of Lubrication Tech*., Vol.101, pp. 251-257.

62. Ohno, N. (2007), High-Pressure Behavior of Toroidal CVT Fluid for Automobile, *Tribology International*, Vol. 40, pp. 233-238
63. Sakai, T., Murakami, T., Yamamoto, Y., Uchiyama, H., Komoto, T. and Tezuka, T. (1992), A Naphthenic Oil of Hydrogeneted Coal Tar Distillate as a Lubricant with Low Solidification Pressure, *Journal of Synthetic Lubrication*, Vol. 9, No. 3, pp. 223-235.
64. Kondo, S., Sayles, R. S. and Lowe, M. J. S. (2006), A Combined Optical-Ultrasonic Method of Establishing the Compressibility of High-Pressure Oil and Grease Films Entrapped in a Ball on Flat Contact, *ASME Journal of Tribology*, Vol.128, pp. 155-167.
65. Kasolang, S. and Dweyer-Joyce, R. S. (2008), Viscosity Measurement in thin Lubricant Films using Shear Ultrasonic Reflection, *Proc. of the ImechE, Part J: Journal of Engineering Tribology*, Vol. 222, pp. 423-429.
66. **Mia, S**. and Ohno, N. (2010), Relation Between Low Temperature Fluidity and Sound Velocity of Lubricating Oil, *Tribology International*, Vol. 43, No. 5-6, pp. 1043-1047.
67. Hayashi, S., Masuhara, K., **Mia, S.**, Morita, S. and Ohno, N. (2008), Prediction of Pressure-Viscosity Coefficient of Mixtures, *Tribology Online*, Vol. 3, No. 2, pp. 86-89.
68. Ohno, N., Kuwano, N and Hirano, F. (1988), Observation of Mechanical Behavior of Solidified Oil by Using Photoelastic Method, *Journal of Japan Society of Lubrication Engineers*, Vol. 33, No. 9, pp. 693-699.
69. Ohno, N., Rahman, M. Z. and Tsutsumi, H. (2006), High-Pressure Short Time Behavior of Traction Fluids, *Lubrication Science*, Vol.18, pp. 25-36.
70. Ohno, N. and Yamada, S. (2007), Effect of High-Pressure Rheology of Lubricants upon Entrapped Oil Film Behavior at Halting Elastrohydrodynamic Lubrication, *Proc. of ImechE, Part J: Journal of Engineering Tribology*, Vol. 221, pp. 279-285.
71. Ohno, N., Rahman, M. Z. and Kakuda, K. (2005), Bulk Modulus of Lubricating Oils as Predominant Factor Affecting Tractional Behavior in High-Pressure Elastohydrodynamic Contacts, *STLE Tribology Transaction*, Vol. 48, pp. 165-170.

72. Keck, P. H. and Horn, W. V (1953), The Surface Tension of Liquid Silicon and Germanium, *Physical Review*, Vol. 91, No. 3, pp. 512-513.
73. Macleod, D. B. (1923), Relation between Surface Tension and Density, *Trans. of Farady Society*, Vol.19, pp.30.
74. Ohno, N., Komiya, H., **Mia, S**., Morita, S., Satoh, N. and Obara, S. (2009), Bearing Fatigue Life Tests in Advanced Base Oil and Grease for Space Applications, *STLE Tribology Transactions*, Vol. 52, No. 1, pp. 114-120.
75. Ohno, N., **Mia, S.**, Morita, S. and Obara, S. (2010), Friction and Wear Characteristics of Advanced Space Lubricants, *STLE Tribology Transactions*, Vol. 53, No. 2, pp. 245-255.
76. **Mia, S.**, Komiya, H., Morita, S., Ohno, N. and Obara, S. (2007), Viscosity Loss in PFPE Lubricant for Space Applications under EHL Conditions, *Tribology Online*, Vol. 2, No. 2, pp.54-58.
77. Ohno, N., **Mia, S**., Tateishi, K., Morita, S. and Shitara, Y. (2009), Construction of Phase Diagram uo to 2 GPa and 200°C for Thermo-Reversible Gel Lubricants by Diamond Anvil Cell, *Lubrication Science*, Vol. 21, No. 5, pp. 183-192.
78. **Mia, S.**, Morita, S. and Ohno, N. (2010), Effect of High-Pressure Rheology of Lubricating Oils on Boundary Lubrication, *Tribology International*, Article in Press, DOI: 10.1016/j.triboint.2010.04.003.
79. **Mia, S.**, Mizukami, S., Fukuda, R., Morita, S. and Ohno, N. (2010), High-Pressure Behavior and Tribological Properties of Wind Turbine Gear Oil, *Journal of Mechanical Science and Technology*, Vol. 24, pp. 111-114.
80. Gresham, R. M. (2009), Tilting at Wind Turbines, *Tribology and Lubrication Technology Magazine*, Vol. 65, No. 2, pp. 38-39.
81. Escobar, W. (2008), Understanding Polyalkylene Glycols (and where to apply them), *Tribology & Lubrication Technology Magazine*, Vol. 64, No. 5, pp. 34-39.
82. Rudnick, L. R. (2005), *Synthetics, Mineral Oils and Bio Based Lubricants: Chemistry and Technology*, CRC Press, Wilmington, USA, p.799.
83. Conningham, B., Battersby, N., Wehrmeyer, W. and Fotherg, C. (2004), A Sustainability Assessment of a Biolubricant, *J. of Industrial Ecology*, Vol. 7, No. 3-4, pp. 179-192.

84. Iowa Soybean Promotion Board and Center for Agricultural and Rural Development (1993), *The Future of the Iowa Soybean Industry*, Iowa State University.
85. Adhvaryu, A. Erhan, S. Z. and Perez, J. M. (2004), Tribological Studies of Thermally and Chemically Modified Vegetable Oils for Use as Environmentally Friendly Lubricants, *Wear*, Vol. 257, No. 3-4, pp. 359-369.
86. Fox, N. J., Tyrer, B. and Stachowiak, G. W. (2004), Boundary Lubrication Performance of Free Fatty Acids in Sunflower Oil, *Tribology Letters*, Vol.16, No. 4, pp. 275-281.
87. Morrison, R. B. and Boyd, R. N. (1983), *Organic Chemistry*, Allyan and Bacon: Boston, USA.
88. Leugner, L. (2003), How to Apply and Maintain Biodegradable Lubes, *Machinery Lubrication Magazine*, July 2003.
89. Siniawski, M. T., Saniei, N., Adhikari, B. and Doezeema, L. A (2007), Influence of fatty acid composition on the tribological performance of two vegetable-based lubricants, *Journal of Synthetic Lubrication*, Vol. 24, pp. 101-110.
90. **Mia, S.**, Hayashi, S. and Ohno, N. (2007), High Pressure Tribological Behavior of Vegetable Oils as Lubricant, *Proc. of International Conference on Mechanical Engineering*, 29-31 December, Dhaka, Bangladesh, FL-07.
91. Jayadas, N. H. and Nair, K. P. (2006), Coconut oil as base oil for industrial lubricants-evaluation and modification of thermal, oxidative and low temperature properties, *Tribology International*, Vol. 39, No. 9, pp. 873-878.
92. Jayadas, N. H., Nair, K. P. and Kumar, A. G. (2007), Tribological evaluation of coconut oil as an environment-friendly lubricant, *Tribology International*, Vol. 40, No. 2, pp. 350-354.

# Appendix A

## Specification of Sing Around Device

| | | |
|---|---|---|
| Product | | : UVM-2-7B |
| Measurement method | | : SING AROUND method |
| Power | | : AC 100V ± 10% 50/60 Hz |
| Power consumption | | : 30VA |
| Working climate condition | | : 0 ~ 40 °C, < 90% RH |
| Dimensions | | : 455 × 355 × 166 mm |
| Weight | | : 8 Kg |
| Working position | | : Keep horizontal |
| Transmission frequency | | : 1 ~ 10 MHz (adjustable setting) |
| Transmission pulse width | | : 0.5 ~ 0.05 μs (adjustable setting) |
| Measurement mode | | : Single probe and double probe techniques |
| Receiving window setting | | : Delay min. 0 μs max. 400 μs (setup 0.2 μs) |
| | | Width min. 0 μs max. 400 μs (setup 0.2 μs) |
| Fixed delay | | : Basic delay time 63.5 ± 2 μs |
| | | Multiple delay time N times 63.5 μs (N = 1 ~ 16) |
| Time base: | Frequency | : 10 MHz |
| | Ageing rate | : ± $1\times10^{-6}$ / year |
| | Temperature characteristics: ± $1\times10^{-6}$ / 0 ~ 50 °C | |
| Display: | Display A | : Sing around period 10 notation 8 ½ digit |
| | | Minimum digit 0.01 ns (average 10000 times) |
| | Display B | : Monitor 10 notation 3 digit |
| Output | | : 1. counter output 0.5 Vo – p 50 Ω |
| | | 2. RS-232C interface |
| | | Asynchronous communication method |
| Carrier velocity | | : 2400 bit/s |
| Data length | | : 8 bit |
| Parity | | : no |
| Stop bit | | : 2 bit |

## Parts Names and Functions

### Front Panel

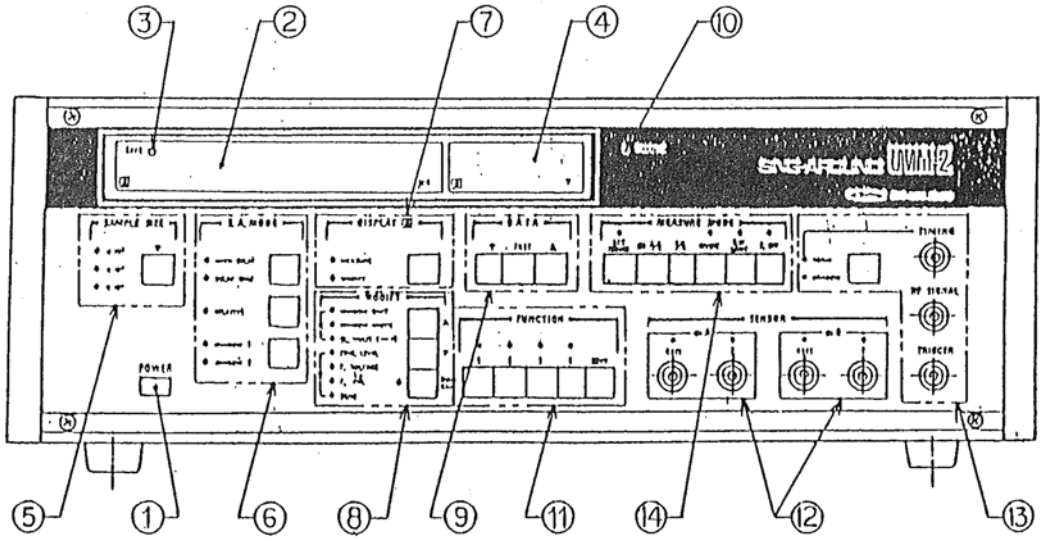


(1) POWER

Pushing the power switch, apparatus can turn on and turn off.

(2) [A]

LED display monitor of 10 notations, 8 ½ digit. The Sing around average cycle (in $\mu$s) is displayed.

Moreover, when (7) DISP [A] is set in “MODIFY” and (8) MODIFY is set to A (WINDOWS SHIFT, WINDOW WIDTH, DL MULTI), a set value of the set item is shown in this monitor. However, when the (14) COPY key is pushed, it is displayed that it is always a state of COPY.

(3) GATE

It lights while the counter is measuring it the cycle of the Sing around, and it turns it off while not measuring it.

(4) [B]

LED 10 notation display monitor of 10 notations 3 digit

The numerical value of MODIFY [B](TRIG. LEVEL, T. VOLTAGE, T. PW and SENS)is displayed in this monitor. When (8) MODIFY is set in A, “TRIG. LEVEL” is displayed.

(5) SAMPLE SIZE

The counter sets how many times to measure the average of the Sing around cycle. It changes whenever the key is pushed ($10^2 \rightarrow 10^3 \rightarrow 10^4$ time average).

(6) S. A. MODE

The delay circuit is installed to prevent the error margin because of a multiple echo in the sample and the Sing around is done including delay time.

“WITH DELAY” : The Sing around cycle is displayed in total including delay time and the propagation time.

“DELAY ONLY” : The Sing around cycle also display only the delay circuit.

“RELATIVE”: It is a function to display the difference with new measurements based on arbitrary measurements.

“WINDOW 1,2” : Two window is prepared with one setting, and when the key is pushed, it is switched. Even if the WINDOW position is not set in every case when the comparison of multiple echoes is measured, it is possible to measure it.

(7) DISPLAY [A]

The state of item of MODIFY A (WINDOW SHIFT, WINDOW WIDTH, DL MULTI) besides it is a Sing around cycle in [A] can be displayed.

“MEASURE” : [A] displays measurements.

“MODIFY” : If (8) MODIFY is A, the state of the selected item is displayed.
If (8) MODIFY is B, measurements are displayed.

(8) MODIFY

WINDOW is set before and behind the reception wave, and detection of the AGC operation and time is done only in WINDOW.

“WINDOW SHIFT” : Time from the transmission to the start of WINDOW is shown.

“WINDOW WIDTH” : Width of time that WINDOW is open, is shown.

“DL MULTI” : 1-16 times time of standards of the delay time (63.5 $\mu$s) can be set.

“TRIG. LEVEL” : The point to exceed the threshold of the voltage with the reception wave is changed when detecting it at the time of the reception wave and the reception wave is selected. The shape of waves chosen by “TRIG. LEVEL” detects 0 potential and the crossing point has been detected at time. “TRIG. LEVEL” comes in changeability within the range from 0to 2.5V. It sets it at the level that S/N of the reception wave is good as measurements are steady. When AGC operates, the amplifier output waveform if controlled to 1.5V. It outputs it to the terminal HF SIG by being divided into1/10 (0.15 V).

“T. VOLTAGE” : The high voltage power supply of the drive circuit of the transmission is set within the range from 0 to 250V, and the high frequency voltage of the transmission is changeable. In an actual setting, reception wave or “SENS” is monitored by thinking about the degree etc. of attenuation and the size of the sample and it sets it to a suitable value.

“T. PW” : When the transmission pulse width is set, it uses it. It sets it to a suitable pulse width for the frequency of the ultrasonic transducer used. The pulse width can be changed within the range from0.05 to 0.5 (1to 10MHz). It is displayed in [B] as a voltage value from 0 to 10V. The setting method makes to “MAIN GAIN” mode, and sets “T. PW” so that the reception wave may become the maximum.

“SENS” : AGC control voltage (0 to 9.99V) is displayed, and the state of the reception wave can be monitored. The monitor voltage increases when the reception wave is large. The monitor voltage decreases when the reception wave is small. If it is a value of “SENS” and a range from 2.0 to 8.0V, it is excellent.

“MAN GAIN” : it “MAN GAIN” key is pushed, the state of a GAIN at that time is maintained, and it becomes a fixed gain mode through it usually measures in the AGC mode. When GAIN is changed in the manual operation, MODIFY is switched to “SENS”, and it changes with the (9) DATA key. At this time, displays B the gain

control voltage within the range from 0 to 10V. GAIN decreases when the voltage increases. GAIN increases when the voltage decreases. It returns to the AGC operation when “MAN GAIN” key is pushed again.

(9) DATA

It uses it for the setting change of the item selected by (8) SELECT. The value of the setting is increased or decreased by operating UP key and DOWN key. When the FAST key is pushed together, the ratio of the change is accelerated to 10 times.

(10) RECEIVE

It lights when in the indicator that shows the state of the reception wave, the reception wave more that the trigger level is in WINDOW, and it turns it off when not is. When the reception wave level is small or another noise exists, it blinks unstable.

(11) MEASURE MODE

“ATT (20dB)” : The indicator lights when the key is pushed with attenuator for the limitation of the reception signal, and the input signal decreases by about 20dB.

“CH A/B”: Two channels A and B are prepared as an ultrasonic transducer connection terminal, and when the key is pushed, it is switched.

“T/R” : Single-probe and double-probe are switched. Connected terminal of the channel has been selected by SH A/B is switched to the connection of single-probe or double-probe.

“INVER” : The polarity that rising edge of the reception wave is good is selected with the key to reserve the polarity of the reception wave.

“BW LIMIT” : LOW PASS FILTER that limits the band of the amplifier is switched. If “BW LIMIT” is used, the high frequency noise is suppressed and when about 1 to 5MHz uses it, it becomes easy to measure.

"T. OFF" : The indicator lights when the key is pushed, and the transmission of each channel stops. It uses when the ultrasonic transducer is detached, and high-pressure shock is prevented.

(12) SENSOR

It is connected terminal of the ultrasonic transducer.

Single-probe → The ultrasonic transducer is connected with terminal R.

Double-probe → The ultrasonic transducer for the transmission is connected in terminal T and the ultrasonic transducer for the reception is connected with terminal R.

(13) CRT MONITIOR TERMINAL

Terminal connected when reception waveform is monitored with oscilloscope. Impedance is 50Ω.

"CRT TRIG" : The pulse that synchronizes with the transmission timing is output with the terminal to put synchronization on the oscilloscope. It connects it with an external synchronous terminal of the oscilloscope.

"HF SIG" : It is a monitor terminal of the reception wave form. The shape of waves after the amplification impedance is converted is output. When AGC operates, it is controlled to the size of 0.15V with HF SIG terminal.

"TIMING" : Reception WINDOW and the NORMAL signal can be monitored. It is switched alternately with a wave change key of WINDOW and NORMAL.

(14) FUNCTION

All the settings that can be operated on the panel side can be memorized as "FUNCTION". Four different settings can be memorized.

**Back Panel** has the electric input.

# Appendix B

## Mathematical Formulation of Falling Ball Viscometer

### Mathematical Formulations

A steel ball is dropped into the oil which is passed through an observation window. As pressure increases, it increases viscosity of the oil in the high-pressure container. The dropping ball speed becomes slower. In this principle this falling ball viscometer works and viscosity is calculated by the measuring speed of falling ball.

Considered the following assumptions:

a) Speed of ball will be small.
b) No slide between ball and the fluid.
c) Fluid is incompressible.
d) Fluid should be Newtonian.
e) Fluid is to expand infinitely.
f) Ball should be a rigid body.

Stocks' law, for the resistance of a sphere moving slowly a viscous liquid,

Buoyancy force, $f_1 = 3\pi\eta dv$ (B1)

Where, $\eta$: absolute viscosity of the fluid which is need to determined

d: diameter of the steel ball

v: speed of the dropping ball

Ball fall freely due to gravitational force,

Gravity force, $f_2 = \frac{\pi}{6}d^3\rho_0 g - \frac{\pi}{6}d^3\rho g$ (B2)

Where,

$\rho_0$: ball density

$\rho$: fluid density

g: gravitational force

Ball falls freely due to the gravity is equal to buoyancy force

$$f_1 = f_2$$

so, the viscosity of fluid, $\eta = \frac{d^2(\rho_0 - \rho)g}{18v}$ (B3)

But, it is unacceptable since the ball is falling down in the container and at high pressure the container expands gradually. Thus expansion of the container should be considered. Considering the influence of wall of the oil container,

$$\eta = \frac{d^2(\rho_0 - \rho)g}{18v} f_w \quad \text{(B4)}$$

$f_w$ : compensation coefficient toward the influence of the pipe wall

as dropping speed, v = d/t so, Eq. B4 becomes

$$\eta = \frac{d(\rho_0 - \rho)g}{18} f_w * t \quad \text{(B5)}$$

t: the time when the light was shut out with the ball falling

So, viscosity of a fluid can be determined by the simple calculation from the Eq. B5 using a falling ball viscometer. Time is measured by using light illuminant and a signal receiver.

**Determination of viscosity η at high pressure**

Pressure p can be found by load,

$$P = X*9.8*Z/\pi(r+u)^2 \quad \text{(Pa)} \quad \text{(B6)}$$

Where, X: load (ton)

Z: syringe coefficient (Z = 0.964)

r: container radius (6mm)

u: expansion of radius of the container

and u is found as,

$$u = 3.8458*10^{-4}*X*0.964/36\pi \quad \text{(mm)} \quad \text{(B7)}$$

viscosity at any temperature, t °C,

$$\eta_0 = \rho_t*\nu_t/1000 \quad \text{(Pa.s)} \quad \text{(B8)}$$

$\rho_t$: density at t °C ($g/cm^3$)

$\nu_t$: dynamic viscosity at t °C ($mm^2/s$)

Here, $\rho_t$ is measured as more than the density $\rho_{15}$ of the oil of 15 °C.

So, at oil temperature t can be measured,

$$\rho_t = \rho_{15} - 0.00064(t-15) \quad \text{(B9)}$$

Now, from WALTHER-ASTM, $\nu_t$ is

$$\log_{10}.\log_{10}(\nu+0.7) = A + B\cdot \log_{10}(273 +t) \quad \text{(B10)}$$

$\nu$ is dynamic viscosity at t °C

A and B are constant depend on oil

Viscosity is done at high pressure up to 3500 $kg_f$. Assumed diameter of the container does not change at the pressure 3500 $kg_f$ is 0.29 GPa. So,

$$\eta = \frac{d(\rho_0 - \rho)g}{18} f_w.t \quad \text{(B5)}$$

d: ball diameter (7.938 mm)

$\rho_0$: ball density (7.8 $g/cm^3$)

if $\rho_p$: density of oil under pressure (Dowson formula), so,

$\rho_p/\rho_t = 1 + 0.58p/ (1+1.68p)$

here p: pressure (GPa), $\rho_t = \rho_{15} - 0.00064(t-15)$

Finally viscosity becomes,

$$\eta = 0.535*(7.8-\rho_t)*t \quad \text{(B11)}$$

now from Baraus equation, $\alpha$ can be determined.

**Pressure-viscosity coefficient $\alpha$ determination**

Barus equation,

$$\eta = \eta_0 \exp(\alpha p) \quad \text{(B12)}$$

i.e. $\alpha p = \ln(\eta/\eta_0)$

$\alpha$: pressure-viscosity coefficient

p: pressure

$\eta_0$: viscosity under atmospheric pressure

$\eta$: viscosity under pressure

In this experiment $\eta$ depends on different pressures. Depending on load its correlation function is computed by a computer program to find out $\alpha$. It has 95 % accuracy limits and indicates how much reliability for the approximation its computation has.

# Appendix C

## Mathematical Formulation of High Pressure Densitometer

A known volume of 2 mL oil is used in the oil container for the experiment. The measurement of the load that is applied to the test oil is determined by load cell. A dial gauge is used in the measurement. The value H of the dial gauge in the volume of V is determined first as a base of the oil inside of the container (volume of the oil in vertical distance = 2L)

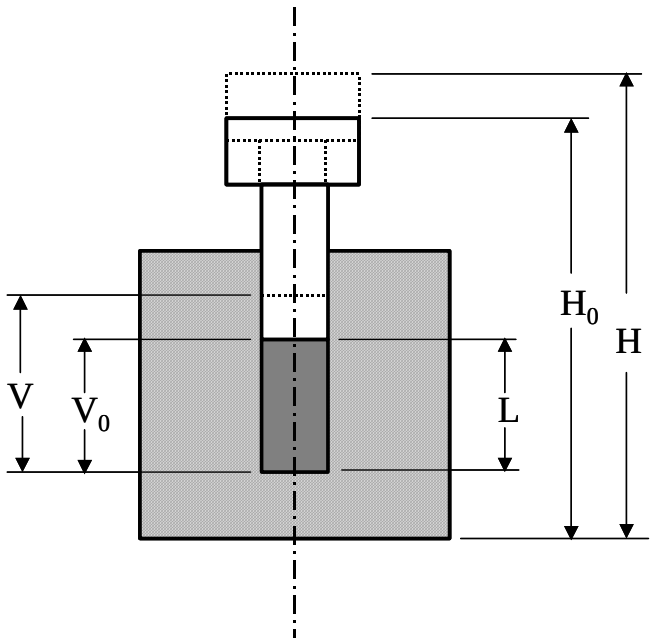


Here, r : inside radius (6 mL)

L: height of oil inside

Then, inside volume of the container, $V = \pi r^2 L$ [C1]

$$So, L = V/(\pi r^2)$$

Actually, the oil volume at the time of experiment is $V_0$

$$V_0 = \pi r^2\{L-(H_0-H)\} \quad [C2]$$

where $H_0$: dial gauge reading at load '0'.

The volume oil the oil from the reading of the dial gauge can be known from the above equation. At high pressure, cylinder may expand and it needs to be checked. If 'u' is the outward direction,

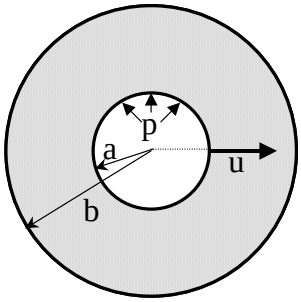


$$\frac{u}{a} = \frac{(1-v)R + (1+v)k^2/R}{k^2 - 1} \times \frac{P_a}{E} \qquad [C3]$$

where, k = b/a

R = r/a

E = $2.1 \times 10^4$ (kg/mm$^2$)

v: poisson's ratio (0.3)

$P_a$: high pressure

a: oil container inside radius (6mm)

b: oil container outside radius (40mm)

r: radius co-ordinate (if r = a)

Again, displacement u

$$u = 3.8458 \times 10^{-4} \times P_a \ (mm) \qquad [C4]$$

Section area of cylinder inside the oil container under high pressure

$$A_p = \pi \times (a+u)^2$$

$$= \pi \times (6 + 3.8458 \times 10^{-4} \times P_a)^2 \qquad [C5]$$

Syringe correction coefficient 0.964, the $P_a$ is

$$P_a = (X_p \times 0.964 \times 9.8) / (\pi \times 6^2) \qquad [C6]$$

$X_p$: reading of the load from universal testing machine ($kg_f$)

Now, Density under the pressure from the above calculation is,

$\rho_p = \rho_0 \times V_0 / V_p$

$$\Rightarrow \rho_p = \rho_0 \frac{36\pi\{L-(H_0-H)\}}{\pi\left(6+3.8458\times10^{-4}\times\frac{X_p\times0.964}{\pi\times6^2}\right)^2\{L-(H_p-H)\}} \qquad [C7]$$

where, $\rho_0$: density at atmospheric pressure

$V_0$: volume at atmospheric pressure

$\rho_p$: density at pressure p

$V_p$: volume at pressure p

$H_p$: reading of the dial gauge in the experiment

From the above calculation, density of test oil can be determined under various pressures up to 1.5 GPa.

***Determination of Tangent Bulk modulus***

Volume of elastic coefficient or bulk modulus determination is given as follows. When compression pressure is received by the liquid, its volume compressed to (V-dV) at pressure (p+dp).

If volume shrinks, this relationship follows the hook's law. So, volume of distortion – dV/V is proportional to pressure increase dp, i.e.

$$dp = -K_T(dV/V) \qquad [C8]$$

$K_T$ is the tangent bulk modulus of the liquid. This is a property which depends on molecular structure of liquid, temperature and pressure as it compressed.